URANIUM OCCURRENCES IN THE GRANITE ZONE

STRUCTURAL SETTING - GENESIS - EXPLORATION METHODS

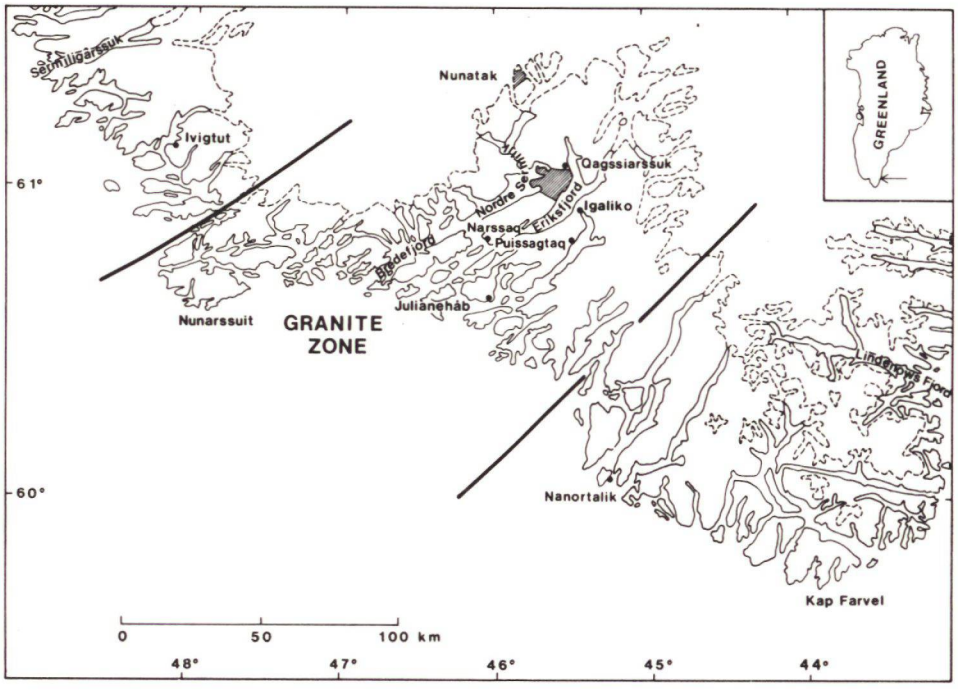

REPORT NO. 1

THE SOUTH GREENLAND EXPLORATION PROGRAMME 1984 - 1986

GRØNLANDS GEOLOGISKE UNDERSØGELSE
The Geological Survey of Greenland
ØSTER VOLDGADE 10, 1350 KØBENHAVN K, DANMARK

URANIUM OCCURRENCES IN THE GRANITE ZONE

STRUCTURAL SETTING - GENESIS - EXPLORATION METHODS

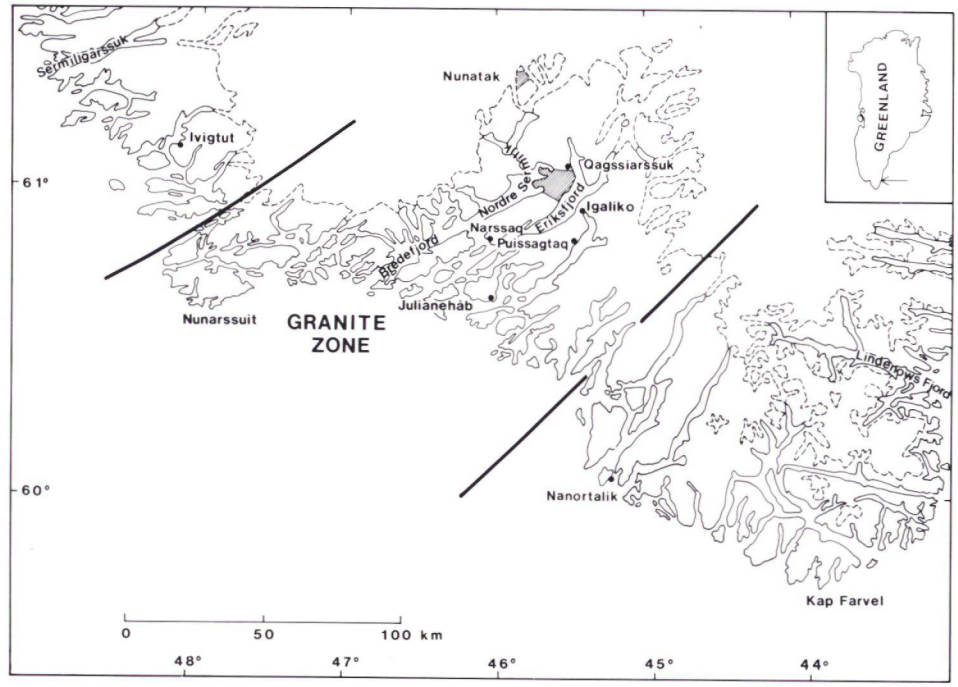

REPORT NO. 1

THE SOUTH GREENLAND EXPLORATION PROGRAMME 1984 - 1986

URANIUM OCCURRENCES IN THE GRANITE ZONE

STRUCTURAL SETTING - GENESIS - EXPLORATION METHODS

The South Greenland Exploration Programme 1984-1986
Report No. 1

Per Nyegaard
Ashlyn Armour-Brown

Pitchblende vein, Nunakutdlak, Qagssiarssuk area

The Geological Survey of Greenland
April 1986

Dansk sammendrag

Den foreliggende rapport indeholder en beskrivelse af foretagne undersøgelser og diskussion af opnåede resultater fra energiforskningsprojektet Sydex´s feltsæson 1984 i den såkaldte Granitzone i den centrale del af Sydgrønland. Den indeholder også en strukturel analyse af Ivigtut-Julianehåb distriktet, der kan være vejledende for fremtidig uranprospektering. Rapporten afsluttes med anbefalinger og forslag til fortsat arbejde af både videnskabelig og prospekteringsmæssig art. Projektet er udført af Grønlands Geologiske Undersøgels (GGU) i samarbejde med Forskningscenter Risø. Det er financieret af energiministeriet.

Den strukturelle analyse er udført under anvendelse af eksisterende geologiske kort, egne feltobservationer samt flyfotografier og satellitbilleder. Større lineamenter i distriktet skyldes Ø-V sinistrale sideværts forkastninger og NØ-SV normalforkastninger. Analysen af de mindre lineamenter viste, at distriktet kan opdeles i tre blokke, der har reageret forskelligt på det regionale stressfelt, der herskede igennem Gardar perioden. Den nordlige blok er påvirket af et ældre forkastningssystem i den arkæiske gnejs, den centrale blok er domineret af en gravsænkning, og den sydlige blok udviser en brat aftagen i forkastningsintensitet mod SØ.

Gravsænkningens begrænsende forkastninger antages at ligge henholdsvis på nordsiden af Nunarssuit halvøen og gennem Vatnahverfi området syd for Igaliko Fjord. De to forkastninger sammenfalder delvist med grænserne for granitzonen, og det antages, at suturzoner dannet i ketilidisk tid (ældre til midt-proterozoisk) har været lokaliserende for gravsænkningen.

Det antages, at et overordnet Ø-V rettet stressfelt, som herskede i hele Gardar perioden, er ansvarlig for den tektoniske udvikling af området. Stressfeltet har maksimal kompression i NØ-SV retningen og minimal i NV-SØ retningen. Tensionen og deraf følgende strækning og fortyndelse af skorpen medførte opstigning af kappemateriale, hvilket igen resulterede i dannelsen af gravsænkningen og intrusionen af magmatiske komplekser i skæringspunkterne mellem de Ø-V gående sideværts forkastninger og de NØ-SV gående normalforkastninger.

Under åbningen af Labrador Havet i mesozoisk tid blev der dannet NØ-SV sinistrale transforme forkastninger. En af disse skærer kysten lige syd for Nunarssuit halvøen, og det ser ud til, at der er en sinistral forsætning på 40 km langs denne forkastning.

Uranmineralisering har fundet sted i de store Ø-V forkastningszoner og i mindre forkastninger med andre retninger. Kendskabet til det regionale forkastningssystem tillader forudsigelse af hvilke retninger, der har givet åbne sprækker, hvorigennem de uranholdige opløsninger har kunnet passere under afsættelse af uranmineraler.

Feltarbejdet i Oagssiarssuk området resulterede i fund af mange nye lokaliteter med uranmineraler. Uranbegblende fandtes i 2 cm brede årer og som hulrumsudfyldninger både i granit og sandsten. De to vigtigste lokaliteter ligger i Eriksfjordformationen i en forkastningsbegrænset sandstenskile. På den ene optræder små spredte uranbegblendeansamlinger over en strækning af 1 km, og på den anden findes tynde radioaktive sprækker diskontinuert fordelt over en strækning på 4 km men knyttet til samme stratigrafiske horisont. På begge lokaliteter er sandstenen omdannet til klorit. Omdannelser til lermineraler er et karakteristisk træk for sidestenen omkring højlødige ´unconformity type´ uranforekomster under Athabasca sandstenen i Canada. Det er derfor nærliggende at tolke kloritdannelsen i Eriksfjordformationen som et analogt fænomen, hvilket betyder, at den ´unconformity´, der ligger ved bunden af Eriksfjordformationen, udgør et lovende prospekteringsmål.

I graniten uden for sandstenen findes uranbegblende knyttet til småsprækker, og mineralet brannerit (med uran og titan) findes i små årer eller spredt i sidestenen til uranbegblendeårer. Branneritens tilstedeværelse kan være tegn på enten, at der er uranbegblende på dybere niveau, eller at uranholdige opløsninger har passeret sprækken. Uranmineralerne findes ofte i

kontakten mellem granit og skærende doleritgange, og sidstnævnte tænkes at være gunstig for uranens udfældning.

På en nunatak nord for Nordre Sermilik blev uranmineraler i små mængder fundet både i gnejs og i Gardar årer knyttet til sprækker. Isotopaldersbestemmelser viste, at uraniniten i gnejser er 1740 millioner år svarende til alderen af Julianehåb graniten, mens uraniniten i sprækkerne er 1350 millioner år svarende til tidlig Gardar. Sidstnævnte er betydelig højere alder end tidligere udførte isotopbestemmelser på uranbegblende fra årer på Igaliko halvøen (1100 millioner år), og det er muligt, at nunatakkens uran er kontamineret med ældre radiogen bly. Den ketilidiske alder på uraninit godtgør, at de ketilidiske suprakrustale bjergarter kan have været kildebjergarter for den omfattende uranmineralisering i sprækkezonerne i Gardar perioden.

Fluorit fra årerne i sprækkezonerne er analyseret for sjældne jordarter for om muligt at bestemme oprindelsen af de hydrotermale opløsninger, hvoraf årerne er dannet. Resultaterne viste, at fluoritprøverne kunne klassificeres på grundlag af værdier normaliseret mod chondrit eller mod en standardprøve, og at de hydrotermale opløsninger sandsynligvis stammer fra eller er stærkt beslægtet med Motzfeldt intrusionskomplekset. I et Tb/La - Tb/Ca diagram plotter de fleste værdier i det hydrotermale felt. Nogle få plotter i det pegmatitiske felt og har tillige højt Th-indhold, hvilket tyder på dannelse ved høj temperatur.

De kemiske analyser af indsamlede vandprøver fra søer, henholdsvis bække, gav sammenlignelige resultater. De to indsamlingsmedier supplerer hinanden godt og påviste tilsammen anomale områder både i graniten og i Eriksfjordformationen. Det konkluderes, at prospektering ved hjælp af vandprøver fungerer godt og med fordel kan kombineres med prospektering ved hjælp af scintillometer.

Tre typer af ionabsorberende materiale blev testet som medium til prospektering efter skjulte uranforekomster. Absorbanterne lå i to måneder nedgravet i jorden over en formodet forlængelse af uranbegblendeåren ved Puissagtaq. Resultatet af analyserne var nogenlunde tilfredsstillende og metoden kan vise sig at blive anvendelig i områder uden blotninger. Yderligere afprøvning er dog nødvendig før dens fulde værdi kan bedømmes.

Tungmineralkoncentrater blev indsamlet i elve både i Puissagtaq og i Qagssiarssuk for at eliminere effekten af organisk indhold i bæksedimentet. Det organiske materiale absorberer uran og kan derved frembringe falske eller transporterede anomalier. Som ventet havde tungmineralkoncentraterne lavere uranindhold end den tilsvarende finfraktion (inkl. organisk materiale). Fire af tungmineralprøverne, samlet i nærheden af en uranbegblendeåre, havde et højt indhold af uran. En mineralogisk undersøgelse viste, at uranen, uventet, optræder som små indeslutninger af uranothorit og uranothorianit i zircon og uranholdige niobium-mineraler. Ingen af disse mineraler er fundet associeret med uranbegblende i åren, og der er derfor tvivl om metodens anvendelighed.

Resultaterne af feltsæsonen 1984 bekræfter, at der i Granitzonen findes udmærkede forudsætninger for at finde uranforekomster, som kan vise sig at være brydeværdige. Prospekteringen skal foretages både i graniten og i sandstenen, hvor der er muligheder for uranbegblendeårer. I sandstenen er der desuden muligheder for 'unconformity' typen på kontakten sandsten/granit langs forkastningszoner, som det kendes fra Athabaska i Canada og Pine Creek i Australien.

ABSTRACT

This report describes the work and results of the South Greenland Exploration Programme (Sydex) during the 1984 field season in the Granite Zone, and discusses the results and conclusions that can be drawn from them. It also contains a structural analysis of the Ivigtut-Julianehåb region, which will help in future exploration by indicating the likely directions of uraniferous faults and fractures. It also includes suggestions for future work with both exploration and scientific aspects. The project was carried out by the Geological Survey Greenland (GGU) in co-operation with Risø National Laboratory. It was financed by the Danish Ministry of Energy.

The structural analysis was carried out using previous geological maps, our own field observations and an analysis of lineament frequencies taken from aerial photographs and satellite images. Major lineaments in the region are due to E-W sinistral wrench faults and NE-SW normal faults. Analysis of the minor lineaments showed that the region could be divided into three blocks which have each reacted differently to the same regional stress field which was active throughout the Gardar period. A northern block which has been influenced by an older system of faults in the Archaean gneiss, a central block dominated by a graben, and a southern block where there is a change to a less intensively faulted area.

The NE-SW striking boundary faults of the graben are believed to be on the northern side of the the Nunarssuit peninsula and along a fault zone which runs through the Vatnahverfi area south of the Igaliko Fjord. These two faults coincide approximately with the boundaries of the Granite Zone, suture zones formed during the Ketilidian, which later influenced the location of the boundary faults of the Gardar graben.

The wide occurrence of E-W striking sinistral faults indicates that the overall stress field during the Gardar was an E-W directed sinistral simple shear over the whole zone. The maximum compression direction in such a stress field would be NE-SW. This direction parallels the tensional features such as the graben and the dyke swarms. The crustal stretching and consequent thinning in the NW-SE minimum compression direction would promote the rise of mantle material and consequent updoming leading to the normal faulting, graben formation and the emplacement of the alkaline intrusions which are coincidentally situated on the major E-W striking faults.

During the opening of the Labrador Sea in the Mesozoic NE-SW sinistral transform faults were formed. Although Mesozoic faults have not previously been recognised in South Greenland it is suggested that one of these cut the coast just south of Nunarssuit peninsula. Based on published information it is proposed that there is a sinistral displacement of 40 km along this fault. Such a movement would place the Nunarssuit alkaline complex along with the Ilímaussaq complex, and the Grønnedal-Ika complex with the Igaliko complex along the same E-W Gardar faults respectively.

Uranium mineral occurrences are found in the major E-W fault zones and in minor faults with other strikes. They naturally occur where openings allowed access of the uranium bearing fluids and traps where minerals could be deposited. Knowledge of the regional structural setting of the Gardar period is, therefore, important for future exploration.

Many new uranium mineral occurrences were found in the Qagssiarssuk area. Pitchblende was found in up to 2 cm wide veins and as cavity fillings both in granite and sandstone. The most important are two anomalous areas occurring in the Eriksfjord Formation sandstone. These are in a fault-bounded sandstone wedge in which scattered small pitchblende occurrences were found discontinuously over a distance of 1 km, and in the southern part of the area where small radioactive joints were found over a distance of 4 km at the same stratigraphic level. The first locality is associated with a well defined fault lineament but no major fault was associated with the latter. Pitchblende has been identified at some of the radioactive joints and at one of the

localities scattered radioactive joints cover an area of 10x250 m. At both these localities the sandstone has been altered by chlorite. Clay alteration is characteristic of the haloes over the high grade unconformity-type uranium mineralisation found below the Athabasca sandstone in Saskatchewan, Canada. It is, therefore, suggested that these are similar haloes and that the underlying unconformity is a very promising target for future uranium exploration.

In the surrounding granite, pitchblende is associated with joints, and the uranium-titanium mineral brannerite is found either as veinlets or in the wall rock as replacements after sphene or other Ti minerals. It is possible that the brannerite occurrences indicate either that pitchblende is associated at a deeper level or that uranium has passed through the joint system. In the granite these occurrences are often found close to the contact between granite and dolerite dykes. It is suggested that the proximity of the dolerite dykes has helped in the precipitation of the uraniferous minerals.

On a nunatak north of Nordre Sermilik uranium minerals were found both in gneiss and in Gardar veins. The occurrences are small but interesting from a genetic point of view as isotopic age determinations showed that the uraninite in the gneiss had an age of 1780 Ma which corresponds to the age of the Late Julianehåb granite. The age of the pitchblende in the veins, on the other hand, is 1350 Ma which is early Gardar. This is considerably older than previous isotopic results from pithblende veins (1100 Ma), and it is possible that this pitchblende was contaminated with older radiogenic Pb. The finding of uraninite of Ketilidian age in the Granite Zone establishes that the Ketilidian supracrustal rocks could have been a source for the extensive uranium vein type mineralisation in the Gardar period.

The rare earth element (REE) content of fluorite was studied in an effort to elucidate the origin and genesis of the hydrothermal activity. From the results it was possible to group fluorite on the basis of their sample/chondrite and sample/sample normalisation values and to suggest that most of the fluorite samples were derived from or related to the Motzfeldt centre. Most of the values plot in the hydrothermal field of the Tb/La - Tb/Ca diagram. A few plot in the pegmatitic field and as these also have the highest Th content it is suggested that they had a higher temperature of formation.

Geochemical prospecting in the Qagssiarssuk area was carried out using lake and stream water sampling, and the results from the two sampling media correspond well. The method outlined anomalous areas both over the granite and the Eriksfjord Formation. It was concluded that these exploration methods worked well and could be combined efficiently with scintillometric prospecting.

Resin and MnO ion absorbers were tested in different soils to see if they could detect buried uranium occurrences. They were buried in the soil over a period of 2 months over extensions of the pitchblende veins at Puissagtaq uranium prospect. The method was partially successful and it may prove to be a viable technique for the evaluation of geophysical anomalies where there is no exposure. But further orientation studies are required in areas where the distribution of buried uranium showings is better known.

Heavy mineral concentrates were collected from streams both in the Puissagtaq and in the Qagssiarssuk areas in order to eliminate the influence of organic matter which absorbs uranium and leads to falsely high and transported anomalies in the stream sediment. Organic material was eliminated by panning and the heavy mineral concentrates had correspondingly less uranium compared with sieved fine fraction of stream sediment; however, four anomalous heavy mineral concentrate samples which were thought to have been due to the presence of pitchblende were investigated mineralogically, and it was found that the uranium was held in inclusions of uranothorite and uranothorianite in zircon and in uraniferous Nb-minerals. Neither of these minerals are known to occur with the pitchblende or brannerite showings. Its usefulness as an exploration technique, therefore, seems doubtful.

TABLE OF CONTENTS

LIST OF FIGURES, TABLES, MAPS AND APPENDICES

MAPS

FIGURES

List of figures, tables, maps and appendices

List of figures, tables, maps and appendices

List of figures, tables, maps and appendices

TABLES

APPENDICES

1 INTRODUCTION

The Granite Zone of South Greenland has been shown by the reconnaissance work carried out during the SYDURAN project to contain numerous occurrences with pitchblende and uranium dominated radioactive minerals (Armour-Brown et al., 1982, 1984). As a spin off of this project the South Greenland Exploration Programme (SYDEX) was started at the beginning of 1984. There was a number of objectives for the Sydex project in the Granite Zone. These included detailed prospecting of the Qagssiarssuk area and of one of the nunataks north of Nordre Sermilik (fig. 1), the interpretation of the Gardar structures and further evaluation of the best exploration methods in the area. This report describes the results of the field work carried out in 1984 and the evaluation of the petrographic, mineralogical, and analytical studies.

The project was financed by the Danish Ministry of Energy under its Energy Research Programme 1984 (EFP ´84). The Geological Survey of Greenland (GGU) in collaboration with Risø National Laboratory (Risø) were responsible for the project and it was under the direction of Agnete Steenfelt at GGU and Leif Løvborg at Risø.

In the field P. Nyegaard worked around Qagssiarssuk while A. Armour-Brown worked at Puissagtaq and on the nunatak. They were assisted by Ole Christiansen, Jens P. Nielsen and Hans Christian Olsen, who carried out much of the water sampling in the Qagssiarssuk area and participated in the scintillometer survey. The geophysical survey was carried out by Leif Thorning and Egon Hansen from GGU´s geophysical section. The laboratory work was carried out by Eva Nørringaard and later by Morten Heegaard of GGU.

1.1 Geology of the Granite Zone of South Greenland

The field area comprised a part of the Precambrian shield of Greenland which consists mostly of the Proterozoic Ketilidian "Mobile Belt". The belt has been divided into four major structural zones (Allaart, 1976) of which the Granite Zone is one (fig. 1).

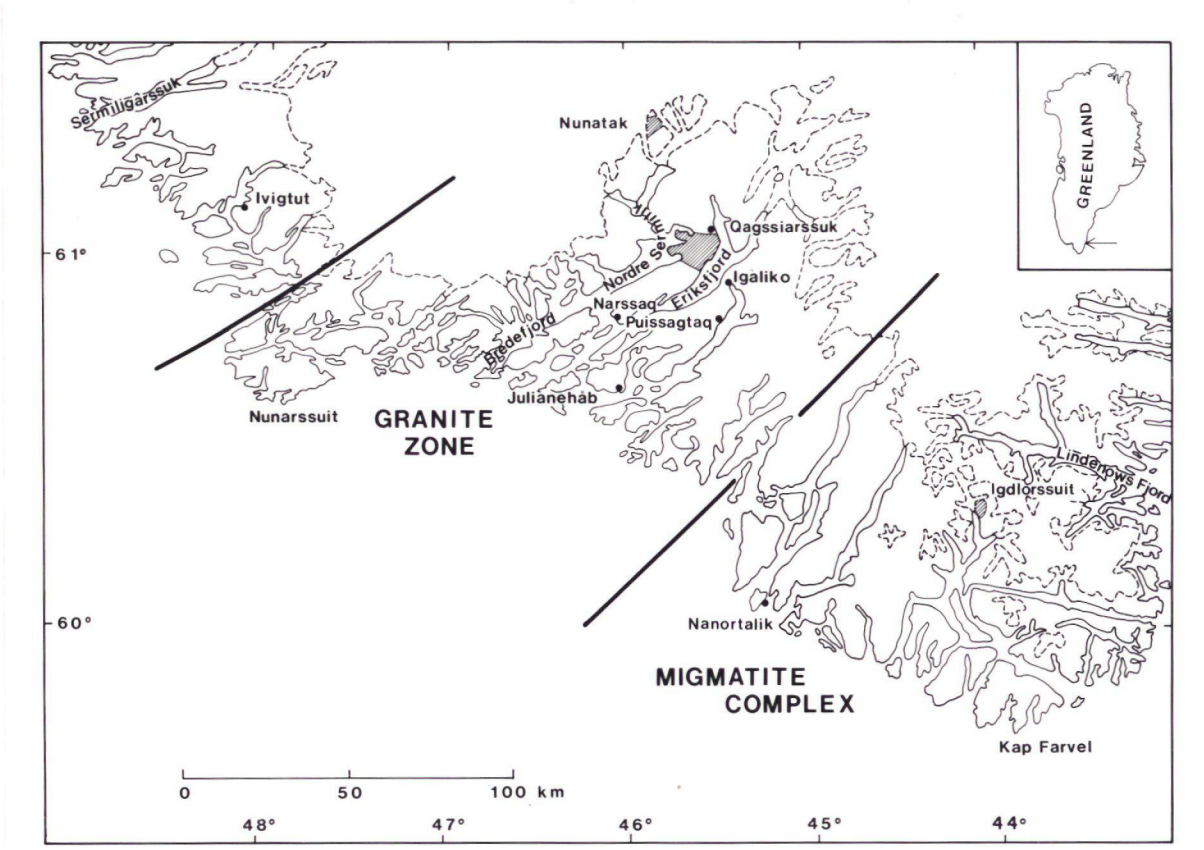

Fig. 1. Map of South Greenland with working areas during the 1984 field season.

The Granite Zone is underlain by a complex of granite, diorite and gneissose granite in a 80-150 km wide belt trending in a NE-SW direction known as the Julianehåb Granite (Allaart, 1976). This granite has been divided into early and late members. The early granite members are foliated, inhomogeneous rocks of adamellitic to granodioritic composition with supracrustal relics. The late granite is less foliated, coarser grained with the same composition as the early members. Basic and intermediate rocks are scattered throughout the Granite Zone. The age of the early granite is around 1840 Ma and the age of the late granite approximately 1780 Ma according to Rb-Sr, Pb-Pb and U-Pb isotopic age dates (van Breemen et al., 1974, Kalsbeek & Taylor, 1985).

After the Ketilidian diastrophism this crystalline basement was subjected to intense faulting accompanied by the cratogenic deposition of sandstone and basalt volcanic flows (Eriksfjord Formation) and igneous activity of the Gardar period (Emeleus & Upton, 1976). Both the Gardar supracrustal rocks and the crystalline basement were intruded by a variety of dykes and alkaline

complexes. Age determinations by the Rb-Sr method (Blaxland et al., 1978) suggest a range from 1330 to 1150 Ma for the intrusion of the complexes.

1.2 Field investigations

The field work in the Qagssiarssuk area (fig. 1) lasted from June 27nd to September 1st 1984. The work was carried out from two inland camps with helicopter support and from two coast camps with a rubber boat. The work along the northwestern coast was partly hindered by ice. Eighteen days were lost due to bad weather but there were enough dry and sunny days to carry out the planned work on schedule. The ground scintillometry was carried out using Scintrex BGS-2 instruments. Fault zones in the area were especially checked for radioactivity. The water samples were collected from lakes and streams. The water was stored in polyethylene bottles and shipped to GGU by air and analysed there for uranium, fluorine, pH and conductivity. Heavy mineral concentrates were also collected in a few streams by panning stream sediment.

The field work at Puissagtaq (fig. 1) was carried out in two periods from June 28th to July 5th and from September 1st to September 5th. The first period was used to place resin ion absorbers in the soil over known uranium mineral veins and the second period to retrieve them for analysis. This was done at the same time as sampling the soils in order to find a technique for locating pitchblende ore concealed under the soil. During the same periods water and seep samples together with heavy mineral concentrates were taken. This was done in order to evaluate these methods as a means of differentiating between true and false or transported uranium anomalies in the stream sediments.

The field work at the nunatak (fig. 1) took place in the last two weeks of August. The field work was concentrated firstly on the location of the source of the gamma-spectrometer anomaly and secondly on general prospecting in the area.

1.3 Acknowledgements

The authors are indebted to a great number of people, who have assisted in the field and in the laboratories, and we would particularly like to thank H. Kunzendorf, E. Johansen and P. Jensen at Risø National Laboratory, Elektronik Afdeling for their analyses of many of the rocks by EDX and DNC and gamma-spectrometry analyses. Also J. Rønsbo from the Institute of Mineralogy, the University of Copenhagen is thanked for his valuable help during the microprobe work.

2 TECTONIC SETTING OF THE JULIANEHÅB-IVIGTUT REGION

2.1 Introduction

At an early stage of the regional uranium prospecting work in the Granite Zone of South Greenland faults were recognised as being a controlling factor of the uranium mineralising process (Armour-Brown et al., 1982). The faults appear to have given access to hydrothermal fluids related to the Gardar igneous activity. A regional evaluation of the lineament pattern combined with mapped faults, therefore, was thought to be helpful in a future exploration, as it would help define the limits of this hydrothermal activity as well as pin point areas favourable for openings with vein type uranium occurrences.

Previously the same fault pattern was recognised in both the Ivigtut and the Julianehåb areas (Berthelsen, 1962). Therefore the whole of southern Greenland and not only the uranium district in the Granite Zone, will be treated as a whole in the following structural analysis.

2.2 Previous work

During the systematic mapping of the Ivigtut and Julianehåb areas in the late fifties and early sixties, the dominant E-W sinistral faults were recognised and used to divide the region into big fault blocks (Berthelsen, 1962). Some of these wrench faults were active both in pre-Gardar and in Gardar times (Henriksen, 1960). The Gardar intrusive ions complexes are found where ENE trending dykes and fault rich zones cut the E-W wrench faults (Berthelsen & Noe-Nygaard, 1965). The Gardar central complexes have an elliptical form, which are explained by ductile deformation of the hot intrusions undergoing large scale simple shear (Stephenson, 1976).

The major E-W Gardar structures are mapped with a fairly regular interval of 10-18 km (Allaart, 1973, 1983, Stephenson, 1976), and a total, sinistral displacement of between 15 and 20 km has been estimated for the central part of the region (Stephenson, 1976). This E-W fault trend with a sinistral sense of displacement has been recognised as far north as the fjord Neria, 50 km north of Ivigtut (Higgins, pers. comm.). Analysis of fault trends in the Ivigtut area (Berthelsen & Henriksen, 1975 - fig. 56a,b) show a decrease in intensity of E-W faulting to the north, where a NNE direction becomes more frequent. To the south E-W faults with a sinistral sense of displacement have not been recognised south of a major ENE lineament through the Vatnahverfi area, south of Igaliko Fjord.

Another important fault trend in the Julianehåb-Ivigtut region is the NNE 10^{o}-30^{o} direction. Faults with this direction show dextral displacements, and they are the first and last active faults in the region (Berthelsen & Henriksen, 1975; Emeleus, 1964). Through Gardar time there seems to be a shift in trend from NNE to more N-S. This direction is thought to be the complementary shear direction to the E-W sinistral faults (Berthelsen Henriksen, 1975).

In the Ivigtut-Julianehåb region lineaments which trend 60^{o}-80^{o} (ENE) are due to crush zones and dyke swarms (Berthelsen & Henriksen, 1975). This is the same direction as the fjord system in the region, and this topographic feature may be partly due to glacial erosion along ENE crush zones (Emeleus & Upton, 1976). This trend, as the E-W direction, becomes less and less important north of Ivigtut and south of Vatnahverfi. The movements along the ENE faults were mainly vertical.

The ENE trend is also the most common direction of the dyke swarms in the region, although the early dolerite dykes south of Ivigtut follow an E-W trend parallel with the E-W faults. In the Ivigtut area three generations of dolerite dykes have been mapped with somewhat varying trends suggesting variations in the orientation of the regional stress field during the period of emplacement of each generation (Berthelsen & Henriksen, 1975). There seems to be a general regional change in strike from around E-W to ENE in the southeast part of the area, to around NE in the northeast part of the area. This indicates an approximately 45^{o} anti-clockwise rotation of the dolerite dykes (Berthelsen & Henriksen, 1975). An anti-clockwise rotation of dykes is also reported from the nunataks northeast of Qagssiarssuk by Upton & Fitton (1985) and in the Julianehåb area by Allaart (1973). On the other hand the early E-W dykes often show signs of shearing along their length and are thought to be intruded in shear zones (Upton, 1974, Emeleus & Upton, 1976), and the rotation is probably only 10^{o}-20^{o} as observed for the two latest generations. Three ENE dyke swarms mapped in the Ivigtut, Nunarssuit and Tugtutôq areas show a crustal opening calculated to 3 % at Ivigtut (Berthelsen & Henriksen, 1975), and approximately 4 % in the Nunarssuit-Tugtutôq-Igaliko area (Upton & Blundell, 1978; Allaart, 1969).

A graben structure in the Tugtutôg-Qagssiarssuk area, in which the lava and sandstone of the Eriksfjord Formation (Poulsen, 1964, Stewart, 1964) were deposited, was already proposed by Ussing (1912), but Berthelsen & Noe-Nygaard (1965) and Allaart et al. (1969) suggested that the E-W wrench faults controlled the basin. A graben structure with an ENE trend was later brought up again by Emeleus & Upton (1976) and Upton & Blundell (1978). An analysis of lineaments on satellite images show that the ENE tension fracture direction is nearly absent southeast of a line through the Vatnahverfi area south of the

Igaliko Fjord (Conradsen et al., 1985). This is regarded as the southern limit of the graben structure (Nyegaard et al., 1986). The Gardar graben structure was correlated in time with the Seal Lake and Keweenewan grabens in the eastern Canadian Shield (Emeleus & Upton, 1986; Baer, 1981). Palaeomagnetic studies of Gardar rocks (Piper, 1976, 1977a, 1977b, 1982; Piper & Stearn, 1977) demonstrated that Greenland was a part of the Laurentian craton. During the Gardar period the same stress field is assumed for both South Greenland and East Canada (Baer, 1981).j

The relative ages between faults, dykes and alkaline intrusions show that repeated movements took place along faults and with the same sense of displacement throughout the Gardar period possibly already starting in late Ketilidian time. A chronology for the Gardar period is suggested by Upton & Blundell (1978) and Emeleus & Upton (1986) with (1) an early rifting (1300 Ma), deposition of lava and sandstone and large undersaturated syenitic volcanic centres; (2) rifting (1250 Ma) marked by intrusion of alkaline basic dykes, transcurrent faults and intrusion of silica oversaturated central complexes; (3) asymmetric rifting (1170 Ma), emplacement of alkaline basic dykes, rejuvenation of older trancurrent faults and late stage intrusion of alkaline central complexes.

The widespread faulting and dyke emplacement in the Gardar period have, according to Berthelsen & Henriksen (1975), developed under the same regional stress system. They suggest an approximately E-W orientation of the maximum stress axis, changing with time to NE-SW. The corresponding minimum axis was orientated N-S, changing with time to NW-SE.

Later fault activity in South Greenland may also have occurred in Mesozoic time during the opening of the Davis Strait. A major NE-SW striking sinistral transform fault from the Newfoundland shelf through the Labrador Sea interpreted from magnetic studies (Hood & Bower, 1973) has been projected along Bredefjord on the basis of topographic features. Mesozoic faults have not previously been recognised in South Greenland.

2.3 Lineament and structural analysis

A map showing lineaments and major faults in the area from Neria in the north to Lichtenau Fjord in the south was compiled on a 1:250 000 scale map (Map 1). The larger faults and crush zones were extracted from field maps, published 1:100 000 geological maps, satellite images at 1:1 000 000 and aerial photos at 1:50 000 and 1:150 000.

The purpose was to obtain an overall structural model of the region, and therefore many small lineaments seen on aerial photos graphs have been omitted

from the lineament map. The most important lineaments or faults in the region have been accentuated on the map. The direction of these fault and crush zones are E-W and NE-SW. Most of the dykes have also been omitted from the map, except for the widest and most extensive dolerite/gabbro and giant dykes. These dykes are of Middle and Late Gardar age, and the dykes with a WNW trend are the oldest (Berthelsen & Henriksen, 1975). The Early Gardar lava and sandstone of the Eriksfjord Formation and the Gardar alkaline, central intrusions are also shown on Map 1. The intrusions have been divided by age according to Upton & Blundell (1978) into Early (1400?-1300 Ma), Mid (1300-1250 Ma) and Late (1250-1130 Ma) Gardar. Early Gardar includes Grønnedal-Ika, Motzfeldt and North Qôroq complexes, the Mid Gardar Kûngnât and Ivigtut complexes and Late Gardar South Qôroq, Igdlerfigssalik, Puklen, Narssaq, Ilímaussaq, Tugtutôq, Klokken and Nunarssuit complexes. On the lineament map the complexes of Early and Late Gardar age are divided into two and three groups respectively.

2.3.1 Major E-W faults

Six E-W faults cut through the region and divide it into slices approximately 15 km wide. The regional trend of these faults is in fact close to 100°, but will be referred to as E-W faults, as earlier authors have done, in order to avoid confusion. Several of these E-W major faults show horse-tailing and they have a curved trend (Map 1). The northernmost lie north of Sermiligârssuk and curves to the SE and probably joins the next fault through Tigssalûp ilua and Arsuk Fjord. They have been correlated with the fault through the area north of the Qagssiarssuk area (Berthelsen, 1962). The next E-W major fault (the Laksenæs fault; Henriksen, 1960) cuts the Ivigtut area. The next major E-W fault is found north of Sânerut. It crosses the southern limit of the Inland Ice and is thought to join the fault through the Ilímaussaq intrusion (Berthelsen, 1962). South of this fault zone two more major zones run from the Nunarssuit area to the Igaliko Fjord.

These major E-W faults are well documented (Berthelsen, 1962; Allaart, 1973, 1983) and show sinistral displacements of several kilometres. The latest movements along these faults seem to have occurred in the Late Gardar approximately simultaneously with the intrusion of the Ilímaussaq intrusion. The faults offset the Early Gardar Motzfeldt complex and the Narssaq intrusion of early Late Gardar age, but the Ilímaussaq complex, which cuts the Narssaq intrusion, shows no offset, although the fault can be traced through the complex as a brecciated zone often with associated fluorite (Steenfelt, 1972). The latest intrusion, the Nunarssuit complex, cuts an E-W fault, and no trace of the fault within the intrusion has been recognised.

2.3.2 Major NE-SW lineaments

Five major NE-SW lineaments intersect the region, and together with the major E-W faults divide it into fault blocks (Map 1). The trend of these lineaments are closer to ENE, but will for simplicity, be referred to in the following as NE-SW. The lineaments are rarely mapped on land but seem to be normal faults and crush zones with mostly vertical displacement. Two NE-SW lineaments border the Nunarssuit area, and they are expressed in the trend of the fjords, and only the northern one is mapped on land. The next major NE-SW lineament goes through Bredefjord, and the fault nature is seen as crush zones along the shores and as a downthrow of the Eriksfjord Formation exposed to the southeast. The continuation of the fault in the Qagssiarssuk area is not clear. A major fault may also be situated in Skovfjord. The next major NE-SW lineament is found in the Igaliko Fjord and partly seen on the shores and it can be traced on land south of the Igdlerfigssalik complex. To the southeast through the Vatnahverfi area another major lineament occurs, but although it is found on land very little is known about it. Only one of the E-W major faults seems to cross this fault zone. To the southeast two NE-SW lineaments go through the Lichtenau Fjord and Unartoq.

2.3.3 Analysis of lineament trends

From the compilation of the lineament map (Map 1) it became clear that the fault and crush zones are developed to different degrees in the region. On the other hand the lineament trends seem to be consistent within the large fault blocks bordered by the major lineaments in the region. Therefore the major E-W and NE-SW faults and lineaments have been used to divide the region into 14 large fault blocks with a size of 300 to 1200 km^2. Within each fault block the direction of the minor lineaments (faults and crush zones) was measured and their frequency distribution plotted at intervals of 10^o. Adjacent blocks with similar lineament distributions are joined, and the final result is 8 large fault blocks each with a different pattern (fig. 2).

The lineament frequency diagrams have not been weighted for the length of the lineaments. To test if this refinement would change the frequency patterns on the rose diagrams the total length of the lineaments in each interval was plotted for two of the blocks. The two types of diagram showed the same pattern; therefore, it is assumed that the unweighted minor lineament frequencies in each block represent the true frequencies of the lineaments.

Block 1: This block is bound by two E-W faults north of Sermiligârssuk where the northern one curves to the SE and joins the southern fault which has a direction of about $100-110^o$. The dominant trend for the minor lineaments is NNE.

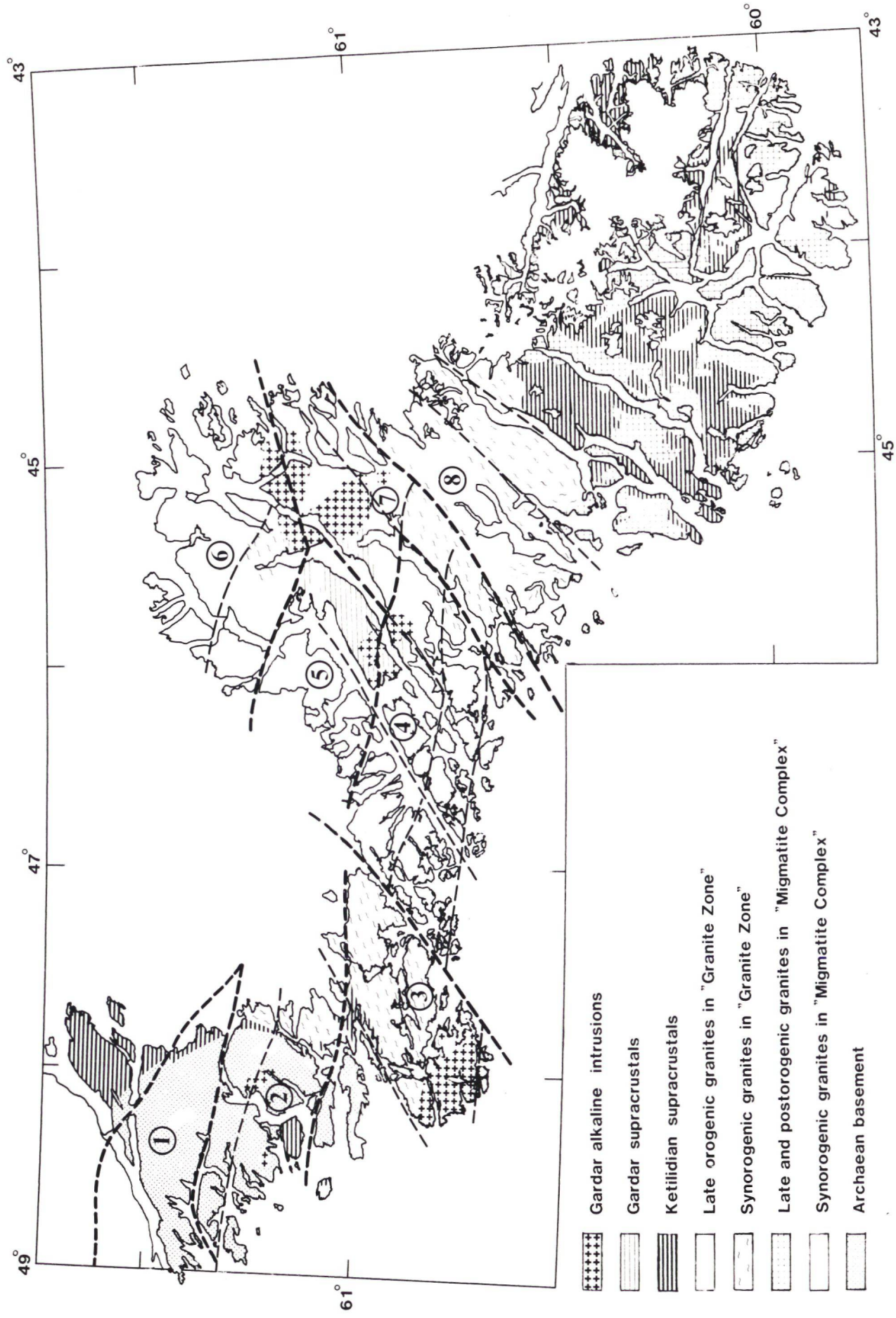

Fig. 2. Geological map of South Greenland with major fault blocks. The heavy dashed lines limit blocks with similar lineament trends and follow mainly major fault zones. The numbers refer to text and fig. 3.

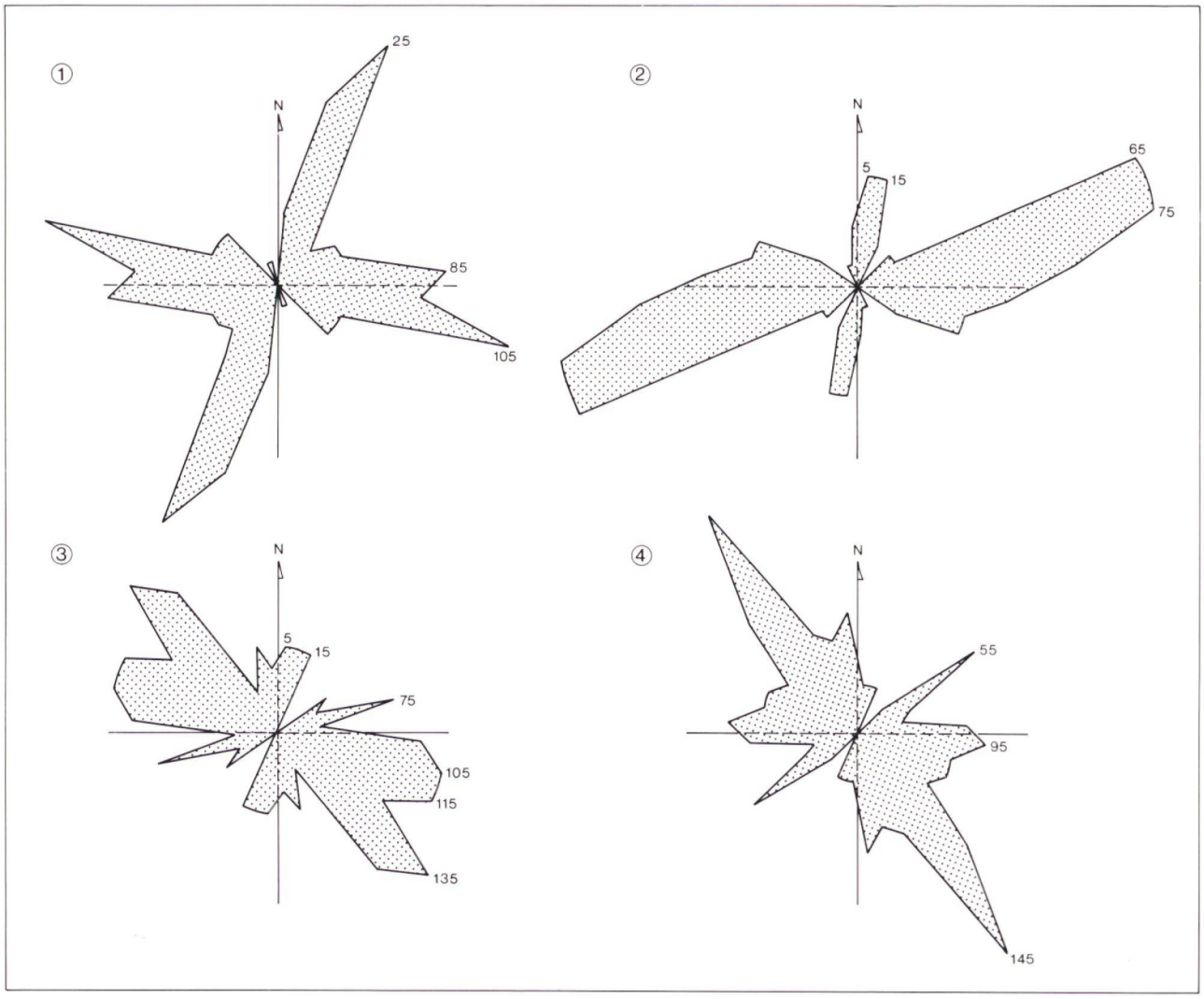

Fig. 3. Rose diagram showing lineament frequencies within fault blocks. The encircled numbers refer to the text and fig. 2. The small figures indicate directions in degrees.

direction and to a lesser extent the E-W direction (with maxima at 85° and 105°)(Fig. 3, 1). The number of measured lineaments (N) within this block is 71.

Block 2: This block is bounded to the south by the E-W fault which runs north of Sânerut and by the Inland Ice. The dominant trend is the NE-SW direction between 65° and 75°, while the N to NNE trend (5°-15°) is diminished (Fig. 3, 2). N = 78.

Block 3: This block is bounded by a NE-SW fault southeast of Nunarssuit and and by the Inland Ice to the NE. The dominant trend has changed to 135° but the E-W (95°-115°) direction is also well developed. The N to NNE and NE trend is also present (Fig. 3, 3). This block is cut by a dense dyke swarm with a NE direction, which is not plotted in the rose diagram. N = 81.

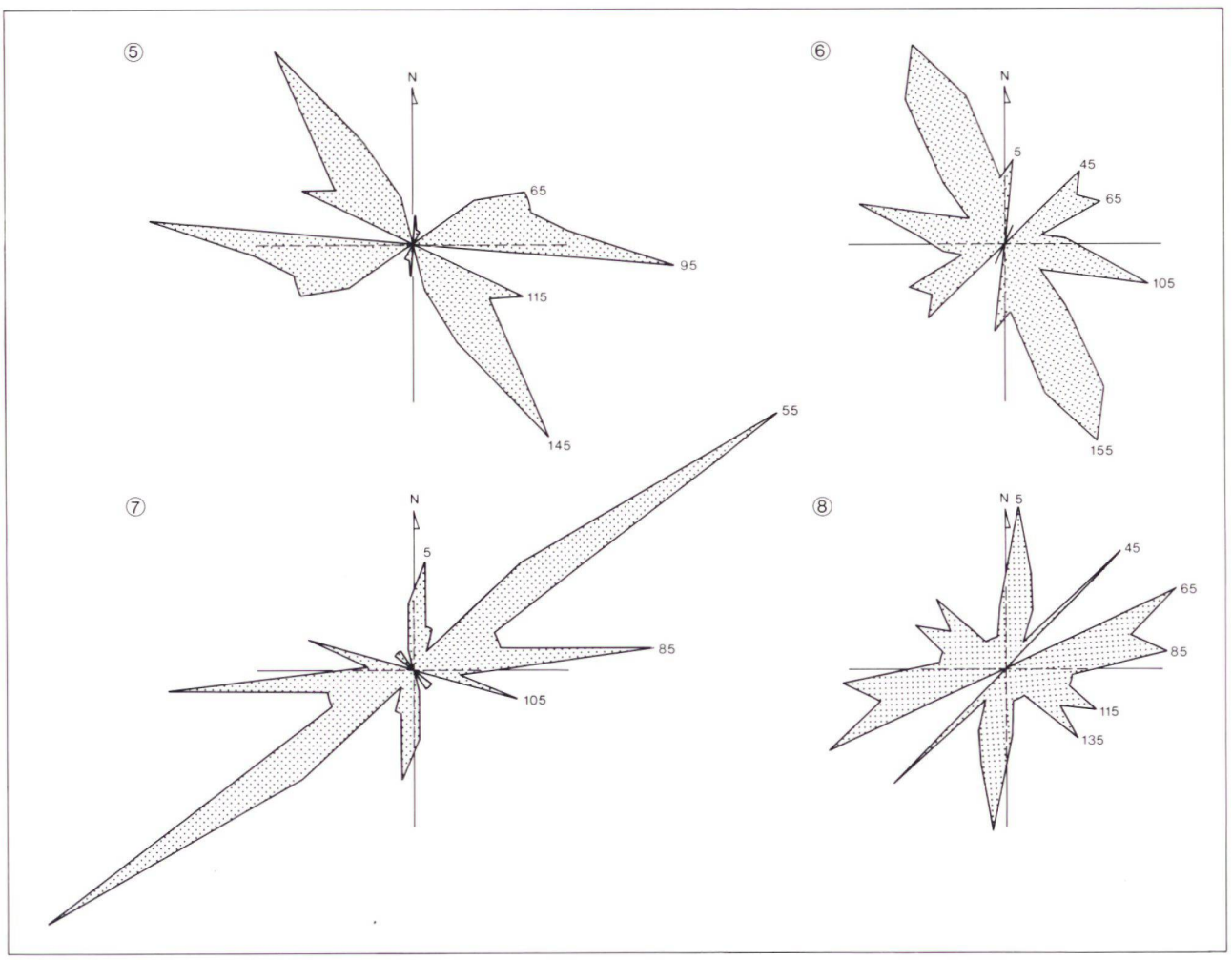

Fig. 3 cont. Rose diagram from fault blocks. The numbers refer to text and fig. 2.

Block 4: This block is bounded to the NE by the E-W fault, which cuts through the Ilímaussaq intrusion and to the southeast by the NE-SW fault through the Igaliko Fjord. SE trending lineaments predominate in this block. The 55° and the 95° trends are seen to a much lesser extent (Fig. 3, 4). N = 141.

The NE-SW trending dyke swarm which cuts both this block as well as blocks 5 and 6 are not included in the rose diagrams.

Block 5: This block is bounded to the north by the E-W fault through the Qagssiarssuk and Motzfeldt Sø areas and to the SE by the fjord Tunugliarfik. Again the SE trending lineaments dominate but the E-W direction is also well developed (Fig. 3, 5). N = 100. From Map 1 it is noted, that the many minor lineaments present in the granite basement throughout the region is mostly lacking in the area of the Eriksfjord Formation between Narssaq and Qagssiarssuk.

Block 6: This block covers the area north of the E-W fault cutting through the Qagssiarssuk and Motzfeldt Sø areas. The SE trend is again dominant and the 105° and 45°-65° trends occur with lesser frequency (Fig. 3, 6). N = 72.
Block 7: This block is not regular as the area between Tunugdliarfik and Igaliko Fjord is included in the fault slice bounded by two NE-SW faults through the Igaliko Fjord and the Vatnahverfi area. In this block the NE-SW trend is predominant with much less frequency of the E-W lineaments. The SE trend is nearly absent (Fig. 3, 7). N = 70.
Block 8: This block lies southeast of the NE-SW fault through the Vatnahverfi area. The trends are the same as in the previous block, but the northern trend has become more frequent, and the 135° much less frequent. Trends about 65° to 85° are also well developed (Fig. 3, 8). N = 48.

From the rose diagrams (fig. 3) and the lineament map (Map 1) it is seen that although the major lineaments in the region follow the same trends, the different fault blocks have reacted in different ways to the regional stress field. The trends along which the faulting, crushing and dyke emplacement has occurred are the same in each block, but are developed to different degrees. Four trends are recognised, and these are:

1) N to NNE with dextral displacements,
2) NE-SW with dyke emplacement and vertical displacements,
3) E-W with sinistral displacements and
4) SE-NW with mainly sinistral displacements, but also to some extent dextral displacements.

Information on their direction of displacement has been illustrated on Map 1.

The N to NNE trend predominates in the northernmost part of the region (Block 1), and the SE-NW trend seems to be best developed in a central area from Nunarssuit down to Igaliko Fjord (Block 3, 4, 5 & 6). South of Igaliko Fjord, in the Vatnahverfi area, the NE-SW lineaments prevail in a 10 km wide zone with extensive faulting (Block 7). South of this zone the lineament frequency decreases drastically and occurs mainly with N to NNE and NE directions (Block 8).

2.4 Discussion and conclusions

Based on the analysis of trends of lineaments the region can be divided into 3 main areas:

A) A northern area north of Nunarssuit with major E-W faults (Block 1 & 2),
B) A central area with major E-W and NE-SW faults (Block 3, 4, 5, 6 & 7) and
C) A southern area south of Igaliko Fjord with major NE-SW faults (Block 8).

2.4.1 The northern area

The lineaments in the northern area, which is underlain mainly by Archaean rocks, are interpreted as resulting from the interaction of older fault systems with the regional stress fields operating during the Gardar period. The Vestland shear belt, which lies just to the north of Block 1 (Fig. 2) (Bak et al., 1975), trends NNE and has been described as one of the major shear zones of West Greenland. This NNE direction is frequent in Block 1 (Fig. 3), but less frequent in Block 2 to the south, where NE-SW trending lineaments predominate. The major movements in this area are sinistral along the E-W faults indicating that the main stress field was simple shear with this sense of movement. The dextral movements along NNE faults is interpreted as a reactivation of older faults along planes of weakness in a complementary direction to the E-W stress system. The many dykes in the Ivigtut area follow a general NE-SW trend, which would have been the tension fracture direction in this stress field.

2.4.2 The central area - the Gardar graben

The central area (Blocks 3, 4, 5, 6 & 7, fig. 2) is bordered by the NE-SW lineaments north of Nunarssuit and south of Igaliko Fjord. These two lineaments are believed by the authors to be deep seated crustal structures possibly of Ketilidian age as they roughly coincide with the limits of the Ketilidian Granite Zone. The southern part of this central area through Vatnahverfi south of Igaliko Fjord is strongly faulted along a NE-SW trend in a 10 km wide zone (Block 7, fig. 3). No major E-W faults cross this southern NE-SW lineament, which has also acted as a geochemical barrier (Armour-Brown et al., 1982).

The statistical lineament analysis of satellite images (Conradsen et al., 1985) shows a high frequency of the NE-SW trend between these two boundary

faults, and that the E-W trend has a low frequency southeast of the NE-NW Vatnahverfi lineament (Block 8, fig. 2). These two lineaments bounding the central area are interpreted as being the limits of the Gardar graben.

The width of this graben is about 85 km. The major alkaline complexes are found within it at the intersection with major E-W sinistral faults and dyke swarms, in association with horse-tailing of the faults. The response to the regional stress system in this part of the region was mainly an opening of the graben along the NE-SW tension direction and displacements along the E-W faults. Within the graben structure the fault blocks have mainly adjusted to the stress system by displacements along minor SE-NW to SSE-NNW secondary faults. This direction is nearly absent outside the graben structure (fig. 3). There is also a change in the frequency of the N to NNE lineaments which are thought to have been the complementary shear direction to the E-W faults. They are best developed in the northern Archaean block by reactivation of older faults and to be much less frequent within the graben structure. The southern boundary of the graben is especially well defined by the many NE-SW faults throughout the Vatnahverfi area. The northern boundary is not so well expressed by intense faulting, but more by a change in the minor lineament trends.

The central part of the graben is possibly the large downthrown area of the Eriksfjord Formation between Narssaq and Qagssiarssuk and further to the SE through Tugtutôq. It is in this area, that the highest density of dykes are found (Emeleus & Stephenson, 1970), and where the dyke swarm is geochemically different from the other swarms in the region (Upton & Emeleus, 1986). The dykes here are more alkaline and richer in P, Ba, Sr, LREE and Nb on the basis of which it is concluded that the crust was thinner in this zone than in the Nunarssuit area. It is also in this area that there is a gravimetric "high", which has been interpreted as a basic rock mass underlying the Ilímaussaq intrusion in the centre of the graben (Blundell, 1978).

The supracrustal rocks of the Eriksfjord Formation reacted differently to the tectonic stress in the Gardar period than the granite basement. Although the formation is dissected by major faults, minor lineaments are infrequent. Brecciated zones in the sandstone which are not apparent as lineaments have, however, been seen in the field. These are presumed to reflect the response of the sandstones to the fault movements in the basement.

2.4.3 The southern area

In the southern area (Block 8, fig. 2 & 3) the Gardar stress field has also acted, but it is not so intensely faulted and has about 60% fewer lineaments. Satellite images (Conradsen et al. 1984) of this southern area also have a low

frequency of the main lineament directions. Although the same lineament directions are apparent, the E-W faults are few and the frequencies of the lineament directions are very different from Block 7 (Fig. 3) immediately to the north which suggests that there is a different structural style in this area.

2.4.4 Regional stress system

According to palaeomagnetic studies South Greenland was part of the Laurentian craton of eastern Canada at least after 1800 Ma (Piper, 1977; Piper & Stearn, 1977; Le Pichon et al. 1977). Palaeolatitude reconstruction and structural considerations suggested to Baer (1981) that the Laurentian shield moved south from about 1350 Ma as if it was being pulled (that is to say under tension, with the tension direction in the NW-SE) until it reached its southerly limit corresponding to the apex of the palaeomagnetic "Logan Loop" at about 1150 Ma. The craton then changes direction of movement to move north again as if it was pushed from the south under the influence of the Grenvillean developments to the south. This reconstruction accounts well for the development of the Gardar tensional features such as the graben and especially for the cessation of the associated igneous activity. It does not account for the regional sinistral stress field which is proposed here. However, it does not contradict it. The palaeomagnetic methods are presumably not sufficiently sensitive to detect the relatively minor sinistral movements. It would seem highly probable that regional stress fields with simple shear could be formed while continental masses were moving as much as 90^{o} of latitude and unspecified and unknown degress of longitude.

2.4.5 Mesozoic faulting and dyke emplacement

Mesozoic dykes with a NW-SE trend are mapped along the coast in the Ivigtut-Julianehåb region, and they have been related to the opening of the Labrador Sea (Watt, 1969). Later displacements along one of the NE-SW major faults may also have occurred. Hood & Bower (1973) suggest that a transform fault runs from Bredefjord across the Labrador Sea towards Hawke Saddle on the Newfoundland shelf and continues in the Cabot fault. This transform fault has a sinistral offset with a displacement of approximately 40 km.

A sinistral fault with 40 km offset does not fit with the geology around Bredefjord, and if it continues to the land it must be correlated with one of the other NE-SW faults. The faults north of Nunarssuit and through Vatnahverfi show no offset of the coast-parallel dyke swarm, but the fault south of Nunarssuit is a possibility. The Mesozoic coast parallel dykes on the islands

south of this line curves from NW to WNW towards the fault and a displacement of 40 km is possible (Fig. 4). This would also bring the major E-W fault pattern in better agreement and the Nunarssuit and Ilímaussaq complexes will be situated along the same E-W fault, as will the Grønnedal-Ika and Motzfeldt-Qôroq-Igdlerfigssalik complexes (fig. 4). It also explains the topographical kink of the coast just south of Nunarssuit. Gneissic rock units mapped around this NE-SW fault (Allaart, 1983; Pulvertaft, 1967) are also brought into better agreement.

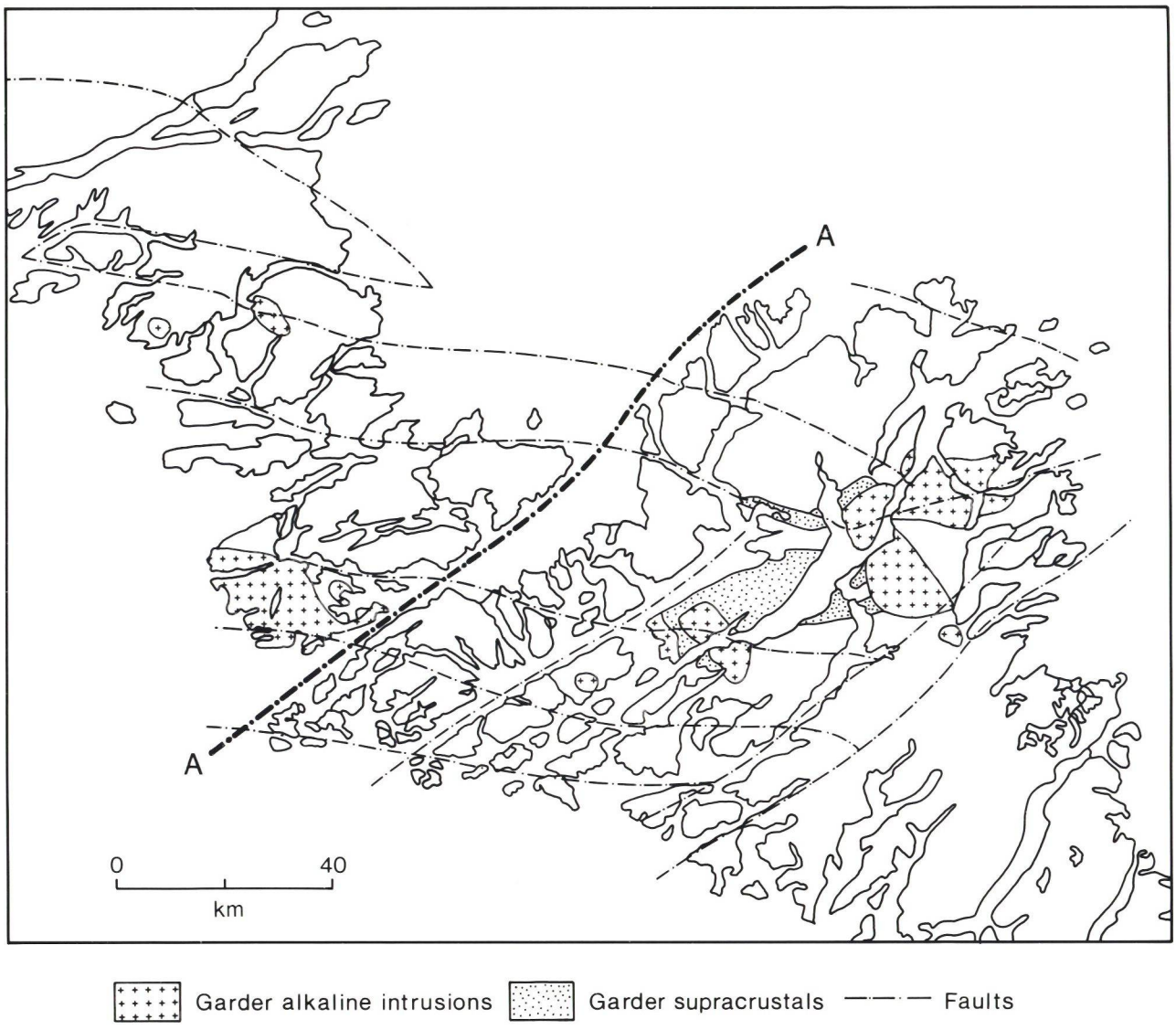

Fig. 4. Map of the Ivigtut-Julianehåb region. The area has been restored along a Mesozoic fault (A-A) with a sinistral, 40-45 km offset.

From the south of Nunarssuit the fault probably continues just north of the nunataks north of Narssarssuaq where a broad magnetic low is found with a possible continuation on the east coast of Greenland (Thorning, pers. comm. 1985).

2.4.6 Relations between uranium occurrences and fault pattern

A comparison between the lineament map of the Julianehåb-Ivigtut region (Map 1) and the distribution of uranium mineral occurrences in the Granite Zone (Map 2) show that the occurrences are associated with both major and minor faults with a preference for the NE-SW tension direction and the E-W fault zones. It must be kept in mind that the map with Uranium mineral occurrences illustrates more the prospected area than the actual distribution of occurrences.

Previous work in the Vatnahverfi area (Block 7, fig. 2) has shown that uranium mineral occurrences seem to have a preference for lineaments with E-W and NE-SW trends (Armour-Brown et al., 1984). Uranium occurrences are also found in faults and crush zones with other trends (Fig. 5). Therefore a more detailed lineament analysis of the major fault blocks must be carried out prior to prospecting in order to locate possible openings most likely to have given access to mineralising hydrothermal fluids. The heavy concentration of uranium mineral occurrences in the Vatnahverfi area (fig. 5) and the intensive faulting along the NE tension direction suggests further prospecting in this wide fault zone, where both the NE and SW parts have not yet been prospected.

A comprehensive correlation between fault pattern and radioactive mineral occurrences cannot be achieved at this stage as only one quarter of the Granite Zone has been investigated. The lineament analysis carried out is, therefore, a framework on which future prospecting can be based in a combination with the geochemical maps of South Greenland (Armour-Brown et al., 1982).

3 RADIOACTIVE MINERAL OCCURRENCES

The field exploration for uranium mineral occurrences has been carried out in two areas of the Granite Zone (fig. 5). The most intensive prospecting was made in the Qagssiarssuk area (fig. 5, area A) and to a lesser extent on the nunatak north of Nordre Sermilik (fig. 5, area B). The following description includes results from the ground scintillometric prospecting, microscopic and microprobe investigations, analytical work and isotopic age determinations.

Fig. 5. Uranium mineral occurrences in the Granite Zone and the location of working areas in 1984 field season.

3.1 Uranium mineral occurrences in the Qagssiarssuk area

3.1.1 Geology of the area

The area is underlain by late Ketilidian, coarse grained biotite granite (1782 +/-20 Ma; van Breemen et al., 1974), aplite and bodies of dioritic rocks commonly veined by granitic rocks. The granite was subjected, during the Gardar period (1330-1150 Ma; Emeleus & Upton, 1976), to extensive faulting and deposition of sandstone and lava (the Eriksfjord Formation; Poulsen, 1964; Stewart, 1964), emplacement of a swarm of basic and alkaline dykes and to carbonatitic volcanism (Allaart, 1983).

The sandstone is red coloured and composed of well rounded quartz grains. The cement is normally siliceous and the sandstone is very pure with only few feldspathic grains. Beds of conglomerate occur at several levels in the sandstone formation, and the pebbles are well rounded and almost all consist of sandstone (Ussing, 1912). The basal layers of the sandstone are arkosic and overlie disintergrated granite. Fanglomerate like beds are found in places which are thought to lie close to the margin of the basin (Poulsen, 1964). They are probably associated with escarpments formed by normal faults. The lavas are mostly basaltic with some high level flows of trachytic composition (Stewart, 1970). The carbonatitic volcanism was explosive and associated rocks pyroclastic in nature. Thin layers of carbonated lava are overlain by bedded tuffs and agglomerates (Stewart, 1970), and cut by volcanic vents. Associated with the carbonatitic rock are barite and a fluorine rich apatite (Knudsen, 1986; Stewart, 1970). The dyke swarm in the Qagssiarssuk area is composed of dolerite/gabbro dykes and of trachydolerites, trachytes and saturated and undersaturated microsyenites (Allaart, 1983). The Ketilidian and Gardar rocks are dissected by two main sets of faults trending ENE and E-W. The E-W faults which strike more commonly in an ESE-WNW direction in the Qagssiarssuk area have a total displacement of about 7 km with a sinistral sense and with a smaller vertical component, which together with the ENE normal faults has contributed to the preservation of the Eriksfjord Formation (Emeleus & Stephenson, 1970).

Pitchblende and other uranium mineral occurrences have been found in major fault zones in the western part of the area (Armour-Brown et al., 1983). Radioactive thorium dominated green or brown dykes have also been found (Hansen, 1968; Armour-Brown et al., 1982).

3.1.2 Results

Prospecting with scintillometers resulted in the finding of many small pitchblende and/or brannerite occurrences in both granite and sandstone associated with fracture zones and joints (Nyegaard, 1985). Radioactive, thorium dominated joints and dykes were also found in the area. In the description of the occurrences, the area has been divided into 4 sub-areas - the Ingnerûlalik, Nunakutlak, Kangerdlua and Sitdlisit areas (fig. 6).

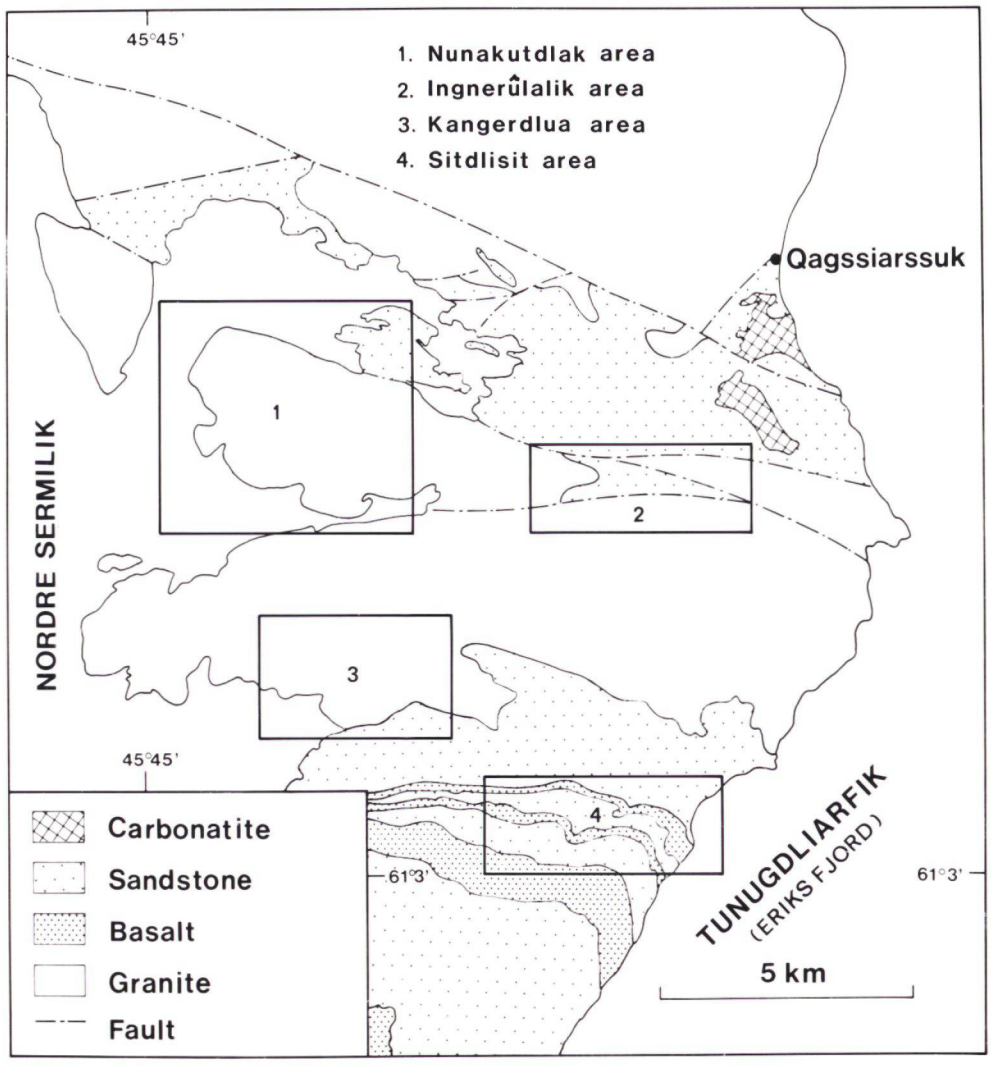

Fig. 6. Index map for description of U occurrences, the Qagssiarssuk area.

3.1.2.1 The Ingnerûlalik area

In the sandstone wedge, bordered by two major fault zones in the central part of the area (fig. 7), many scattered small pitchblende occurrences were found along an 5 m high fault-controlled E-W wall. These occurrences were traced for about 1 km in a 2-3 m wide zone adjacent to the fault. Pitchblende is found as cavity fillings up to 0.5 cm wide, but also as smears along tension joints striking 40-60°. The distance above the contact between granite and sandstone is roughly calculated to 50-100 m.

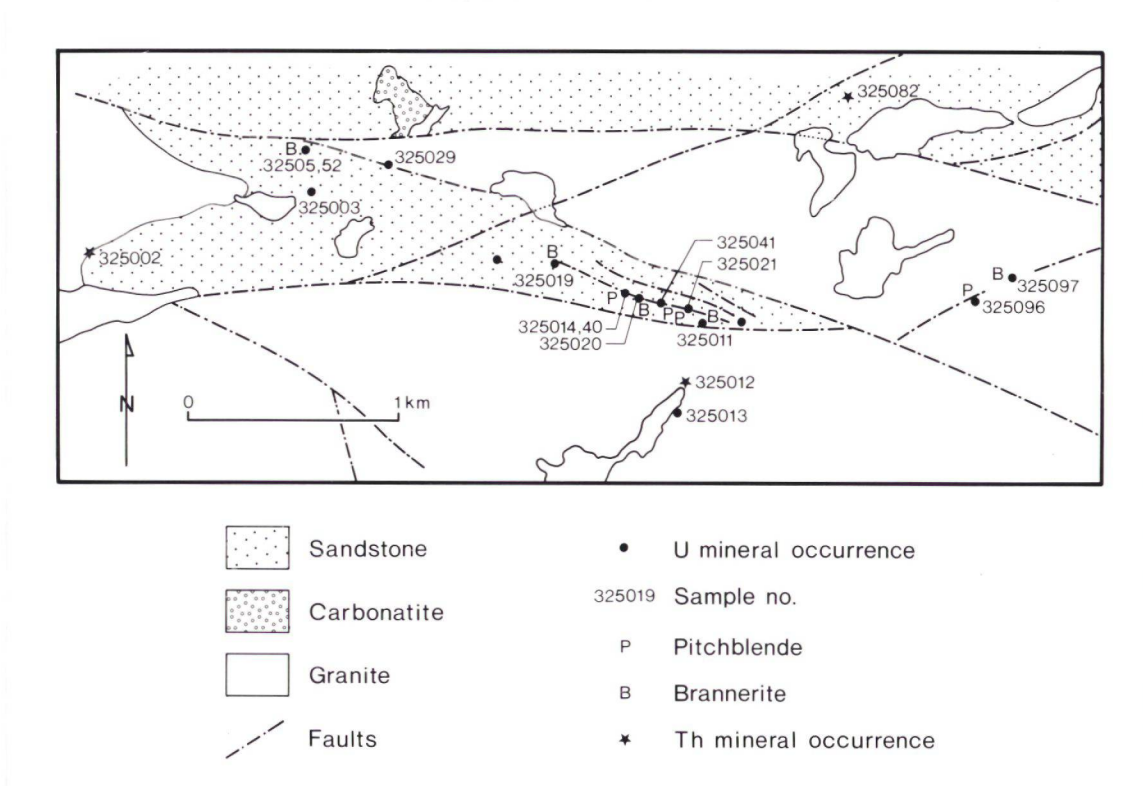

Fig. 7. Geological map with U and Th occurrences in the Ingnerûlalik area.

The sandstone is grey to light brown in the fault zone and brecciated. The rock is a rather pure quartz sandstone with very few feldspar grains. The quartz grains are rounded and overgrown with newly formed quartz, but the old grain boundaries can still be recognised. Layering associated with sorting of the quartz grains are noted in the samples. In the brecciated parts of the sandstone chlorite is present in the matrix, and the rock is cut by late quartz veins. In the mineralised parts of the brecciated sandstone yellow, secondary U minerals, pyrite and hematite are associated with the pitchblende.

The pyrite is altered to limonite, which is also seen as veinlets. The hematite of the specularite type occurs as thin laths overgrowing other minerals and also in quartz veins as cavity fillings with a spherulitic texture. Cryptocrystalline hematite is overgrown by a specularitic form.

Pitchblende is found in holes and as veinlets with yellow, secondary U-minerals rich in Pb, of which one is probably kasolite ($Pb(UO_2)(SiO_3)(OH)_2$), which is partly surrounded by later quartz (fig. 8). The other is a U-mineral rich in Fe, which is mainly seen as veinlets and replacements of pyrite. Microprobe data of the secondary U-minerals gave the following average results:

Sample no. 325041	UO_2	PbO	FeO	SiO_2	CaO
Kasolite -	43.870	34.483	0.177	9.826	n.d.
U-Fe mineral -	29.229	5.933	37.689	4.466	0.597

The uranium content in the rock samples is assayed by gamma-spectrometry at GGU and delayed neutron counting (DNC) at Risø. The DNC results are normally much lower than the gamma-spectrometry measurements indicating radiogenic disequilibrium in the pitchblende due to surface leaching of uranium:

Sample no.	Gamma-spec. ppm	DNC ppm
325011	374	37.7
325019	152	22.4
325020	811	19.8
325021	6038	126
325041	1766	1160

Microprobe data systematically measured over pitchblende grains show a rather large variation in the UO_2, PbO, SiO_2 and CaO contents (fig. 9 - Grain I,II). UO_2 seems to be positively correlated with CaO and negatively correlated with SiO_2. The calculated chemical ages (Delaloyle, 1979) vary considerably from 1003 to 1355 Ma (average 1168 Ma) in pitchblende grain I and from 615 to 1177 Ma (average 994 Ma) in grain II. Only the average for grain I is reasonably compared with isotopic ages from other localities (1184 Ma). The

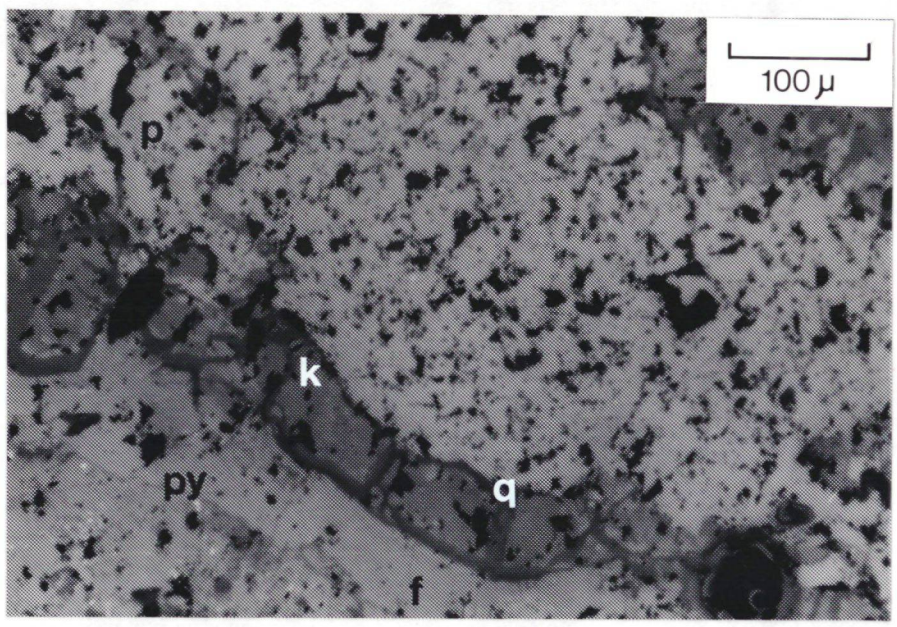

Fig. 8. Photomicrograph of pitchblende altered to kasolite (k) and a secondary U-Fe mineral (f). Kasolite is bordered on three sides by quartz (q). Pyrite (py) occurs in the matrix. Sample no. 325041.

average composition and chemical age of the pitchblende by microprobe analysis is:

Sample no.	UO_2	PbO	TiO_2	FeO	CaO	Ce_2O_3	SiO_2	Ma
325041	77.998	12.733	n.d.	0.068	3.689	0.071	0.671	1096

Other small radioactive localities with brannerite ($(U,Ca,Fe,Th)(Ti,Fe)_2O_6$) are found in the sandstone to the west. In the granite fault wedge to the east two localities, one with yellow, secondary U minerals, and one with brannerite, are found (fig. 7).

In the Ingnerûlalik area Th occurrences in sandstone are associated with heavy mineral layers 0.5 to 1.5 m above the granite/sandstone unconformity (fig. 7, 325002), and also associated with a brown, radioactive and brecciated dyke rich in pyrite. In the granite one radioactive locality with Th minerals in joints was found (fig. 7, 325012). Coatings with malachite and azurite are also observed in fault zones within this area.

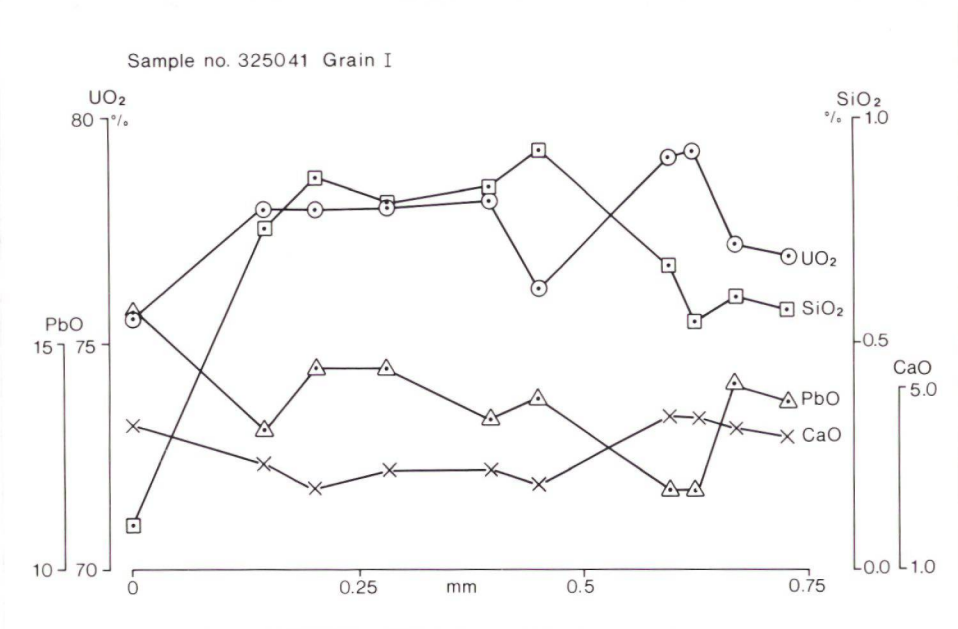

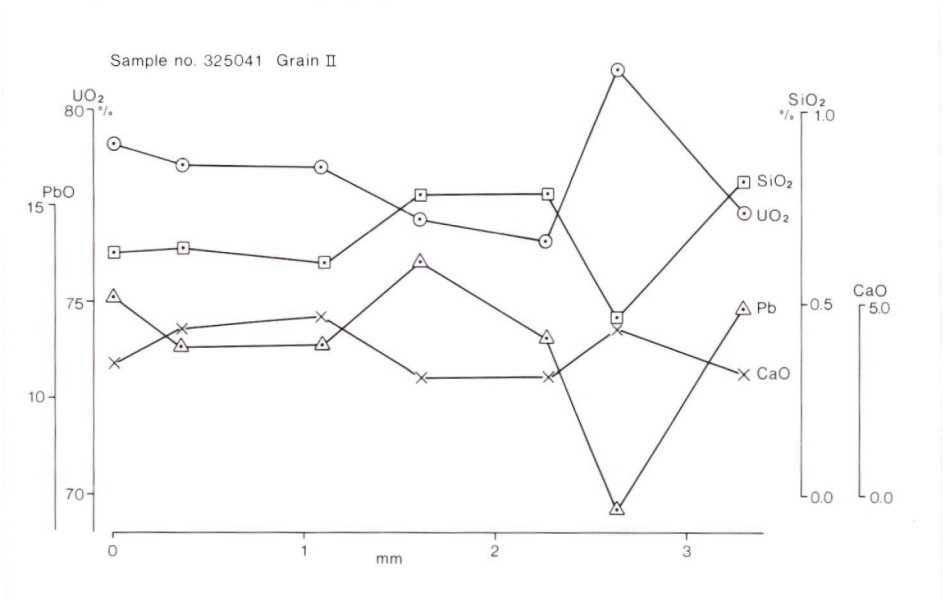

Fig. 9. Microprobe data over two pitchblende grains. Grain I: short axis, Grain II: long axix. UO_2, PbO, SiO_2 & CaO. data.

3.1.2.2 The Nunakutdlak area

In the granite area to the west (fig. 10), which is dissected by many faults and fractures, uranium mineral occurrences were found at several localities. One of these (fig. 10 - 325066) has two small pitchblende veins with secondary yellow U-minerals. The veins lie 'en echelon' 0.5 m apart and they can be traced 1.5-2 m striking 60^{o} with a width of up to 1-2 cm. The veins are situated approximately 0.5 m from the apophysis of a dolerite dyke. The granite is red altered in a zone of about 15-20 cm around the veins and secondary U minerals occur in thin cracks in the granite.

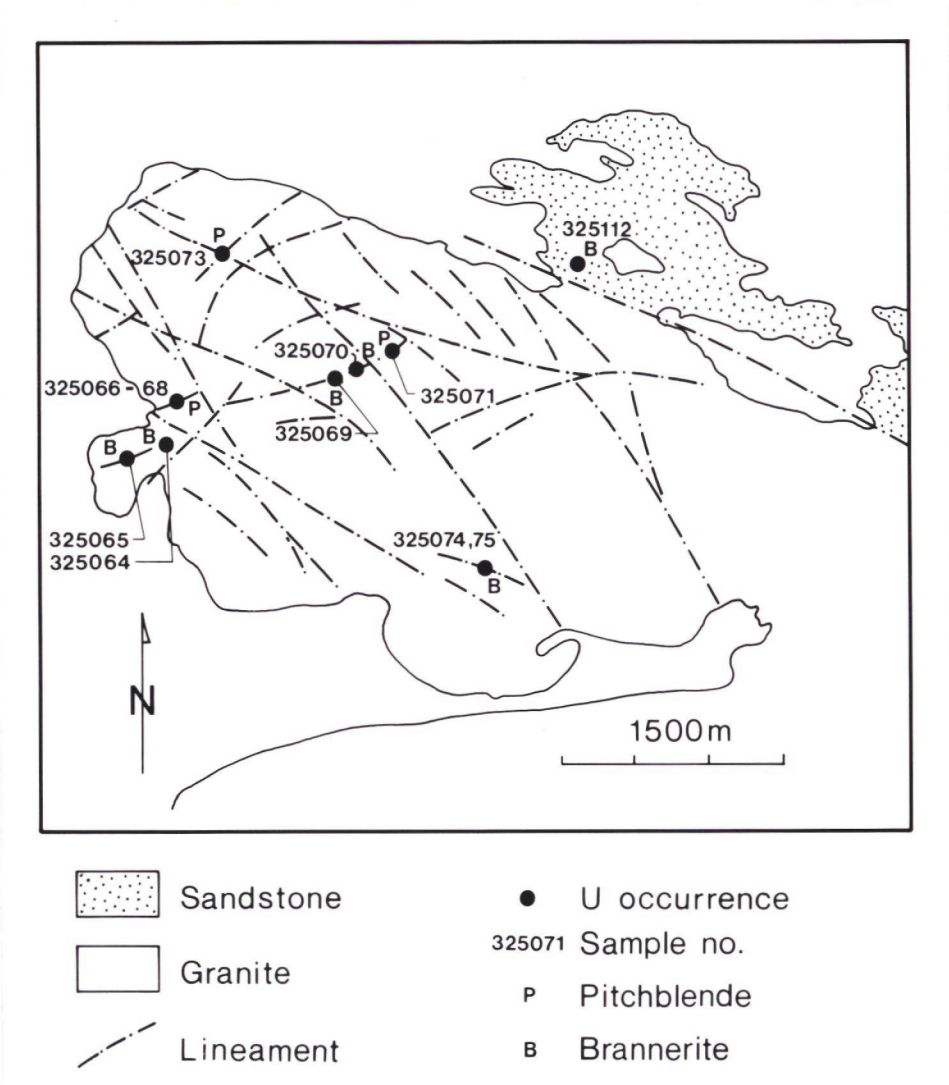

Fig. 10. Geological map with U occurrences in the Nunakutdlak area.

The granite is very altered and brecciated with quartz veinlets, and dolerite fragments are found in the brecciated wall rock. The pitchblende is botryoidal and replaced by a yellow secondary U mineral (probably kasolite) and chlorite. Brannerite is found in the wall rock replacing other Ti-minerals, mainly sphene (fig. 11). Associated with the uranium minerals are hematite and pyrite, the latter partly altered to limonite.

Microprobe analyses of the pitchblende (sample no. 305065) give a rather low UO_2 content and the chemical ages are high, varying fom 1404 to 1966 Ma. The chemical composition also differs from the pitchblende found in the sandstone wedge to the east, in being richer in PbO, FeO, TiO_2, SiO_2 and Ce_2O_3 and lower in UO_2 and CaO. Microprobe data gave the following average pitchblende composition:

Sample no.	UO_2	PbO	TiO_2	FeO	CaO	Ce_2O_3	SiO_2	Ma
325066	66.319	17.824	0.203	0.527	1.630	0.458	1.083	1679

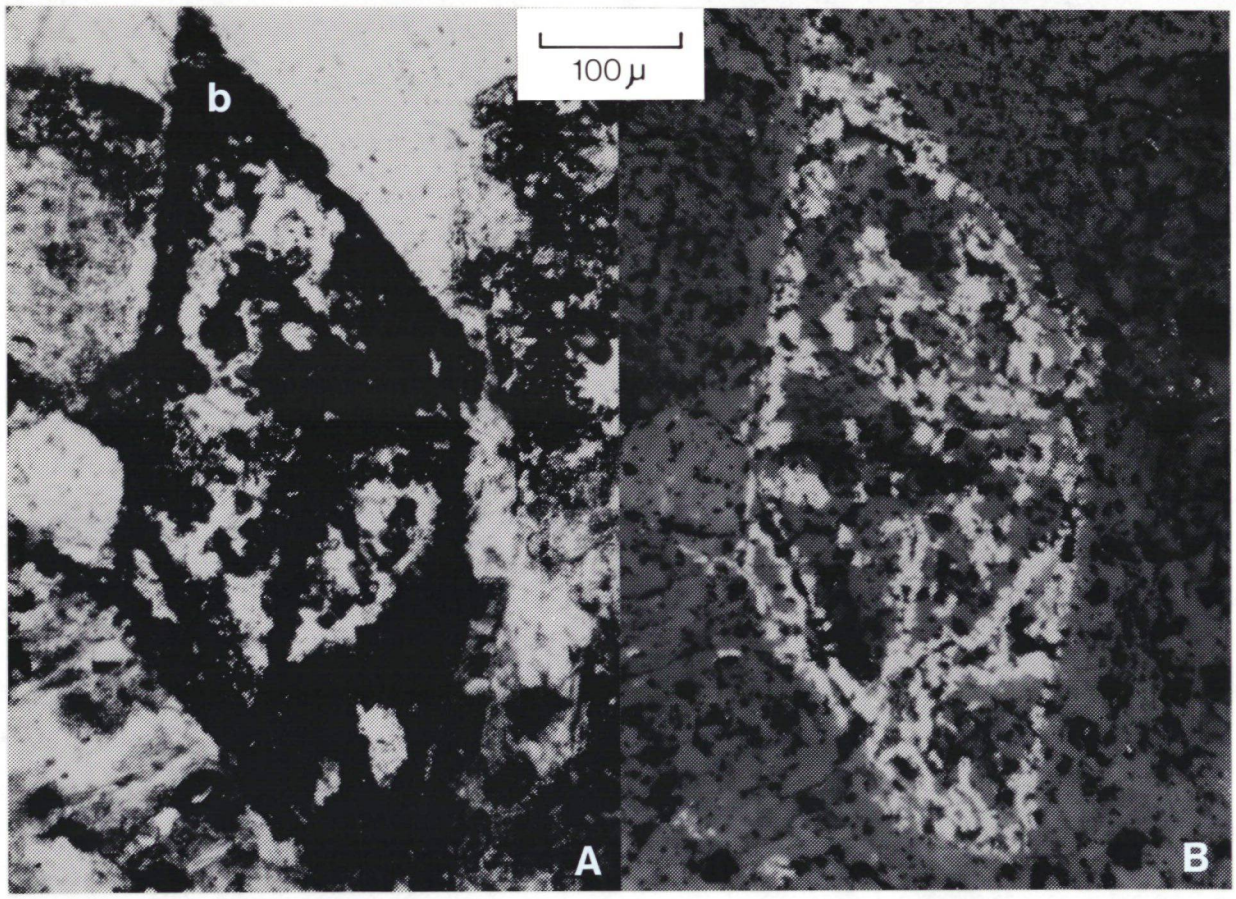

Fig. 11. Photomicrograph of brannerite (b) pseudomorph after sphene. A: transmitted light, B: reflected light. Sample no. 325068.

Approximately 300 m to the south of the pitchblende veins a small radioactive zone is traced 2-3 m along the contact between granite and a 10 m wide dolerite dyke with a 50° strike (fig. 10 - 325064). The granite is red altered in a 3 m wide zone and cut by few quartz veins. The dolerite is also fractured and cut by calcite veins. The U-mineral is brannerite associated with hematite.

To the west of this locality, about 300 m, a irregularly radioactive fracture is located in the granite (fig. 10 - 325065). The zone can be traced about 10 m trending 76°. The granite is altered to a brown colour surrounded by a violet/brown zone. The sample is rich in fluorine (1.04%). The granite is cut by veinlets of calcite, quartz and chlorite/quartz veinlets. The radioactive mineral is brannerite replacing other Ti-bearing minerals, and much hematite occurs.

The boggy area, which covers a great part of the terrain around these localities, has a distinctly high radioactivity level. The top layer of the bog is black organic material 10 cm thick. Then follows approximately 10 cm of brown clayish soil with 520 ppm U, which overlie at least 20 cm black organic soil with 1490 ppm U. Water samples from this area (Armour-Brown et al 1982)

gave very high U values which can not be explained by the now known uranium mineral occurrences.

Three radioactive localities were found about 1200-1500 m to the northwest of the pitchblende veins in the contact between granite and a 10-15 m wide dolerite dyke (fig. 10 - 325069,70,71). The granite is red, altered and brecciated with many calcite/fluorite veins. The radioactivity is only found as small spots of cm-size.

Samples of altered dolerite are rich in chlorite, brecciated and with both calcite-fluorite veinlets and a few quartz veinlets. Sphaerolitic pitchblende is found in one of the samples overgrowing chalcopyrite (fig. 12). The spherulitic pitchblende is confined to areas, which suggest a replacement of idiomorphic pyrite grains. Microprobe data show, that pitchblende has lost PbO resulting in too young chemical ages. The following data are the average composition and chemical age of the pitchblende:

Sample no.	UO_2	PbO	TiO_2	FeO	CaO	Ce_2O_3	SiO_2	Ma
325071	74.227	10.774	0.510	0.542	4.356	1.157	0.454	987

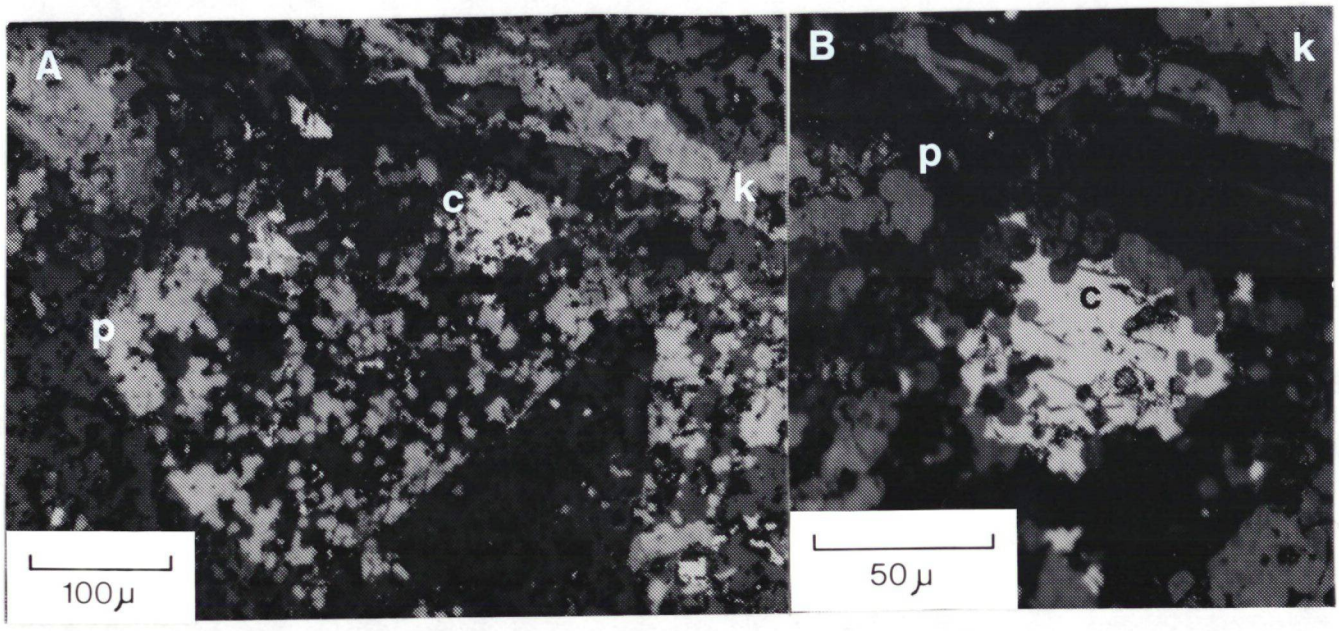

Fig. 12. Photomicrographs of sphaerolitic pitchblende (p) replacing chalcopyrite (c) with a vein of kasolite (k) The outline of the area with pitchblende indicate a replacement of pyrite. Sample no. 325071. B: Enlargement of area c of photomicropraph A.

The major radioactive minerals are yellow secondary U minerals seen as fracture fillings and also replacing chalcopyrite. The U minerals are kasolite and probably curite ($3PbO.8UO_3.5H_3O$). They are analysed by microprobe with the following averaged results:

Sample no. 325071	UO_2	PBO	FeO	SiO_2	Ce_2O_3
Kasolite:	45.098	34.567	0.338	9.215	n.d.
Curite? :	64.710	21.367	0.096	n.d.	0.055

Another uranium mineral is brannerite, which is seen as crystal skeletons intergrown with calcite and replacing titanomagnetite (fig. 13). Euhedral pyrite is disseminated in the samples associated with chalcopyrite and both minerals are altered to limonite and replaced by hematite. Galena and malachite are also observed.

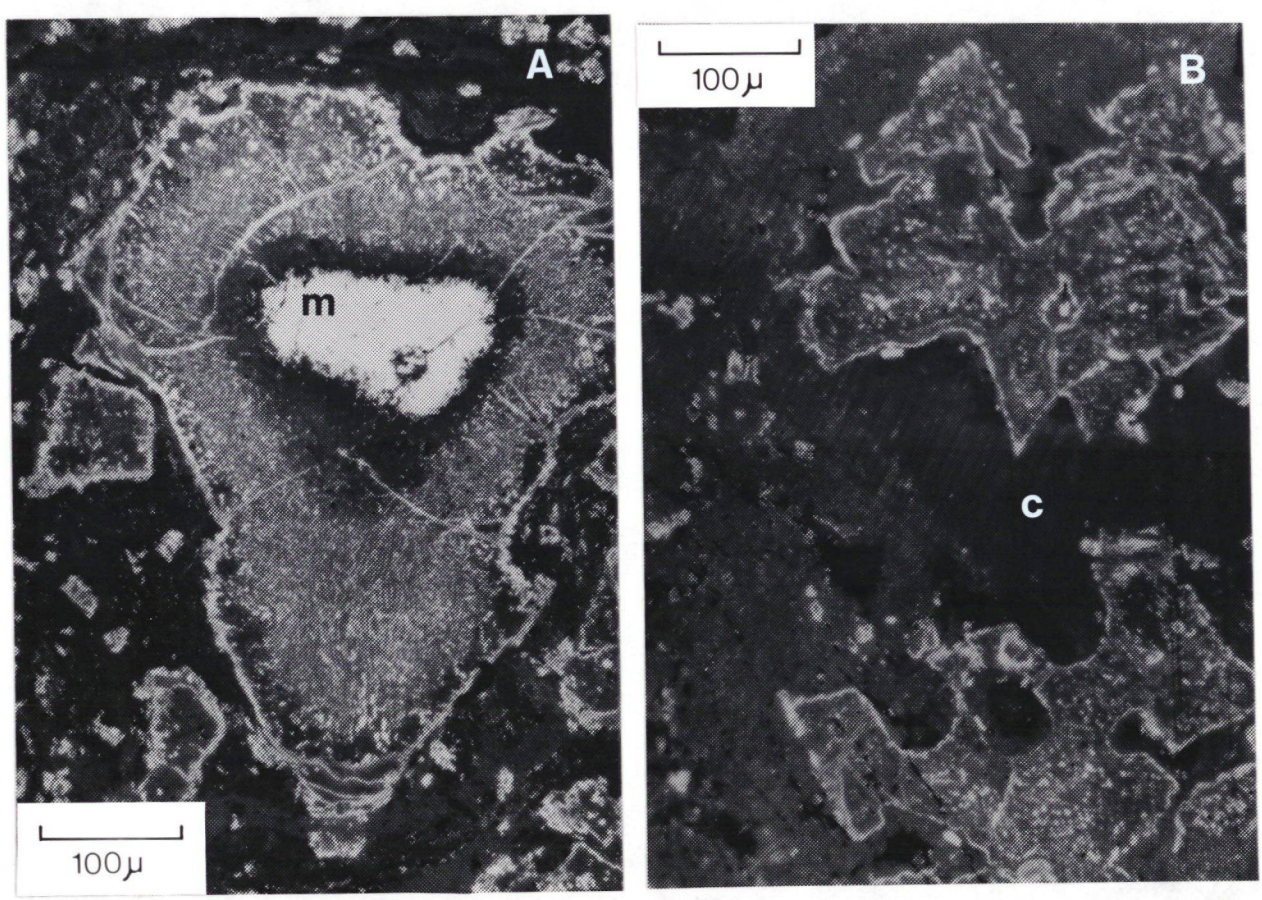

Fig. 13. Photomicrograph of skeleton brannerite (A) probably replacing titanomagnetite with remnant of magnetite (m) and (B) intergrowth with calcite (c). Sample no. 325069.

To the northwest (fig. 10 - 325073) a locality with pitchblende was found at the intersection of two lineaments. The 40° trend is a dolerite dyke and the 120° trend a fault/crush zone. The radioactivity can be traced about 2-3 m in the 120° direction. The granite is red, altered and with quartz/fluorite and calcite veins. Pitchblende and yellow secondary U-minerals are found as smears a few millimetres wide along cracks striking 20°.

The botryoidal pitchblende (fig. 14) is seen as fracture fillings often with a spherulitic texture. It has shrinkage cracks filled with hematite (fig. 15) and is altered to a secondary U-mineral probably kasolite, which seem to be partly replaced by hematite (fig. 16). The age relations in the pitchblende veinlets are:

1. Chlorite, 2. pitchblende, 3. quartz, 4. kasolite and 5. fluorite

Hematite is younger than pitchblende, but its age relationship to the other minerals is not known, except that it is late and may be younger than kasolite. At other localities the genetic sequence may differ. In the granitic wall rock brannerite is observed.

Microprobe analyses of the pitchblende show a depletion of PbO with chemical ages ranging from 770 to 1121 Ma. The FeO and Ce_2O_3 content are a little higher compared to the previously mentioned pitchblende analyses and SiO_2 is lower. The microprobe analyses show that the single sphaerolites of pitchblende have a fairly regular composition although they differ from grain to grain. The average composition and chemical age is:

Sample no.	UO_2	PbO	TiO_2	FeO	CaO	Ce_2O_3	SiO_2	Ma
325073	72.902	10.731	0.233	0.754	2.821	1.213	0.266	999

In the southeastern part of this area (fig. 10 - 325074) a locality with two radioactive spots approximately 30 m apart are located along a dyke trending 95° in the granite. The granite is strongly red/violet altered and brecciated with calcite veins. The radioactive samples are rich in calcite, fluorite and hematite, and the U-mineral identified is brannerite.

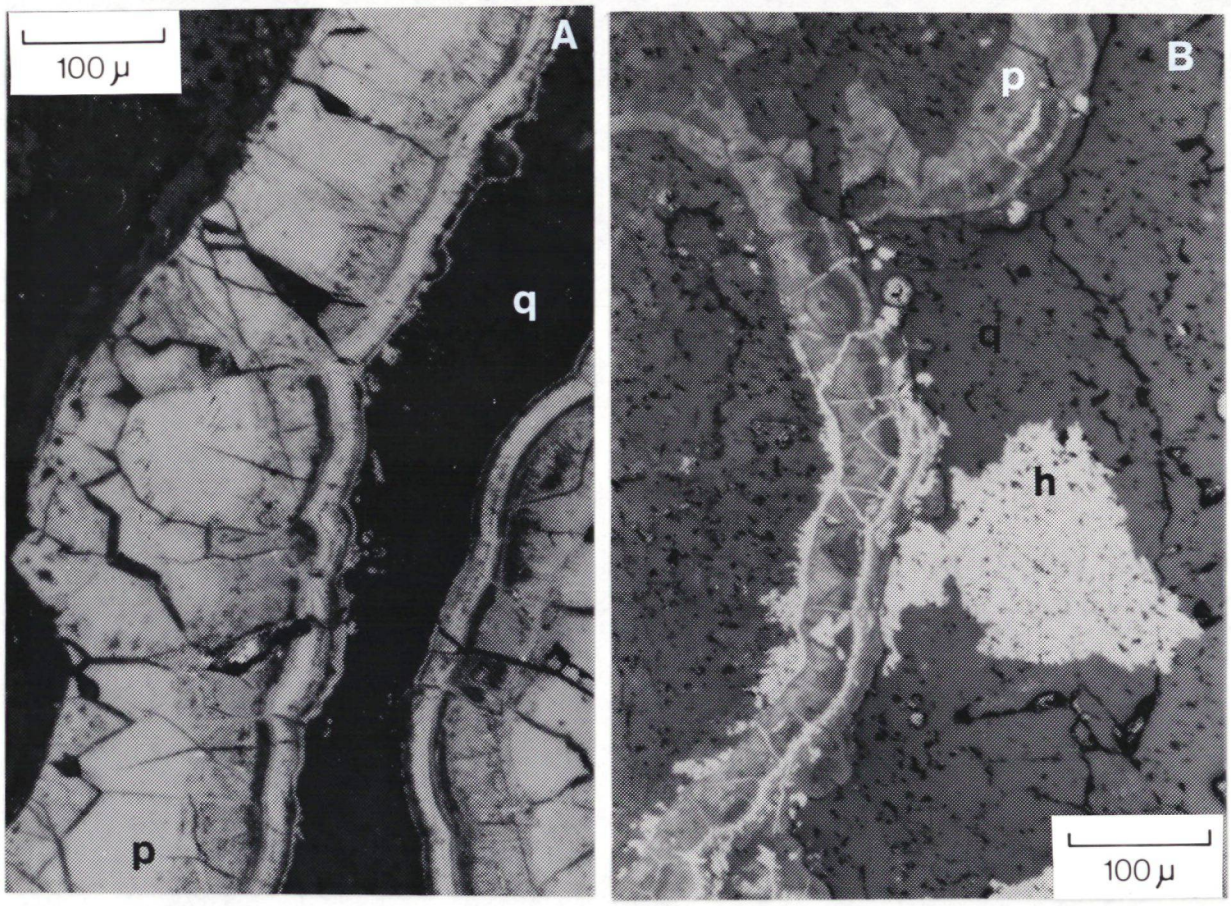

Fig. 14. Photomicrograph of A: botryoidal pitchblende (p) with quartz (q), B: botryoidal pitchblende vein with shrinkage cracks filled with hematite (h). Quartz (q) and hematite in the centre of the vein. Sample no. 325073.

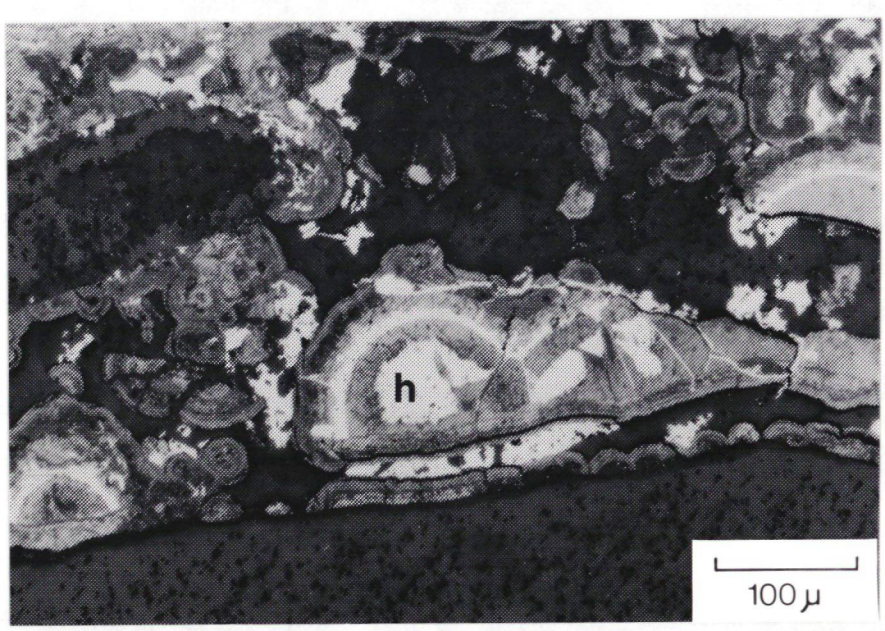

Fig. 15. Photomicrograph of botryodial pitchblende, partly with spherolitic texture, and completely replaced by secondary U minerals and later hematite (h). Sample no 325073.

To the north in this area (fig. 10 - 325112) a small radioactive locality is found in the sandstone close to a major E-W fault zone. The radioactivity was traced for 3 m along a 150/60-E joint with associated hematite. The U-mineral form a 1-2 mm fracture filling with associated chlorite. Microprobe analyses showed that the U-mineral is brannerite and that it is associated with a Ce-rich mineral, which is probably a REE-phosphate or carbonate with fluorine (see Appendix IV). One grain of Th-rich brannerite - absite - was also identified in the sample (see Appendix IV).

3.1.2.3 The Kangerdlua area

In the southwestern part of the area (fig. 16), in the granite and net-veined diorite, many small localities with uranium mineral occurrences were found along thin joints. The radioactive localities can be divided into two groups. One group seems to be associated with a poorly defined lineament striking approximately 120°. The other group lies to the northwest scattered within a small fault block and is not associated with a lineament. Otherwise the localities within the two groups are found in the same rock types and with the same type of U-minerals. All these radioactive localities lie in the granite, but must have been within 15-25 m below the granite/sandstone unconformity.

The mineralised rock types are granite/aplite and diorite, which in connection with U occurrences are red, altered and brecciated. The radioactivity is associated with thin joints with varying trends. The radioactive occurrences are U dominated with pitchblende or secondary yellow U-minerals. Th dominates over U only at one locality. Mostly the radioactive joints can only be traced for 0.5 m, but in some cases up to 3 m. They normally occur within limited areas of about 1.5x3 m, but at one locality the area is 50x10 m (fig. 16 - 325133,34) with a rather dense pattern of highly radioactive joints with pitchblende. This zone is bordered on the southeast by a dolerite dyke. Several of the rock specimens are more examples of wall rocks than the uraniferous fracture filling, which is more deeply eroded and can only be properly sampled by blasting.

The radioactivity is found to be caused by pitchblende, secondary yellow U-minerals and brannerite. Pitchblende occurs as fracture fillings associated with hematite and secondary U-minerals, or as scattered, massive grains (fig. 17) in the wall rock as cavity fillings associated with chlorite. Brannerite occurs as pseudomorphs after sphene (fig. 18), associated with altered titanomagnetite, intergrown with specular hematite replacing magnetite and as veinlets with calcite.

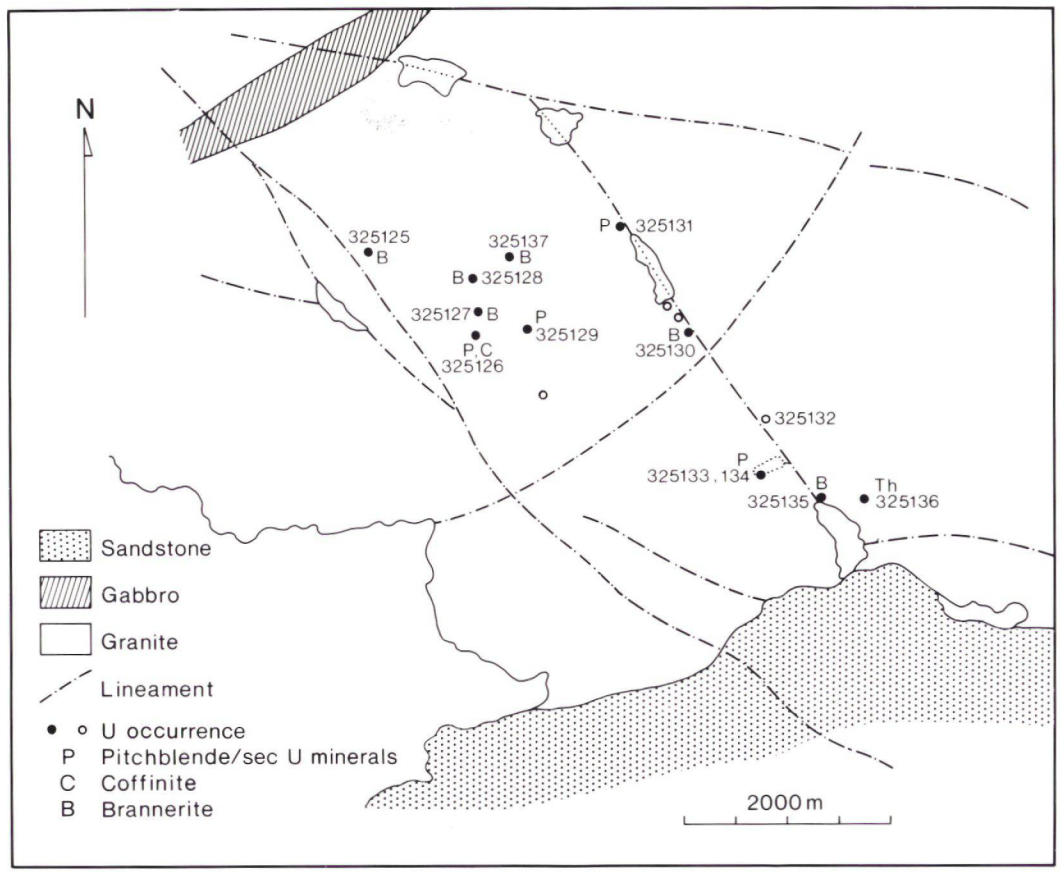

Fig. 16. Geological map with U occurrences in the Kangerdlua area.

Microprobe data from one of the pitchblende samples show both UO_2 and PbO loss with chemical ages varying from 760 to 1750 Ma, although the pitchblende is massive and only little altered. The average composition and chemical age is:

Sample no.	UO_2	PbO	TiO_2	FeO	CaO	Ce_2O_3	SiO_2	Ma
325133	63.235	11.991	0.426	0.505	2.822	1.026	3.825	1250

In sample 325131 the botryoidal pitchblende is completely replaced by a secondary U-mineral (fig. 19) with the following averaged composition:

	UO_2	PbO	CaO	FeO	SiO_2
Sec. U-mineral	39.553	25.711	4.267	2.041	3.459

A REE-rich mineral, probably bastnasite, was identified by microprobe (see Appendix IV).

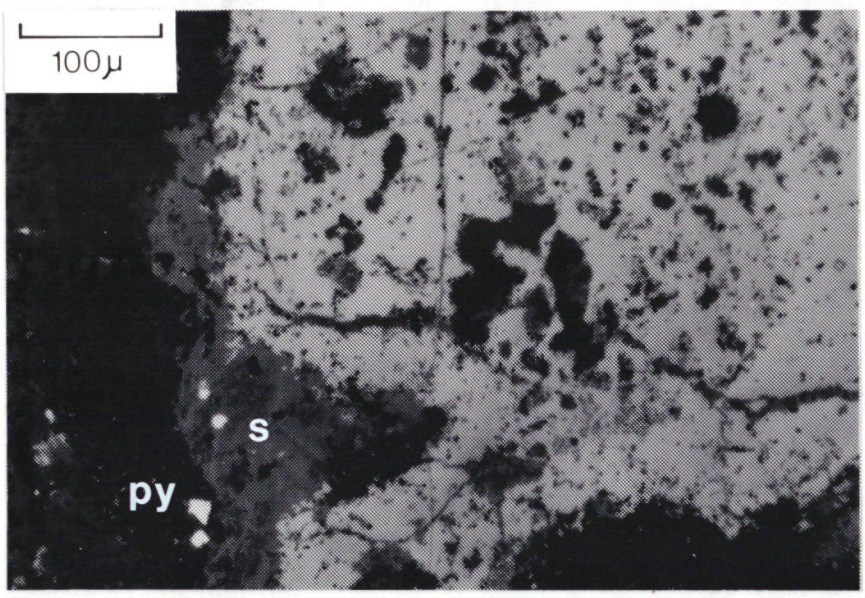

Fig. 17. Photomicrograph of massive pitchblende partly altered to secondary U minerals (s) associated with pyrite (py). Sample no. 325133.

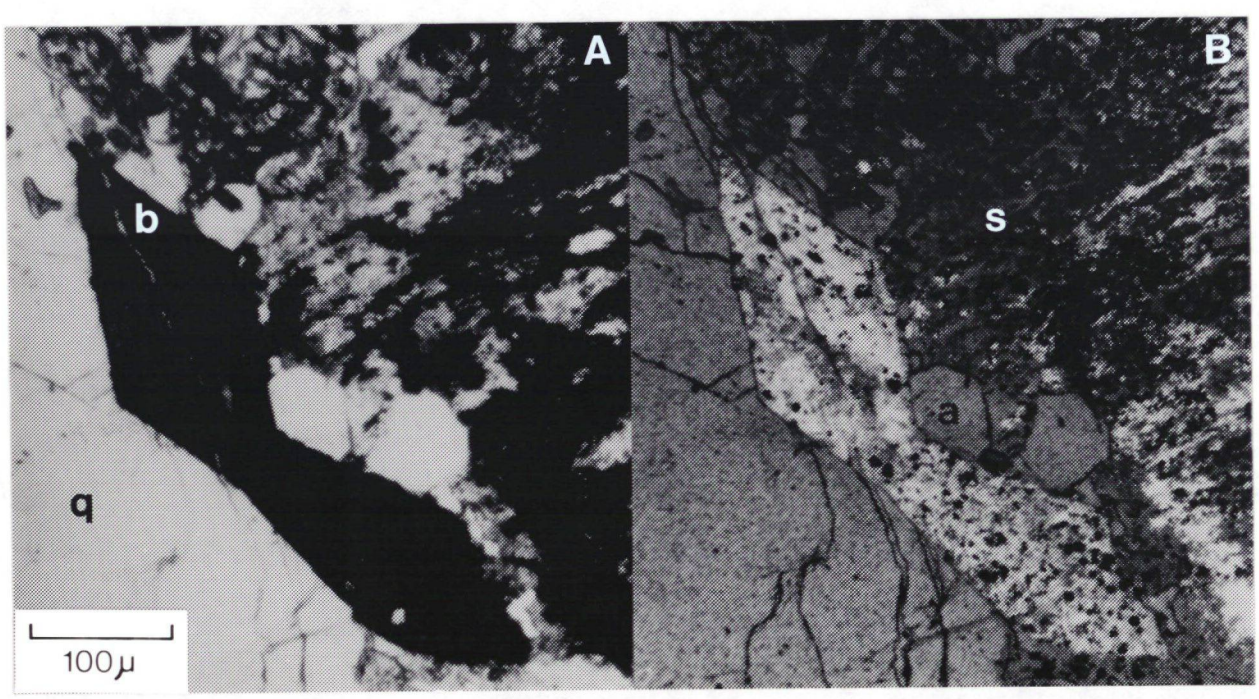

Fig. 18. Photomicrograph of brannerite pseudomorph after sphene in granitic wall rock. a - apatite, q - quartz, s - seritised plagioclase with hematite. A: transmitted light, B: reflected light. Sample no. 325137.

In sample 325126 the microprobe work results show three different uranium phases with the following compositions:

Phase	UO_2	PbO	FeO	CaO	SiO_2
A	61.094	1.496	1.624	6.337	14.331
B	61.943	6.236	2.841	11.912	1.142
C	43.558	23.843	1.926	0.732	10.624

Phase A could be coffinite ($U(SiO_4)_{1-x}(OH)_{4x}$), phase C kasolite and phase B is unknown (phosphate or carbonate?).

The U content in brannerite from the wall rock vary from 26.41 to 49.98 with the following average composition:

Sample no.	UO_2	PbO	TiO_2	FeO	CaO	Y_2O_3	Ce_2O_3	SiO_2
325126	47.950	1.112	36.593	3.364	4.983	0.801	0.335	n.d.
325133	40.883	2.295	33.953	3.109	3.018	0.765	0.894	3.388
325137	34.666	0.666	37.993	5.850	1.974	1.241	0.644	3.326

The brannerite is low in PbO, which has possibly been expelled from the mineral.

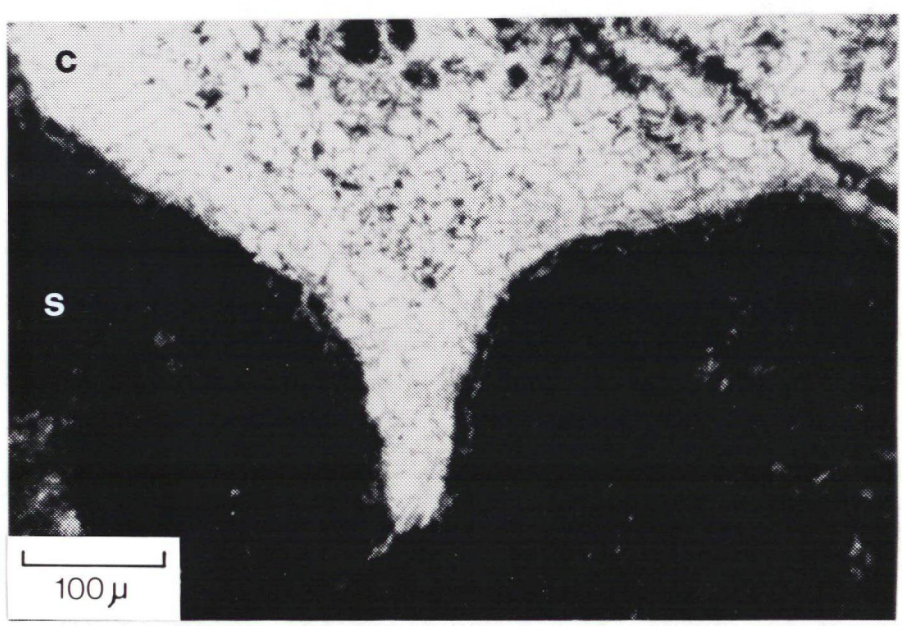

Fig. 19. Photomicrograph of secondary U mineral (s) in a chlorite (c) matrix. Transmitted light. Sample no. 325131.

3.1.2.4 The Sitdlisit area

In the southern part of the area (fig. 20), in the Eriksfjord Formation, several localities with uranium mineral occurrences were found in the sandstone just below a sandstone/basalt sill contact. Only the eastern half of this stratigraphic level was prospected. The localities are found at the same stratigraphical level over a length of 4 km (fig. 20). The distance down to the unconformity is roughly calculated to 250-300 m. The sandstone is strongly fractured with vertical joints mainly striking 40-60° and 130-150°. The radioactivity is normally rather weak (75-110 ur, background: 15 ur) and follow mostly the 40-60° tension joints. At the two sampled localities (fig. 20) the radioactivity reached 530 and 1700 ur. The radioactivity is normally traced 1-5 m along the joints within 5x10 m areas, and at one locality the radioactive joints were scattered within an area of 250x10 m with the long axis trending 70°.

The fresh rock type is a pure quartz sandstone with only few magnetite grains altered to martite. The brecciated rock has veinlets with chlorite and limonite and chlorite at the quartz boundaries. Pitchblende is found as small massive fracture fillings and also as pseudomorphs after pyrite (fig. 21) often altered to a secondary U mineral. The pseudomorphs are embedded in chlorite. Yellow, secondary U minerals are found in veinlets (fig. 22)

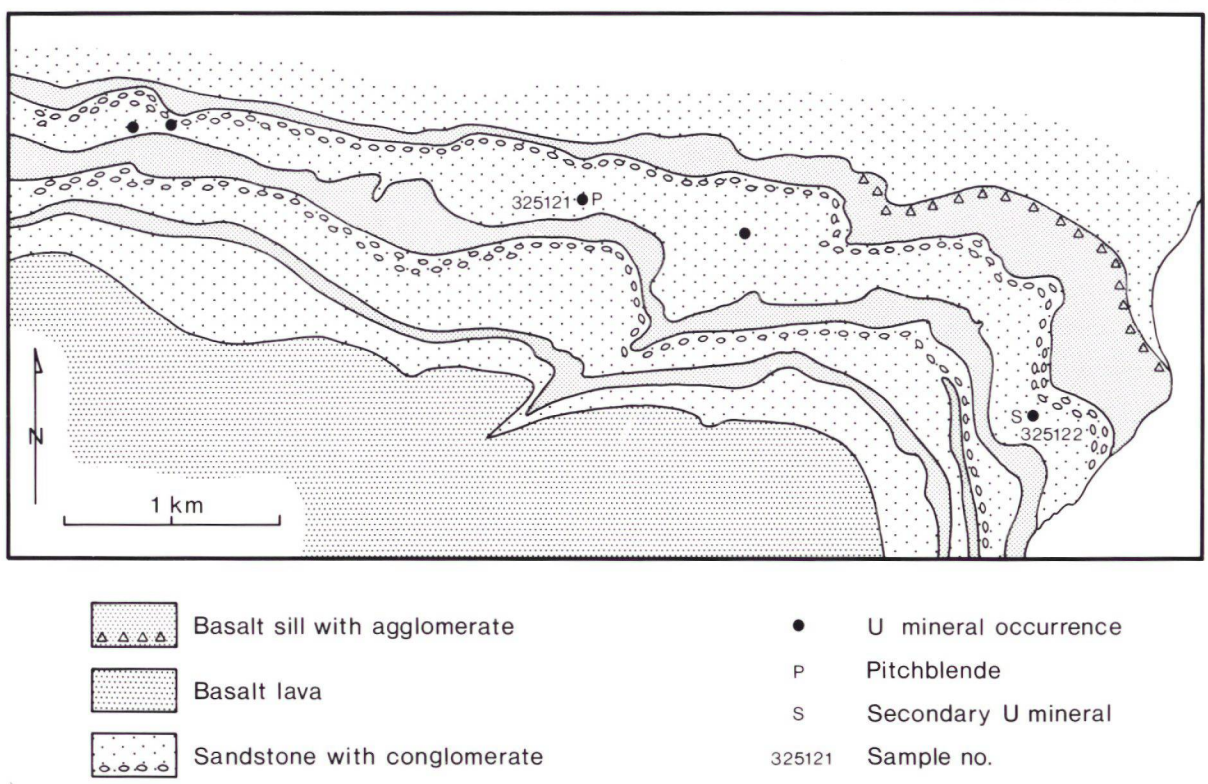

Fig. 20. Geological map with U occurrences in the Sidtlisit area.

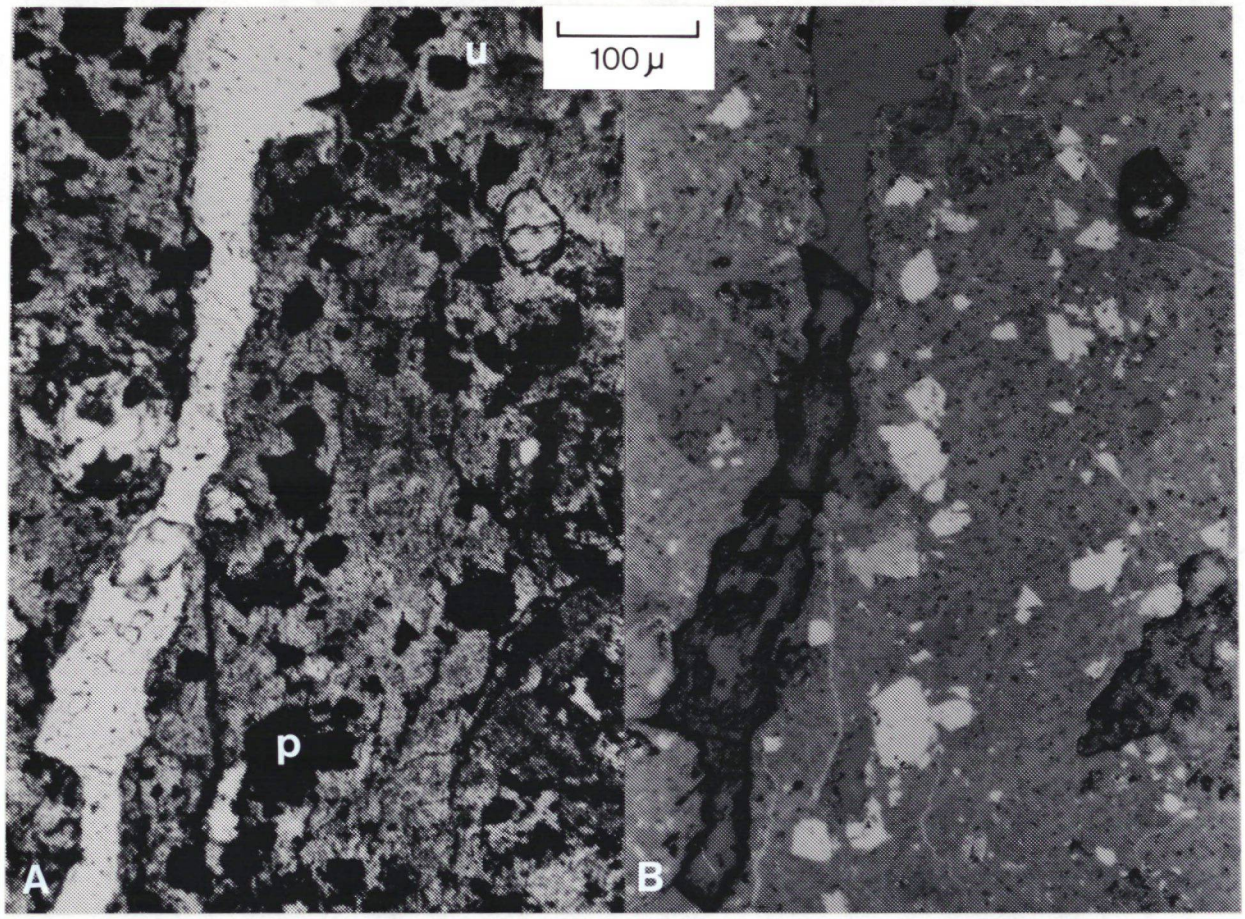

Fig. 21. Photomicrograph of pitchblende (p) pseudomorphs after pyrite in a chloritic ground mass. The pyrite is completely altered to U rich limonite (u). A: transmitted light, B: reflected light. Sample no. 325121.

associated with chlorite veins. These minerals are kasolite and a uranium rich limonite. Brannerite also occur as veinlets and as small idiomorphic grains.

Microprobe analyses of the pitchblende gave the following average composition and chemical age:

Sample no.	UO_2	PbO	FeO	CaO	Ce_2O_3	SiO_2	Ma
325121	78.439	13.469	0.246	1.693	0.050	0.208	1146

The pitchblende grains are homogeneous and gave reasonable chemical ages between 1124 and 1179 Ma.

Wulfenite with approximately 2% UO_2 was identified by microprobe, in addition to brannerite and kasolite:

Brannerite:

Sample no.	UO_2	PbO	TiO_2	FeO	CaO	SiO_2
325121	46.732	1.780	32.033	4.468	1.820	2.554
325122	47.588	1.021	35.151	4.183	3.066	1.840

Kasolite:

Sample no.	UO_2	PbO	FeO	CaO	SiO_2
325122	46.795	31.464	1.004	0.580	11.488

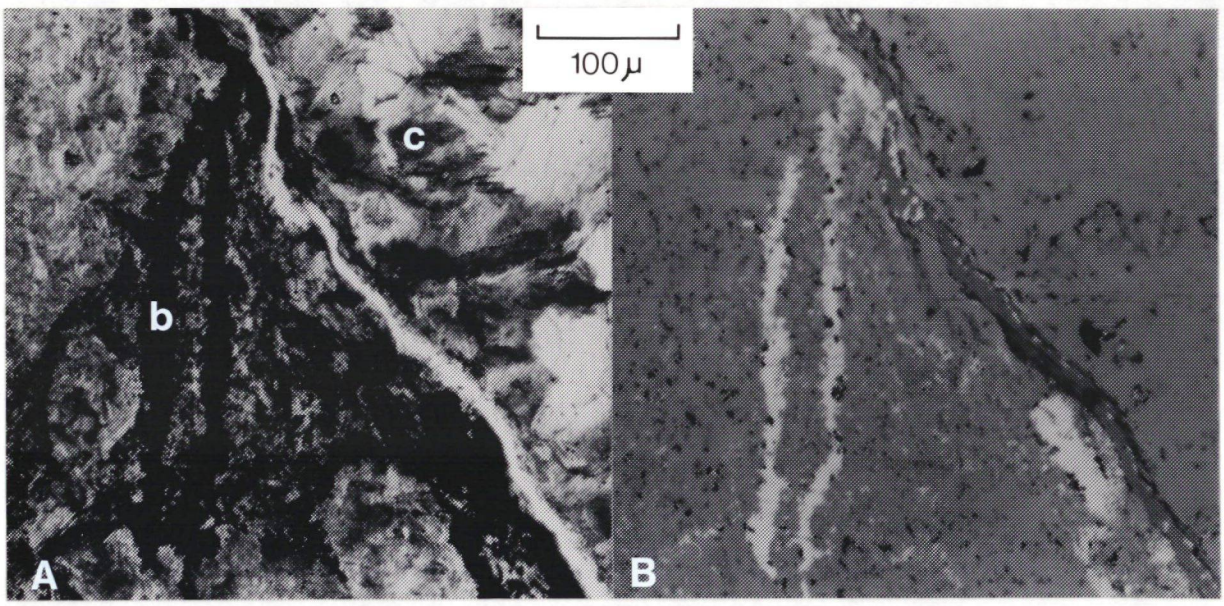

Fig. 22. Photomicrograph of brannerite veinlets (b) in chlorite (c) rich sandstone. A: transmitted light, B: reflected light. Sample no. 325121.

REE minerals, among which one is probably bastnasite, (see Appendix IV) were also detected by microprobe associated with these occurrences. The mineral contains about 20% Ce_2O_3.

Major element analyses of the sandstone (Appendix II, sample no. 325122) gave rather high Al, Fe, and Mg values which indicate the chlorite which has been observed along fractures and was possibly emplaced during the mineralisation process.

3.1.2.5 Other radioactive occurrences

In the north in the prospected area a small radioactive locality in a NW-SE major fault zone was found associated with a fluor-rich apatite (fig. 5). The radioactivity was traced about 5 m over a 0.5 to 1 m wide zone covered with soil and vegetation. The sample taken contained about 27% P_2O_5, 1.8 % Ba, 3% F and 500 ppm U (analytical results - Appendix II, sample no. 325104).

Thorium-dominated mineral occurrences were found both as small joint fillings and as radioactive dykes. The radioactive joints are located in the vicinity of the carbonatitic volcanics around Qagssiarssuk. The joints strike mainly 60^{o}, and the radioactivity can be traced 1.5 to 10 m. Carbonate and pyrite, sometimes with fluorite and hematite, are associated with these joints. The samples are also rich in Ba - 0.3-3.0 % and in RE elements (Appendix II - sample no. 325086, 325103) and a REE mineral was identified by microprobe in sample 325103 (Appendix IV).

Several types of radioactive dykes occur in the area, and they all trend about 60°. The width is 3-5 m and they can be traced for more than 10 km. The most common type is a weakly radioactive (55 ur - 35 ppm Th, 16 ppm U) red trachyte dyke. Three other types of more radioactive (400-500 ur) dykes are found. The most common of these is a brown, fine to medium grained dyke (265-595 ur - 565-1167 ppm Th, 6-242 ppm U). Another is a green, aegirine-rich, medium to coarse grained dyke, which may be found along the same trend as the brown dyke (380-550 ur - 347-743 ppm Th, 108-173 ppm U). In one case a green dyke with a brown center was found (1390 ur , 3108 ppm Th, 177 ppm U). The third type is a fine grained, dark brown microsyenite (440-775 ur - 432-893 ppm Th, 82-205 ppm U). At one locality close to a major fault zone this type contained disseminated pyrite. The dykes cut both carbonatite, sandstone and granite, which are strongly altered in an 1-2 m zone from the contact. The red sandstone is either bleached or green and the granite may be red or green with aegirine. The contacts of the green and brown dykes are sheared, and flow structures occur in the dyke. At one locality the bedding in the sandstone is in contact to the dyke. The dykes are often cut by quartz veins, and willemite (Zn_2SiO_4) was found in one of these veins.

The unconformity between the granite and the Eriksfjord Formation was prospected. It is normally very poorly exposed due to talus. At several localities weak radioactivity was associated with black layers of heavy minerals about 0.5-1 m above the contact. The individual layers are up to 5 cm thick and are concentrated in a 1 m section. The radioactivity is caused mainly by thorium (144-477 ppm Th, 8-27 ppm U). At one locality the basal conglomerate showed a weak elevation in radioactivity, which is also due to thorium (80-204 ppm Th, 7 ppm U).

3.1.3 Discussion and conclusions - the Qagssiarssuk area

The Qagssiarssuk area has proved to contain equally as many uranium mineral occurrences as elsewhere in the Granite Zone of South Greenland although they are still small in size. The ground scintillometric prospecting has proved successful and it is probably the cheapest and quickest method of prospecting in this area, and it can easily be combined with geochemical water sampling.

The field work resulted in findings of uranium mineral occurrences both in the basement of Ketilidian Julianehåb granite and in the Gardar sandstone of the Erikfjords Formation. The main uranium minerals are pitchblende and brannerite. They are found as veins and fracture fillings, smears, cavity fillings and brannerite, and also as pseudomorphs after sphene in the granite wall rock. The uranium mineral occurrences are found in the granite at some

distance below the unconformity between granite and sandstone as in the Nunakutdlak area and other previously prospected areas (Nyegaard et al., 1986). Occurrences are also found close to the unconformity and in the granite as in the Kangerdlua area, where the distance to the unconformity is calculated to be about 25 m below the unconformity , and most importantly in the sandstone from 50 to 250 m vertically above the unconformity.

The uranium vein type occurrences deep in the granite are mostly associated with major and minor fault zones, while the occurrences just below the unconformity are located in brecciated granite and diorite in association with poorly defined lineaments. In the sandstone some occurrences are associated with a major fault as in the Ingnerûlalik area, but in the sandstone to the southwest in the Sidtlisit area faults are not seen associated with the brecciated and sometimes mineralised sandstone. The brecciation may be due to faulting in the basement.

The above mentioned features show a strong resemblance to the uranium mineral deposits described from the Athabasca Basin in Canada (Hoeve & Sibbald, 1978 and Tremblay, 1978), and the Pine Creek Geosyncline in Australia (Ferguson & Goleby, 1980).

The pitchblende and brannerite occurrences in the Julianehåb granite from the Qagssiarssuk area (this report) and in the rest of the Granite Zone (Nyegaard et al., 1986) show the same geological setting as the well known pitchblende veins of the Beaverlodge area north of the Athabasca Lake in Canada (Koeppel, 1968). The mineral assemblages are here divided into two groups, a simple one with pitchblende, hematite and pyrite and a more complex one with Bi, Co, Ni, Au and Ag sulphides and arsenides (Trembley, 1958). This second complex assemblage is not present in the Granite Zone, where the paragenesis is simple with pitchblende, brannerite and rarely coffinite and associated hematite, pyrite and chalcopyrite. Brannerite is also reported from the Beaverlodge deposits (Ruzicka & Littlejohn, 1982). The main gangue minerals from Beaverlodge are hematite, calcite, quartz and chlorite. Calcite is the dominant gangue mineral, hematite is conspicuous and occurs locally as specularite (Tremblay, 1978). This corresponds well with the features found in the Granite Zone although here quartz and fluorite are the main gangue minerals associated with the pitchblende veins. Quartz and calcite veins and veinlets are very common in the Granite Zone also without any trace of uranium occurrences. The calcite veining is particularly well developed in dolerite dykes.

The wall rock alteration at Beaverlodge is reported as red colouration with hematite, dark green chloritisation, white carbonate replacement and formation of quartz and albite (Tremblay, 1978). Widespread epidotisation is also reported but not related to the uranium mineralisation. In the Granite Zone the same types of alteration are noted (Nyegaard et al., 1986) and a little epidote occurs in fracture zones but never in association with uranium minerals.

In the Beaverlodge area the pitchblende veins are mainly located at a specific stratigraphic level with metasediment, basaltic metatuff, gneiss and granite (Tremblay, 1978) with a preference for the basic rocks (Robinson, 1955). In the Granite Zone the basement geology is not so complex as in the Beaverlodge area, and the veins occur both in granite and associated with dolerite dykes. The chemical contrast between dyke and granite seems to have facilitated the precipitation of uranium minerals.

In the Beaverlodge area epigenetic mineralisation has given rise to deposits of simple mineralogy at 1780 +/- 20 Ma and a reworking with a complex mineralogy at 1110 +/-50 Ma, and it is during this latest event, that the unconformity type of uranium deposits of the Athabasca Basin originate (Hoeve et al., 1980). In the Granite Zone pitchblende in the veins has been dated at 1180 Ma (Armour-Brown et al., 1982) and this is the only event recorded in the pitchblende veins. From gneiss in the northern part of the zone uraninite occurrences are reported with an age of 1780 Ma (this report - next section), which is probably the source of the uranium in the hydrothermal fluids responsible for the formation of the Gardar veins.

In the Athabasca Basin unconformity related uranium deposits occur around the contact between sandstone and basement rocks as structurally controlled veins, breccia fillings and associated impregnations (Hoeve et al., 1980 and Ruhlmann, 1985). Mineralisation is known to extend along faults 200 m below the unconformity and at least 200 m above it into the Athabasca Formation (Hoeve et al., 1980). Such relations are also found in the Qagssiarssuk area, where uraniferous veins and joint (breccia) fillings occur from 25 m below the unconformity in the Julianehåb granite to about 300 m above in the sandstone of the Eriksfjord Formation. The occurrences found up till now are small, but they could probably be the expression of a halo surrounding more extensive occurrences associated with hidden faults below the Eriksfjord Formation.

The mineral assemblage in the Athabasca uranium deposits is complex with several uraniferous phases with different associated sulphide phases (Ruhlmann, 1985). The mineralogy is much more simple in the Qagssiarssuk area with a uraniferous phase of pitchblende and brannerite and an associated

pyrite and chalcopyrite phase. Specularite is commonly associated with the occurrences in both areas. The difference between the Athabasca deposits and the Qagssiarssuk occurrences are probably caused by the fact that in the Athabasca area the elements Bi, Co, Ni, Se, Au, Ag, Cu, Mo and Fe were present in the basement there but are missing possibly in South Greenland which is primarily a uranium province (Armour-Brown et al., 1983) with only few base metal occurrences (Harry & Oen Ing Soen, 1965; Ghisler, 1968 and Schönwandt, 1983).

The mineralisation process in the Athabasca Basin is associated with widespread chloritisation, sericitisation and tourmalinisation which envelope the ore bodies (Hoeve et al., 1980; Hoeve & Quirt, 19 5 and Mellinger et al., 1985). The same processes occurred in the Qagssiarssuk area with exception of the tourmalinisation. The primary mineralisation phase in the Athabasca area was associated with red hematite and pale green chlorite (Hoeve et al., 1980) which is also the case in the Eriksfjord Formation where major element analyses of mineralised sandstone gave relative high MgO results varying from 0.37 to 1.36 %. The sandstone is also rich in iron, which is mainly contained in hematite and chlorite. Hoeve & Quirt (1985) describe a plume-shaped shell of clay alteration halo around the unconformity uranium deposits at Athabasca and Wilde et al. (1985) describe the same phenomena from the Alligator River area in Australia. The uraniferous occurrences and the associated clay minerals in the Eriksfjord Formation could well be similar halos above unconformity type pitchblende mineral occurrences.

All the uranium mineral occurrences found in the prospected area are associated with joints and fractures, and they mostly follow the 60^{o} tension fracture direction. Many of the mineralised samples contain brannerite associated with pitchblende, and brannerite is found in the wall rock as veinlets and replacing other Ti-bearing minerals. Therefore, where only brannerite is identified in the rock specimens, pitchblende may occur at a deeper level, or uranium rich fluids have passed through the joints. The brannerite is usually low in Th (> 1%), except for one grain of the Th variety absite identified by microprobe. The Pb content in brannerite is low and very variable. Following other workers (Williams-Jones & Sawiuk, 1985), it can be concluded that the radiogenic Pb cannot be retained in the brannerite lattice. Coffinite was also identified at one locality. Associated with pitchblende and coffinite secondary uranium minerals occur. Most common is kasolite but also curite and several other unidentified secondary uranium minerals occur. REE minerals associated with the uranium minerals were found by microprobe work. Hematisation and chloritisation are associated with the radioactive

occurrences, but are also found without any trace of uranium minerals.

The paragenetic sequence described for a pitchblende vein with 1. Chlorite, 2. pitchblende, 3. quartz, 4. kasolite, 5. fluorite and 6.? hematite is only one of several in the Granite Zone. There are possibly many phases of uranium mineralisation considering that the Gardar period spanned about 300 Ma.

The chemical ages for pitchblende grains are very variable and largely unreliable although they give the right order of magnitude. Compared to the 1184 Ma age found earlier by isotopic analysis (Armour-Brown et al., 1984), some pitchblende appears to have lost U while others Pb.

Thorium mineral occurrences are found both in joints and as radioactive dykes. The joints seem to be associated spatially with the carbonatitic rock around Qagssiarssuk, whereas the radioactive dykes have been associated with the central complexes (Hansen, 1968).

The mineralogy and structural setting of the uranium mineral occurrences in the Qagssiarssuk area show many of the same features as described from the Athabasca Basin in Canada and the Pine Creek Geosyncline in Australia. In the Granite Zone the mineralogy is possibly simpler as the underlying rocks have another composition in trace elements, and it is easier to explain the source and the hydrothermal system responsible for the uraniferous veins in the Gardar province. The source of the uranium is probably the uraninite found in the Ketilidian metasediment in the southernmost part of the region (Armour-Brown & Wallin, 1985) and the uraninite in Ketilidian gneisses found in the northern part of the Granite Zone (this report). The hydrothermal system was probably set up during the intrusion of the alkaline complexes. The study of REE content in fluorite from the Granite Zone indicates strongly that the Early Gardar complex of Motzfeldt is the source of the major part of the fluids probably with a mixture of meteoroic water.

The two anomalous areas in the Eriksfjord sandstone are particularly interesting targets for future exploration because their characteristics suggest that they are haloes to unconformity type uranium occurrences similar to those found in the Athabasca in Canada and Pine Creek in Australia.

One locality in the Qagssiarssuk area is the Ingnerûlalik area where pitchblende and brannerite smears and cavity fillings with associated hematite and/or pyrite are scattered along a 1 km minor fault zone parallel to a major E-W faults. The unconformity is exposed approximately 2 km to the west and the vertical distance is roughly 50-100 m. The Sitdlisit area also is of interest, but geochemical and scintillometric prospecting must be carried out in the whole area within the Eriksfjord Formation as well as a geophysical survey to locate fault zones in the basement.

3.2 Uranium mineral occurrences on the nunatak north of Nordre Sermilik

3.2.1 The geology of the nunatak

The nunatak lies to the north of the fjord called Nordre Sermilik outlined as area B (fig. 5). The area was first explored in 1982 by Bjarne Wallin because of high gamma-spectrometer anomalies in the area (Armour-Brown et al., 1982). He found a number of uraniferous gneiss boulders in which the uranium bearing minerals appeared to be contemporaneous with the country rock rather than in cross-cutting Gardar veins. In addition he defined a radiometric U-anomaly, with a detailed gamma-spectrometer survey, which could have been a source for these boulders. It was felt that this anomaly was interesting firstly for its own sake and secondly because it was the first indication in the Granite Zone that there was uranium in the pre-Julianehåb granite supracrustal rocks which could have been a source of the uranium in the younger Gardar veins (Armour-Brown et al., 1983).

Field mapping and prospecting were carried out in the northern half of the nunatak during the last week of August and the first week of September 1984 by A.Armour-Brown and his assistant Hans Kristian Olesen. The mapping was done on 1:25 000 aerial photographs and on 1:10 000 scale map prepared by Olav Winding on the PG2 photogrammetric plotter at GGU from the high quality aerial photographs taken by the Geodetic Institute in 1980. Many geological features could also been seen on these photos, especially Gardar dykes and lineaments due to faults and fractures, and these were also mapped using the photogrammetric plotter. The field work was concentrated firstly on locating the source of the gamma-spectrometer anomaly and secondly on general prospecting and geological observations in the area as a whole.

The geology of the area is dominated by a medium grained biotite-hornblende granodiorite with diorite phases and late magmatic appinitic rocks (Allaart, 1983). It has been classified, on the 1:100 000 scale geological map, as Late Julianehåb Granite which is foliated in places (Allaart, 1983). In detail this is more complicated because there are numerous inclusions some of which resemble gneissic rafts, and others neosomes and aplitic dykes. The gneissic rafts are composed of white, leucocratic, quartzo-feldspathic sheets varying from 0.5-50 m in thickness and from 10-500 m in length. They are horizontal or dip gently to the NW or SE. They tend to be stacked in sheafs separated by the intruding granodiorite. There is a general impression gathered from the field observations, that the pink-reddish inclusions are

neosomes. They are semiconcordant with the white gneiss and, therefore difficult to differentiate from them, but in some places they cross-cut them at low angle. There are in addition much younger white aplite veins and dykes, which crosscut both these rock types and the granodiorite. They are presumably related to late magmatic events. Major element analysis tends to confirm these observations (Table 2). The white paleosome (325330) contains 89% SiO_2 and only 5% Al_2O_3 and approximately 4% ($CaO+Na_2O+K_2O$ - Table 2, 325309), whereas the red neosome contains 11% Al_2O_3 and 10% $CaO+Na_2O+K_2O$ at the expense of SiO_2 (Table 2, 325308). The same trends are seen in the 2 aplite samples (Table 2, 325308). The area is cut by numerous Gardar dykes. These are mostly wide (20-50 m), steeply dipping or vertical dolerite dykes striking ENE-WSW but there are alxso red and grey microsyenite dykes often radioactive. These tend to be narrower (1-10 m) and strike more commonly on a NNW bearing and have a vertical dip.

A possibly important geological observation was the finding of a large boulder of conglomerate (see fig. 24 for location). This was unmetamorphosed but well cemented polymictic conglomerate made up mostly of sub-rounded cobbles of foliated biotite granite, grey quartzite, black amphibolite and angular fragments of grey fine grained sandstone with fine bedding features (fig. 23). The matrix is a fine to coarse grained, well indurated, greenish-grey pebbly-sand. There is no outcropping conglomerate in the vicinity so this must be a glacial erratic which has travelled from the north,

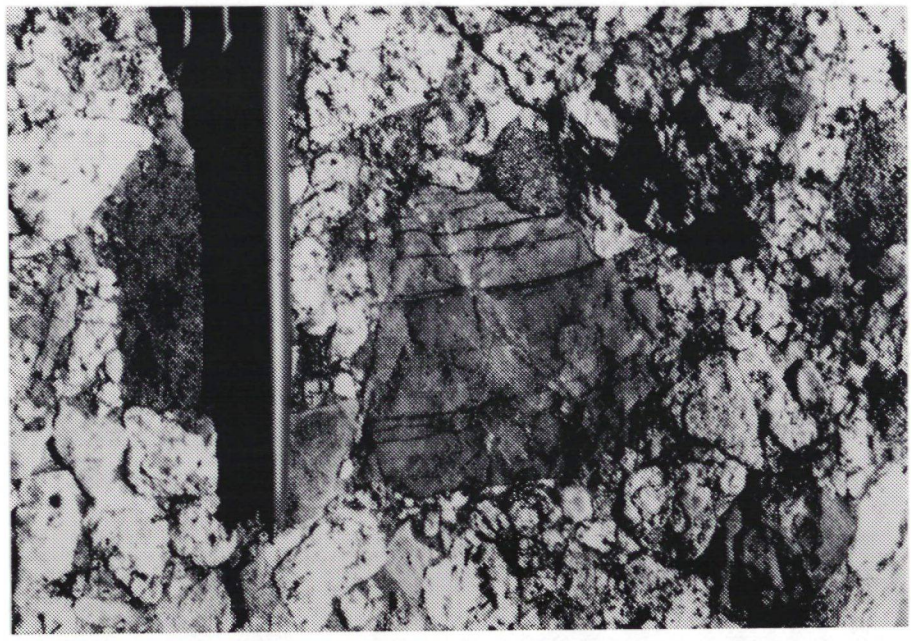

Fig. 23. Photograph of erratic conglomerate boulder

because all the glacial striae in the area indicate that that was the direction of ice movement. It is presumably derived from a unit comparable in age to the Eriksfjord Formation. If this is the case then the northern limit of the Gardar sedimentary environment extends much further north than previously known.

3.2.2 Radioactive mineral occurrences in Ketilidian gneiss

The radioactive elements are enriched to various degrees and have differing U/Th ratios in these gneissic rafts. The gamma-spectrometer anomaly found in 1982 (Armour-Brown et al. 1983) occurs on the summit slopes of the peak north of the lake (Sø 975) (Fig. 24 & 25). This area is dominated by these gneiss

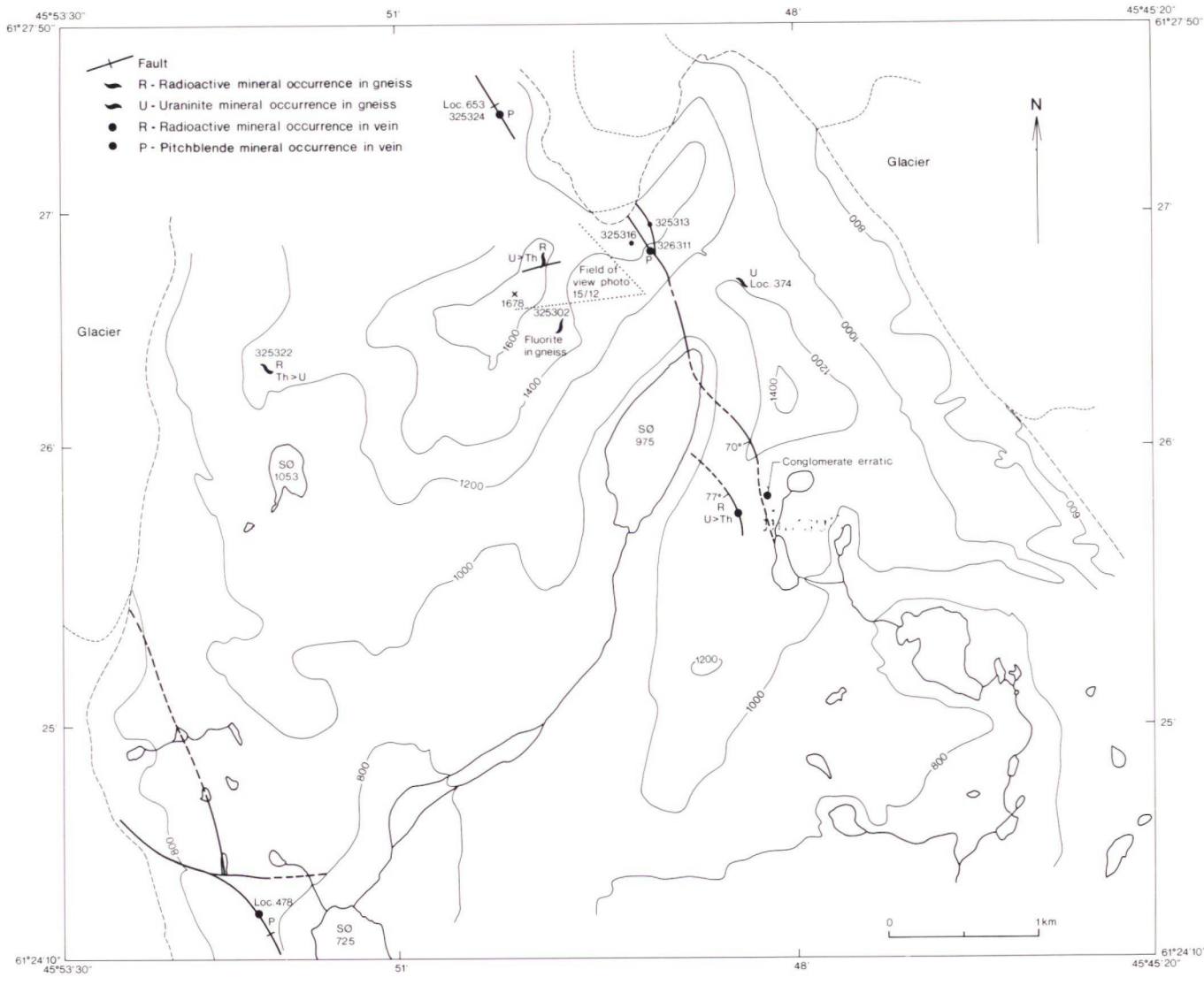

Fig. 24. Index map of observation and sample locations on the nunatak north of Nordre Sermilik.

rafts some of which are highly radioactive with 70 - 700 ur, which is 7 - 35 times background. They contain variable amounts of radioactive elements with large variation in U/Th ratios (Table 1). In general the white gneiss appears to be more uraniferous relative to thorium and the red gneiss and the aplite are thorium dominated.

A particularly large area of red and white gneiss outcrops on the summit of the mountain where the gamma-spectrometer anomaly was found. Because it covers a relatively large area and contains up to a few hundred ppm U and Th (Table 1, sample 325392) it is quite enough to account for 20 - 40 ppm U found in the radiometric anomaly mentioned earlier. The southern slopes of the summit are a dip slope for this radioactive white gneiss and the whole area tends to have a higher radioactive background than the granite and contains radioactive enclaves. Near one of these enclaves a small fluorite occurrence was found (fig. 26, sample 325302). The fluorite is concentrated in small sigmoidal veinlets and were presumably crystallised from late stage volatiles in the gneiss. Although this fluoritic gneiss is not radioactive itself, adjacent outcrops are (325301 contains 630 ur). This proximity suggests that the radioactive elements may have a genetic relationship to the fluorite.

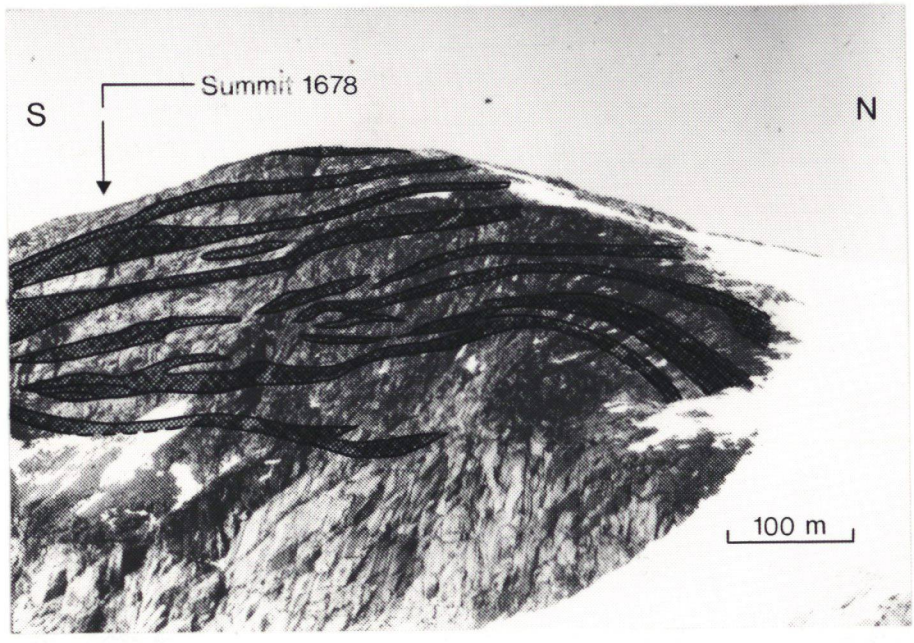

Fig. 25. Oblique photograph illustrating radioactive gneissic sheets (stippled bands) in granite on the summit 1678 of the nunatak. See fig. 24 for field of view.

Table 1. Trace element analyses for rock samples from the nunatak in ppm except for K, Ca, Ti & Fe which are in % by weight

rock type	white gneiss			red gneiss		biotite aplite	magnetite rich aplite
Sample no.	325292	325295	325300	325294	325299	325316	325322
U	430	893	126	29	22	65	191
eU	406	-	103	21	17	43	142
eTH	63	-	646	69	74	263	688
U/eTh	6.82	-	0.20	0.42	0.30	0.25	0.28
eK %	4	-	2	5	2	5	2
Ca %	1	3	1	0	0	1	2
Ti %	0	0	0	0	0	1	1
V	0	0	0	1	0	176	89
Mn	483	642	363	119	115	1370	1252
Fe %	2	1	2	1	1	8	7
Ni	6	0	17	0	0	0	2
Cu	3	0	16	15	0	33	45
Zn	2019	42	80	49	32	197	193
Ga	35	17	41	12	13	33	29
Rb	369	25	167	300	196	382	176
Sr	126	139	127	56	16	137	205
Y	126	149	511	62	73	83	256
Zr	616	396	1037	515	294	1631	1342
Nb	55	72	282	65	67	76	89
Pb	140	303	65	27	40	35	91

rock type	Radioactive microsyenite red	Gardar dykes red	Gardar dykes grey	Gardar radioactive fracture
Sample no.	325298	325320	325321	325317
U	34	38	22	291
eU	23	28	19	212
eTH	50	65	62	24
U/eTh	0.68	0.58	0.35	12.13
eK %	4	3	3	0
Ca %	0	1	1	4
Ti %	0	0	0	0
V	0	0	0	60
Mn	409	910	950	404
Fe %	2	2	2	3
Ni	0	0	0	0
Cu	13	8	11	0
Zn	169	234	263	33
Ga	44	49	48	11
Rb	520	487	482	20
Sr	67	220	36	98
Y	204	163	157	37
Zr	2004	2021	1824	470
Nb	248	262	216	16
Pb	17	19	70	10

N.B.
U analyses were made by Delayed Neutron Counting with a precision of better than +/-2%.
eU, eTh, eK were made by gamma-spectrometry with a precision of +/-3%
The rest of the elements were measured by Energy Dispersive X-ray analysis and are semi-quantitative.
All analyses were done at the Electronics Department of the Risø National laboratory.
eK, Ca, Ti and Fe: %

Table 2. Major element analyses of rock samples from the nunatak

Rock type	Red gneiss	White gneiss	Magnetite rich aplite	White sulphide rich aplite	Biotite aplite	Biotite grano-diorite
Sample no.	325308	325309	325322	325313	325316	325310
SiO_2	76.80	89.01	61.84	70.30	59.66	61.36
Al_2O_3	11.89	5.06	10.33	11.67	17.07	17.26
Fe_2O_3	1.01	0.02	11.40	0.70	2.88	2.70
FeO	0.59	1.31	5.60	1.57	1.00	2.66
MgO	0.34	0.10	0.40	0.28	0.81	1.91
CaO	0.21	1.61	1.71	0.23	0.46	3.67
Na_2O	3.00	2.12	4.09	1.44	6.22	4.66
K_2O	7.13	0.23	2.59	7.19	6.67	4.59
TiO_2	0.05	0.06	1.72	0.16	0.39	0.68
MnO	0.01	0.01	0.17	0.01	0.06	0.09
P_2O_5	0.02	0.00	0.10	0.02	0.11	0.30
SUM	101.05	99.53	99.95	93.57	94.33	99.88

Major elements in %

Sample no.	325308	325309	325322	325313	325316	325310
V	5	6	126	4	not	71
Cr	24	59	0	20		54
Ni	0	0	3	0	analysed	7
Cu	0	9	0	0		9
Zn	14	11	241	22		79
Ga	18	8	27	19		23
Rb	158	8	125	201		133
Sr	86	90	178	149		673
Y	12	3	70	14		28
Zr	620	445	1330	321		382
Nb	11	5	16	24		24
Ba	86	31	261	126		2181
La	8	20	1835	27		46
Ce	10	21	1658	25		60
Nd	0	0	913	1		44
Pb	75	15	174	61		23
Th	29	18	898	22		7
U	48	23	233	12		17
U/Th	1.66	1.28	0.26	0.55		2.43

Minor elements in ppm

N.B. Analyses were made by XRF at Durham University in 1985. Major elements were made on fused discs with a lithium tetraborate flux.

The most important finding in this area was the uranium occurrence in white gneiss at locality 374 (fig. 24). This is a 0.5 - 1 m thick raft of white gneiss with up to 1.3 % eU and relatively low levels of thorium (Table 2 & 3). A sketch map and section (fig. 26) illustrates the size and geology of this occurrence. The uranium minerals are concentrated in two small zones of a few square metres but the whole gneissic raft has a distinctively higher radioactivity than the surrounding biotite granodiorite. The gneiss is made up of a white, granular, medium-grained (50 - 200 micron) microcline, plagioclase and quartz (sample 325309) and a reddish aplitic gneiss (sample 325308). The uranium minerals are distributed along the poorly developed gneissic banding. Uranium is mostly in uraninite with minor yellow secondary phases. The uraninite is fine-grained (20 - 100 micron) and occurs as inclusions, for example in biotite (fig. 27) or as aggregates of fine minerals (fig. 28) associated with microcline and pyrite. The secondary U-mineral occurs as yellow or orange borders around the uraninite or as fracture fillings. They have not been identified with certainty, but microprobe analyses show that they contain appreciable lead in addition to uranium and SiO_2 (Table 4) and are probably kasolite and/or U-Pb silicates.

Table 3. U and Th contents of uraniferous gneiss and a Gardar vein

rock type	uraniferous white gneiss with uraninite		uraniferous Gardar fractures with pitchblende	
Sample no.	325306	325307	325312	325318
	ppm		ppm	
eU	13355	9911	11590	16386
eTh	600	90	0	19
eU/eTh	22	110		862

N.B. Analysed by gamma-spectrometer at GGU with a precision of +/-5%.

Both microscope and microprobe observations indicate that the uraninite is usually inhomogeneous (fig. 29), although the uraninite in biotite is not so altered (fig. 30). Isotope analyses, described below, indicated a high lead loss, which is also indicated by the much lower chemical ages than the lead isotopic ages.

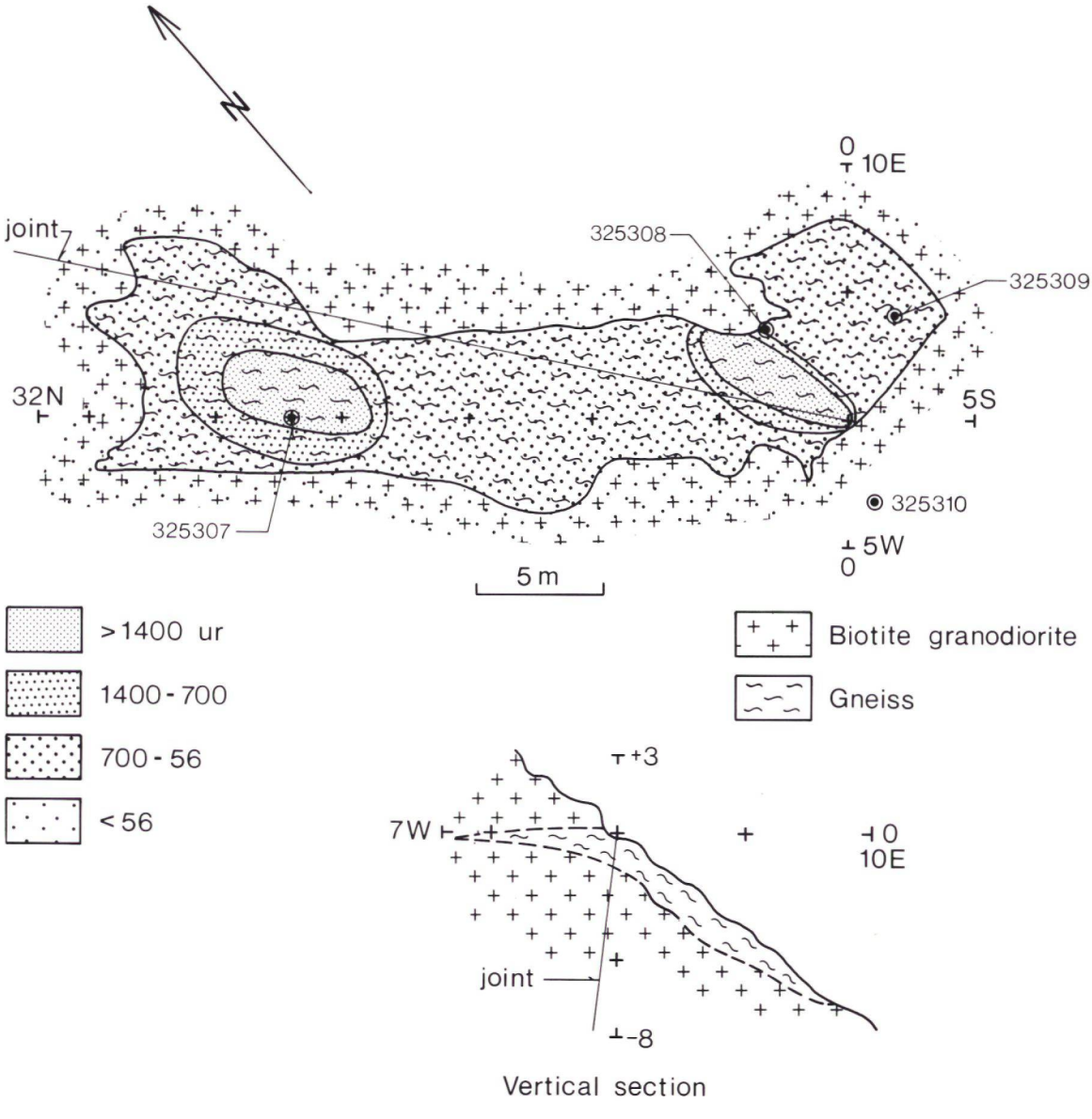

Fig. 26. Geology, radiometry and vertical section of locality 374 on the nunatak

Table 4. Microprobe analysis of uranium minerals from two samples from the nunatak. Analyses were by crystal spectrometer. U analysed with a precision of better than +/-1% and Pb +/-3%. Numbers are averages of 1-4 measurements (n).

Sample no.	Gno	UO_2	PbO	ThO_2	FeO	CaO	Ce_2O_3	Y_2O_3	SiO_2	sum	n
SU-8326		88.528	7.665	0.036	0.020	0.664	0.101	0.071	0.017	97.102	4
325307	1	31.605	9.152	0.098	0.109	0.000	0.123	0.092	36.706	77.885	1
325307	2	67.038	18.779	0.275	0.290	0.780	1.766	0.854	0.400	90.182	3
325307	2	64.616	20.317	0.005	1.117	0.929	0.570	0.080	3.389	91.023	2
325307	5	58.862	0.755	0.001	0.312	6.151	0.185	0.044	12.099	78.409	4
325306	1	39.683	25.990	0.000	2.270	0.003	0.165	0.287	9.733	78.131	2
325306	2	67.099	17.681	0.651	0.095	0.555	1.422	3.531	0.386	91.420	2
325306	4	63.707	17.679	4.163	0.447	0.367	1.213	3.419	0.100	91.095	3
325306	5	36.415	20.791	1.458	8.510	0.340	0.433	0.228	13.077	81.252	3
325306	6	43.855	26.392	0.849	3.563	0.219	0.473	0.145	10.516	86.012	4

Sample no.	grain no.		Chemical age
SU-8326		Pitchblende in standard	
325307	1	Secondary uranium mineral veinlet.	
325307	2	Light phase on BEI of uraninite.	1735 Ma
325307	2	Dark phase on BEI of uraninite.	1650 Ma
325307	5	Fibrous secondary U-mineral surrounding pyrite. Kasolite?	
325306	1	Yellow secondary U-mineral. U-Pb silicate	
325306	2	Uraninite grain.	1646 Ma
325306	4	Homogeneous uraninite in biotite.	1698 Ma
325306	5	Yellow secondary U-mineral. Fe-rich U-Pb silicate	
325306	6	Orange secondary U-mineral. U-Pb silicate	

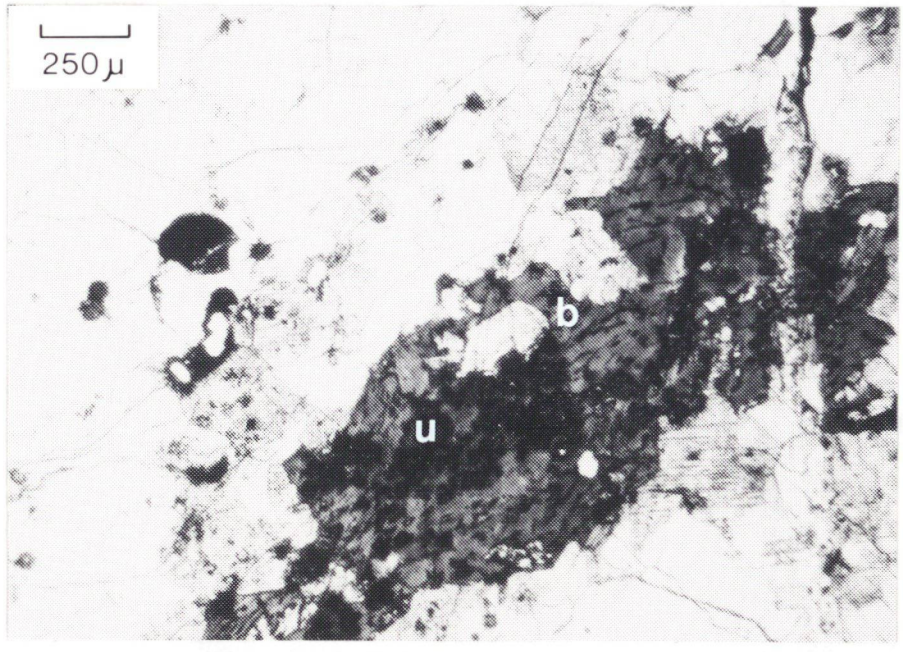

Fig. 27. Photomicrograph of uraninite (u) in biotite (b) in sample 325306.

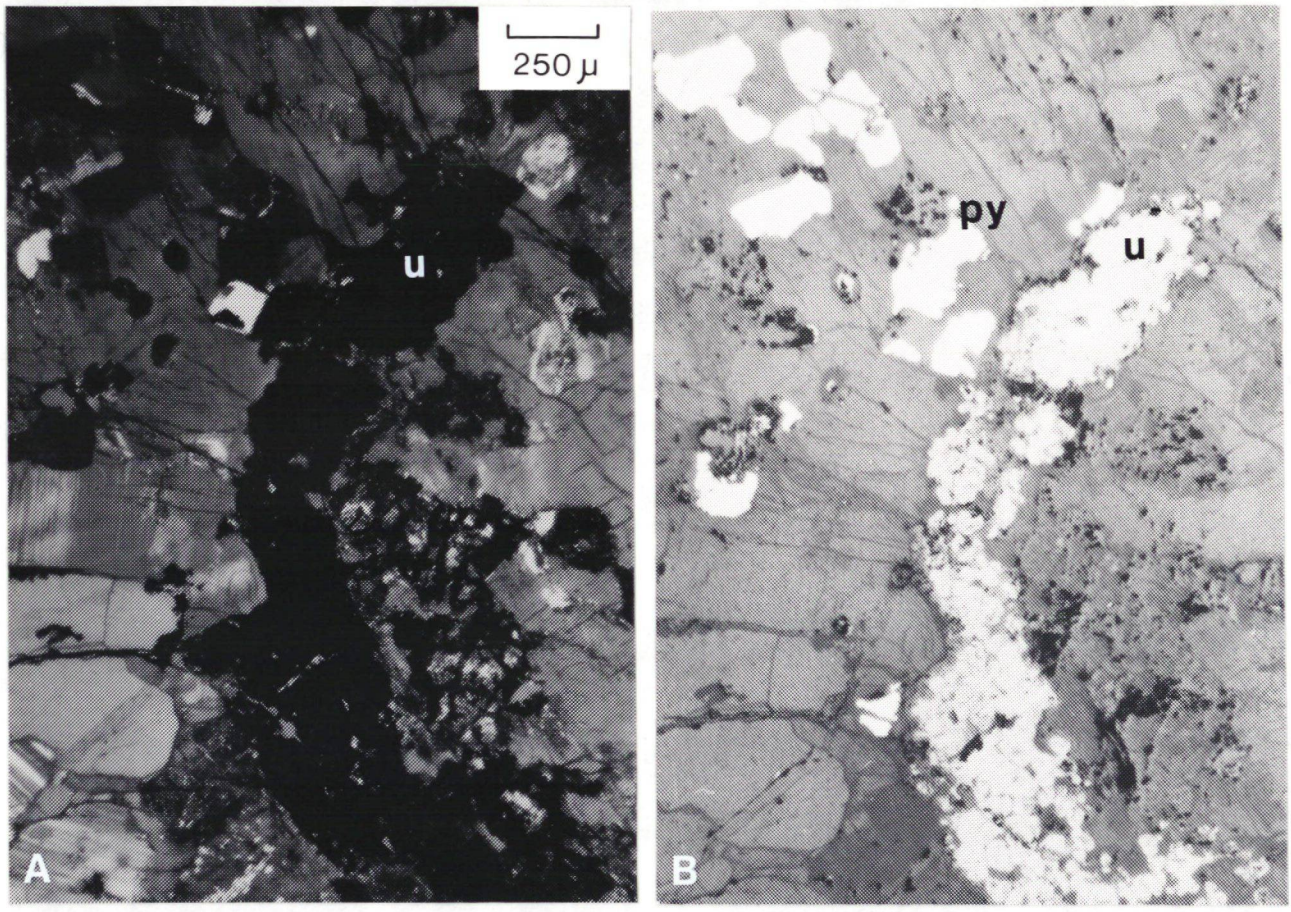

Fig. 28. Photomicrograph of aggregates of uraninite (u) in microcline sample no. 325306. A: transmitted light and X nicols, B: reflected light.

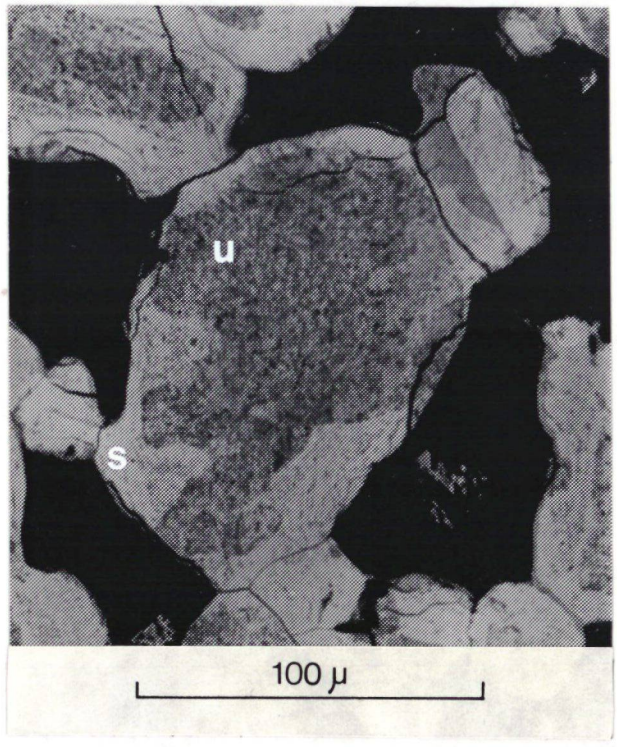

Fig. 29. Back-scattered electron image (BEI) of uraninite (u) surrounded by yellow secondary uranium minerals (s) in sample no. 325307.

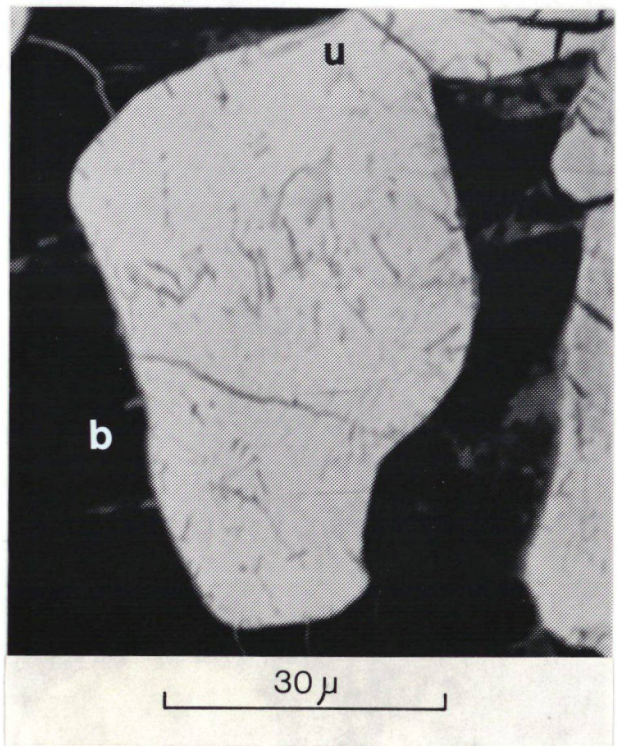

Fig. 30. BEI of uraninite (u) in biotite (b) in sample 326306.

3.2.3 Uraniferous Gardar Veins

Three Gardar vein type pitchblende occurrences were found on the Nunatak during the course of mapping. One of them (fig. 24, sample 325324) is the northernmost known pitchblende location in the Granite Zone. They all occur in altered fracture systems with a 150° strike and vertical to 70°W dip. The fracture zones can be traced over distance of 1 - 2 km and contain various degrees of alteration, hematitisation, quartz and fluorite veining and radioactive mineral occurrences. The radioactive minerals can usually be traced over only a few metres. Vein material which occurs to the northeast of the lake (Sø 975) gives a particularly clear paragenetic sequence (sample 325311). The texture suggests that uraninite was precipitated as vein filling after the growth of euhedral quartz crystals into the vein cavity (fig. 31, A). Pyrite was also associated with this early quartz growth. Later hematite associated with a fine-grained or crypto-crystalline quartz filled in the cracks in the pitchblende (fig. 31, B) and corroded the pyrite.

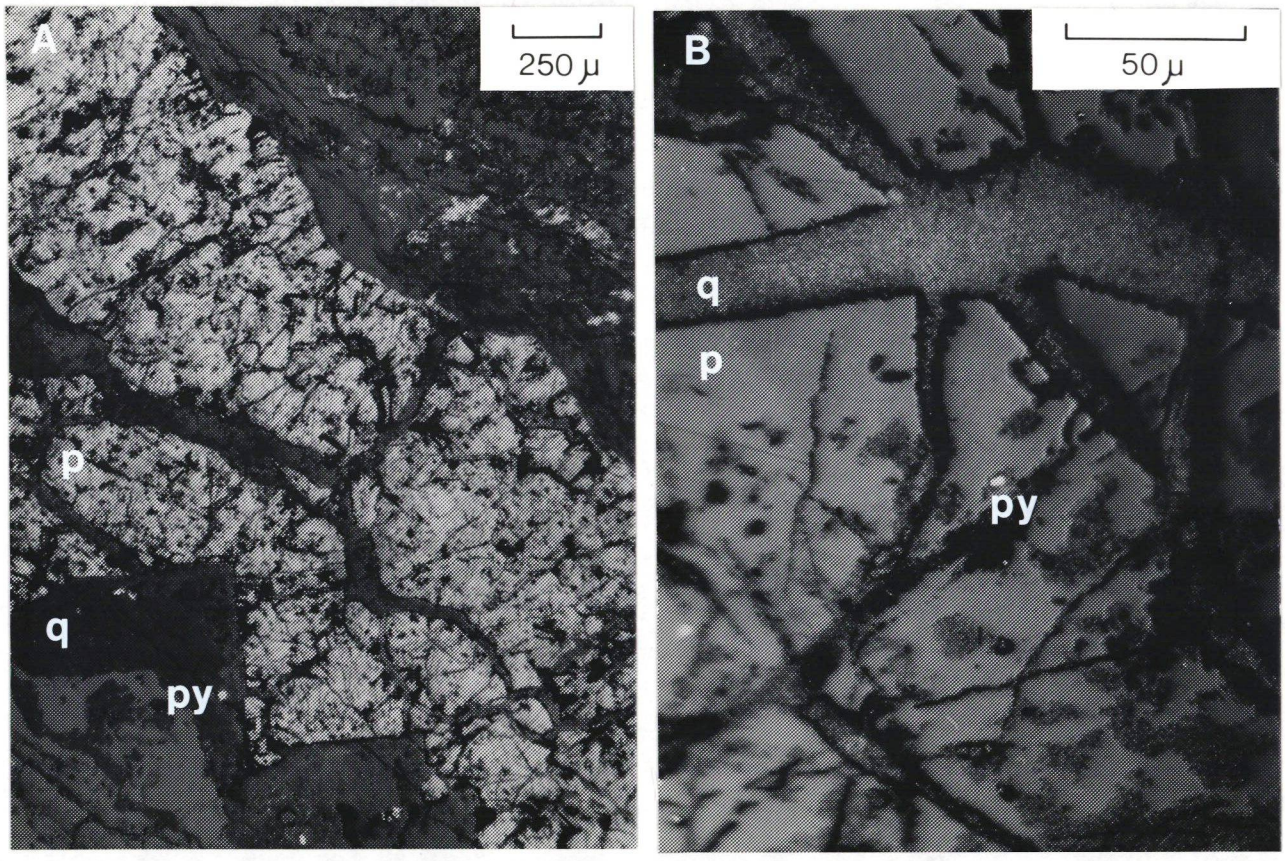

Fig. 31. Photomicrograph illustrating the paragenesis of pitchblende in a vein sample no. 325311. A: uraninite (p) with shrinkage cracks growing over euhedral quartz crystal terminations (q) with fine pyrite inclusions (py), B: cracks in uraninite (u) filled with crypto-crystalline quartz (q) with a reddish internal reflectance due to included hematite. The white inclusions in the uraninite are pyrite (p).

3.2.4 Isotopic results

Uraninite has been separated from three samples by the same method as that outlined in the Igdlorssuit report (Armour-Brown, 1986), and the U and Pb isotopes measured by Ian Swainbank at the British Geological Survey. The results give highly discordant ages showing considerable Pb loss (Table 5).

The 206Pb/207Pb ratio indicates an age of 1780+/-8 Ma (Table 5) This is distinctly older than the 1300 - 1100 Ma isotope ages from the Gardar pitchblende veins. It corresponds to the 1776 +/-37 Ma age for the Late Julianehåb granite determined by van Breemen et al. (1974).

Table 5. U-Pb isotopic analyses of uraninite and pitchblende from three samples on the nunatak. Analyses were made by the isotope dilution method by Ian Swainbank at the British Geological Survey. Samples 287136, and 298026 are pitchblende samples from Gardar veins on the Igaliko peninsula for comparison. Note lower ^{208}Pb level than in 325324.

	Isotopic composition in atom %				Concentration in weight %	
Sample no.	^{204}Pb	^{206}Pb	^{207}Pb	^{208}Pb	U	Pb
325307	0.00224	89.73	9.82	0.447	70.51	20.47
325306	0.00215	89.39	9.75	0.863	59.15	16.69
325324	0.25699	79.84	9.40	9.400	70.92	18.45
287136	0.06570	89.33	8.02	2.586	54.48	10.88
298026	0.06980	89.18	8.07	2.689	49.85	10.19

	Isotopic ratios			Ages in Ma		
Sample no.	206/238	207/235	207/206	206/238	207/235	207/206
325307	0.3029	4.5587	0.1091	1705.9	1741.7	1784.1 +/-5
325306	0.2934	4.4014	0.1088	1658.3	1712.6	1778.6 +/-5
325324	0.2287	2.7257	0.0864	1327.6	1335.5	1347.1 +/-5
287136	0.2050	2.2450	0.0794	1202.0	1195.0	1182.0 +/-15
298026	0.2093	2.2910	0.0794	1225.0	1210.0	1181.0 +/-15

Isotopic analysis of the vein pitchblende (sample no. 325324), on the other hand, suggests age of 1347 +/-5 Ma (Table 5). This is clearly a Gardar event rather than one related to the granite. It is, however, older than the other dated pitchblende veins by nearly 200 Ma. If this is a true age then it extends the period of possible vein type pitchblende mineralisation over a very long period. It is not completely impossible that the Gardar hydrothermal activity extended over such a long period. The lower age limit to the Eriksfjord has never been established but has been assumed to be in the region of 1400 Ma. There is no reason to eliminate the possibility of this type of pitchblende U-mineralisation being formed as early at 1347. It has to be noted, however, that this sample contains a rather higher proportion of common lead (208Pb) compared to the other veins for which there is isotopic data (Table 4). This suggests that it may have been contaminated by older

radiogenic lead. Since the older uraniferous gneiss described above showed signs of mobilisation of uranium and lead and was depleted in lead and further cut by a Gardar joint (fig. 24, loc. 374), the possibility of contamination appears plausible. In which case the true age will be younger, presumably in the range of 1050-1100 Ma corresponding to the other pitchblende veins.

3.2.5 Discussion and conclusions - the nunatak area

The textural and isotopic results establish that the uraninite found at locality 374 and in the area of summit 1678 crystallised during the emplacement of the Late Julianehåb Granite. The fact that thorium is not dominate over uranium in the paleosome whereas it is in the neosome and aplitic dykes suggests that uranium and thorium partitioning took place prior to, rather than during metamorphism. This implies that uranium was already present in the parent rocks of the gneiss before their metamorphism. The nature of this early uranium mineralisation, and whether the uranium was concentrated or depleted during metamorphism remains an open question. The present composition of the paleosome with 89% SiO_2 suggests that they were originally sandstone or arkosic sandstone. As a first working hypothesis, therefore, it is suggested that this occurrence was originally a sandstone type deposit.

None of the uranium occurrences in the gneiss that have been found so far have an economic potential. This is due either to their low grade of a few hundred ppm U as on the mountain summit 1678 m or else the limited size of the rafts of locality 374. The possibility of finding a larger raft of uraniferous metamorphosed supracrustal rocks cannot be ruled out, so this type of occurrence, which is very similar to those at Igdlorssuit in the Migmatite Complex (Armour-Brown & Wallin, 1985), must also constitute a target for future exploration in the Granite Zone. It must be added, however that the metamorphosed supracrustal rafts in the Granite Zone are relatively limited in extent, which limits their uranium mineral potential.

The real significance of these showings lie in the fact that they demonstrate the availability of uranium in non-resistate minerals before the Gardar. During the Gardar this uranium would have been leached out by weathering, meteoric and hydrothermal water during the erosion of the Ketilidian basement. Redeposition of the uranium along the Gardar faults and fractures could have been activated by meeting and mixing of oxygenated uranium bearing meteoric waters with alkaline hydrothermal fluids derived from the alkaline igneous activity.

The finding of the pitchblende and uraniferous veins in the nunatak area extends the northern limit of the Gardar hydrothermal activity. The reliance that can be placed in the 1347 +/-5 Ma U/Pb isotope age for the sample 325324 is, unfortunately, not strong enough to do more than suggest that this represents a lower limit for this Gardar hydrothermal activity. If it is correct it shows that the activity continued over some 200 Ma which appears a rather long period of time. But, on the other hand, there is no reason to suppose that there were not a number of hydrothermal regimes either isolated in time and space or running into one another in response to new surface and sub-surface conditions throughout the Gardar.

3.3 Rare earth elements in fluorite from the Granite Zone

In the Granite Zone of South Greenland fluorite is found throughout the area as fracture fillings together with quartz, calcite and U/Th mineral occurrences. To get a better understanding of the mineralising processes and also to see if it was possible to differentiate fluorite in U and non U bearing veins 13 samples were selected for REE analyses. In two of the samples the fluorite has been separated in two fractions by colour, so in total 15 samples of fluorite have been analysed (Table 6). Three of the samples are from the Motzfeldt Centre (Igaliko alkaline intrusion), two from brecciated albitite in the contact to the Ilímaussaq alkaline intrusion, one is from a Ketilidian leuco-gneiss and the rest are from small fractures in the Julianehåb Granite. The sample locations are shown on fig. 32. The fluorite from the fractures in the granite are associated with U and with Th mineral occurrences as well as with U/Th barren occurrences (Table 6).

The REE analyses were funded by the Danish Science Research Council (grant: j.nr. 11-5327).

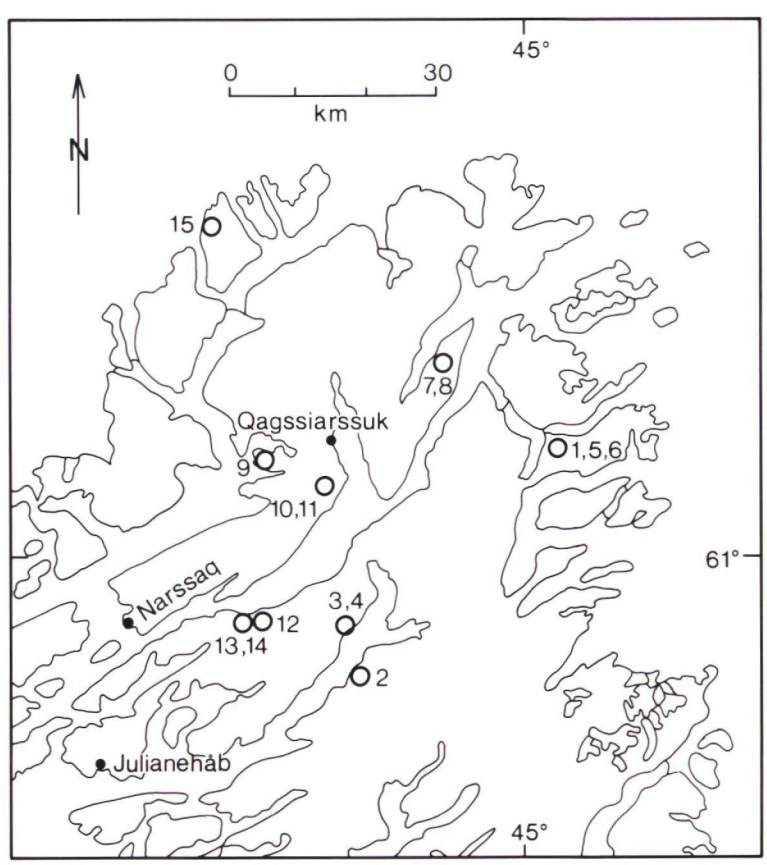

Fig. 32. Index map for fluorite sample locations in the Granite Zone.

3.3.1 Sample treatment

The rock samples with fluorite were first crushed and sieved, and magnetic separation was carried out on the 80-250 micron fraction. The non-magnetic part was separated into three fractions by heavy liquid separation (2.94 and 3.30 specific gravity). Since fluorite has a specific gravity of approximately 3.18 the middle weight fraction contained 70-90% fluorite. About 0.05 to 0.15 g of fluorite was hand picked from each fraction and analysed by instrumental neutron activation (INAA) at Risø National Laboratory for the following elements: La, Ce, Nd, Sm, Eu, Tb, Yb, Lu, Na, Sc, Cr, Fe, Co, Zn, Sr, Hf and Th. Some analyses also included the elements K, As, Ag, Sb, Rb, Cs, Ba and Ta. Semi-quantitative results for Ca were also obtained. The Br results are not considered as the samples have been contaminated by the heavy liquid. The analytical results are listed in Appendix III.

Table 6. Sample locations, fluorite colour and association

GGU no	ID no	Locality	Colour	Remarks
297940	AA1	Motzfeldt Centre	violet	Alkaline pegmatite cutting a basalt raft in nepheline syenite
304240	AA2	Vatnahverfi	violet	U mineral occurrence in granite/lamprophyre contact
304282	AA3	Puissagtaq/Vein 1	very dark violet	U mineral occurrence in granite
304506	AA4	Puissagtaq/Vein 2	very dark violet	U mineral occurrence in granite/dolerite
304606	AA5	Motzfeldt Centre	yellow	Boulder with coarse crystals of fluorite with galena
304609	AA6	Motzfeldt Centre	violet	Veinlet in hydrothermal altered microsyenite
304812	AA7	Mellemlandet	violet	Associated with quartz veining
304812	AA8	Mellemlandet	dark violet	Same sample as AA7
325069	AA9	Qagssiarssuk	light violet to blue	U mineral occurrence in granite/dolerite contact
325085	AA10	Qagssiarssuk	light violet to colourless	Sulphide mineral occurrence in granite
325086	AA11	Qagssiarssuk	violet	Same locality
325224	AA12	Agpat/Puissagtaq	very dark violet	U mineral occurrence in granite
325230	AA13	Agpat	light violet to colourless	Brecciated albitite
325230	AA14	Agpat	violet	Same sample as AA13
325302	AA15	Nunatak	violet	Ketilidian leuco-gneiss

3.3.2 Fluorite colour

The colour of the fluorite seems partly to be correlated with the Fe content where the highest contents give the darkest colour (Table 7), but the radioactivity may also account for some of the dark colouring.

Table 7. Colour and Fe content in fluorite samples

Fe %	U ppm	Colour	Fe %	U ppm	Colour
0.68	1300	very dark violet	0.23	50	violet
0.67	48	very dark violet	0.16	139	violet
0.17	35	very dark violet	0.05	17	violet
0.05	2	dark violet	0.01	2	violet
			0.13	120	violet
			0.08	11	violet
			0.08	26	violet

Fe %	U ppm	Colour
0.003	1	yellow
0.16	15	light violet/bluish
0.24	85	light violet/colourless
0.04	11	light violet

3.3.3 Sample/chondrite normalisation

The fluorite samples show a variation in the total REE content from 10 up to 1600 ppm. The highest content is found in sample AA1 from the Motzfeldt Centre and the lowest in the U,Th barren sample AA8 from Mellemlandet. The REE results have been chondrite normalised and plotted (fig. 33), and they show very varied trends. The results are summarised below. The chondrite values used in the normalisation are from Wedepohl (1978).

AA1 & AA13 : Same shape of curve with a strong enrichment in light REE (LREE), and a clear negative Eu anomaly.

AA9 : Same as AA1 and AA13, but with only a weak negative Eu anomaly.

AA5 & AA6 : Weaker enrichment in LREE and with a strong negative Eu anomaly.

AA3, AA11 & AA14 : Enriched in LREE with a steep fall to Eu from which the curve is much more flat lying.

AA2, AA10, AA12 & AA15: Relatively flat lying curves but with a negative Eu anomaly.

AA4, AA7, AA8 : No Eu anomaly and flat lying curves especially for AA7 and AA8.

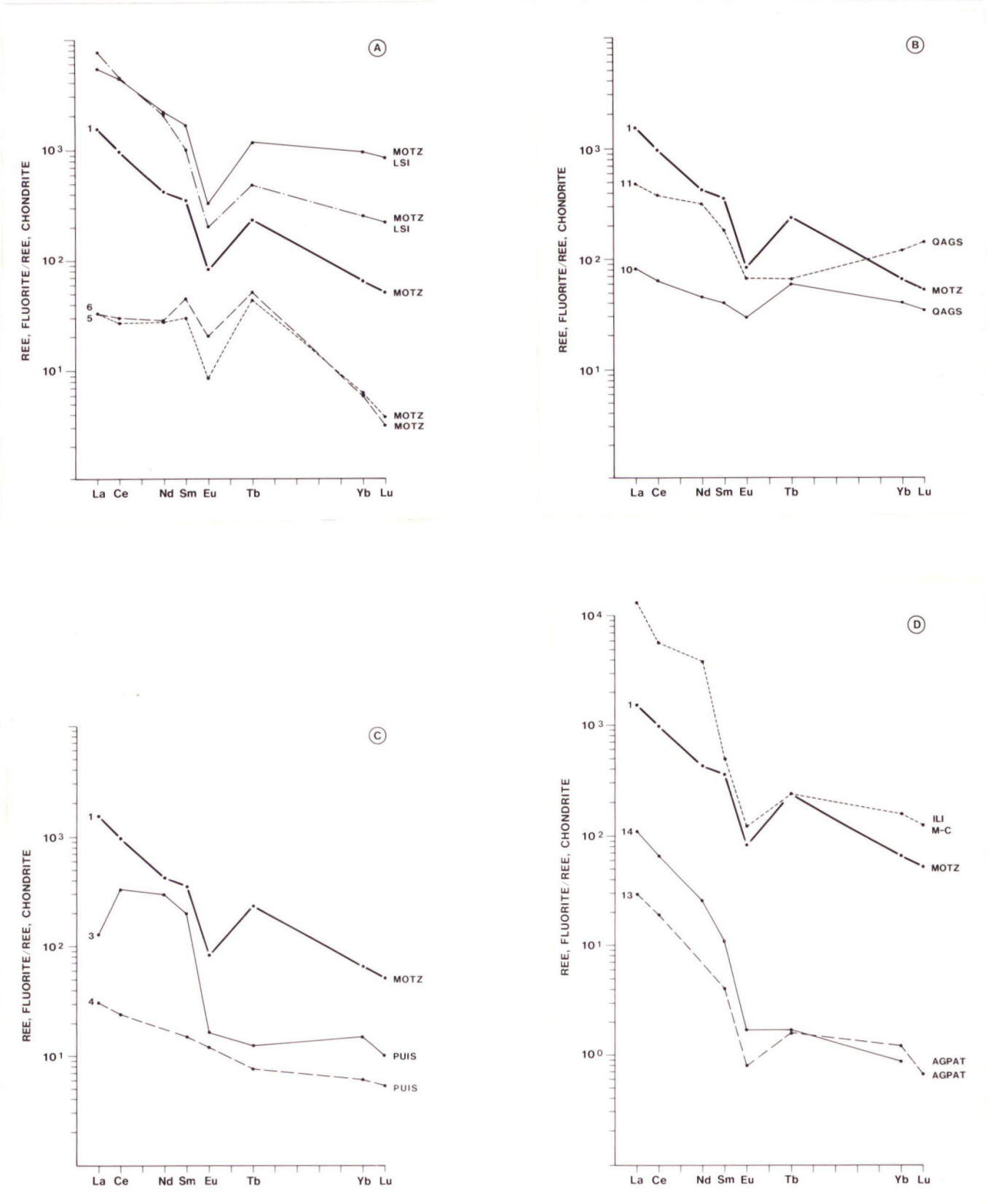

Fig. 33. Chondrite normalised REE distribution in fluorite samples. The samples have been grouped into 6 classes according to their location. See text for reference. MOTZ LSI: Late sheeted intrusions, Motzfeldt centre, ILI M-C: M-c lujavrite, Ilímaussaq intrusion.

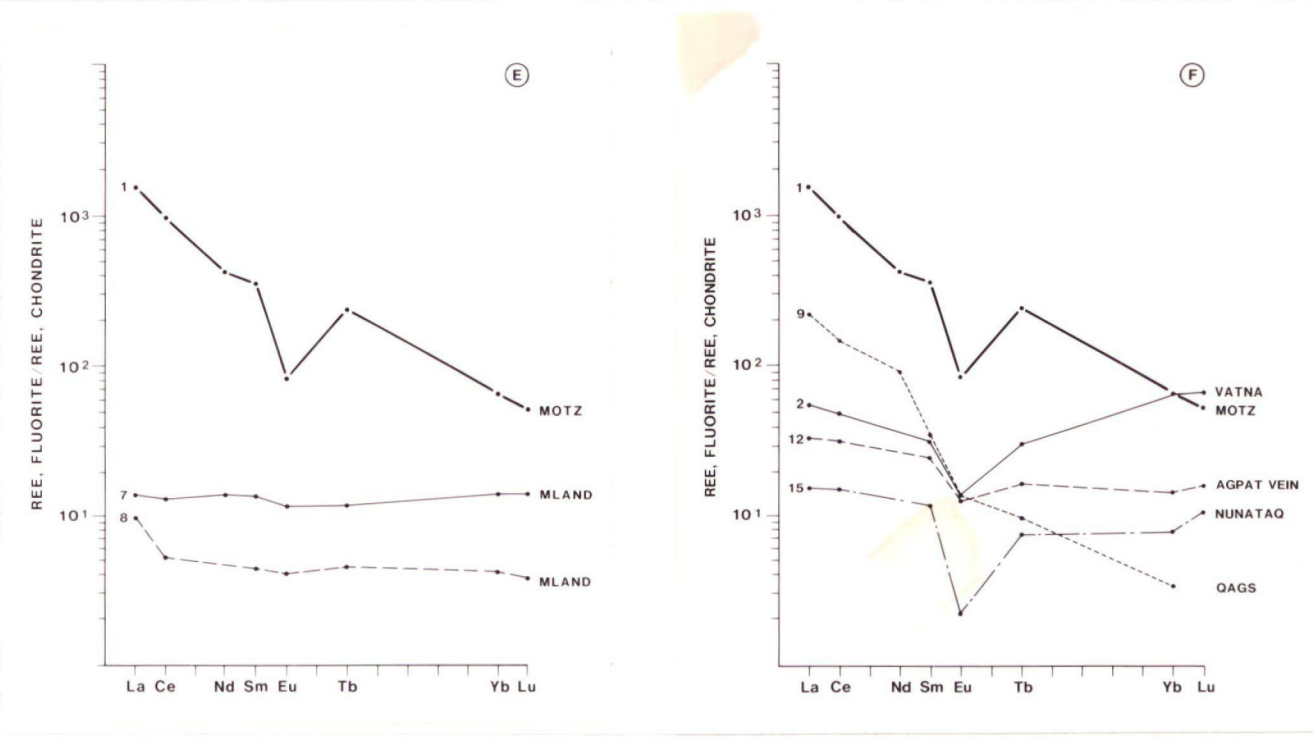

Fig. 33. cont.

The three samples from the Motzfeldt Centre (AA1, AA5 & AA6 - fig. 33-A) show a REE pattern with a decrease in the total content from AA1 to AA5 and AA6, but with a pronounced differentiation between the light (LREE) and the heavy REE (HREE) with Yb/La ratio from 0.029 to 0.125. For comparison the pattern for the late sheeted intrusion, the Motzfeldt Centre (Armour-Brown et al. 1984) is included on fig. 33-A. The two samples from the fracture zone in the granite at Qagssiarssuk (AA10 & 11 - fig. 33-B) also show fall in total REE content with a differentiation between the LREE and the HREE with Yb/La ratio from 0.165 to 0.323. The two samples AA3 and AA4 are both from a pitchblende mineral occurrence in a wide fault zone at Puissagtaq and taken at two localities about 500 m apart. There is a fall in the REE content from AA3 to AA4 (fig. 33-C), which is most pronounced in the LREE group, with a Yb/La ration change from 0.079 to 0.130. Sample AA3 has a very high Ba content and is probably contaminated by barite. Barite is normally rich in the light group of REE and this sample will not be considered in the following. Fluorite sample AA13 and AA14 from the same sample at the Agpat locality at the border of the Ilímaussaq intrusion (fig. 33-D) show roughly the same development as the previous two samples (AA3 and AA4). For comparison the pattern for M-c lujavrite is also shown at the fig. (Bailey et al. 1978). The two samples AA7 and AA8 from Mellemlandet (same rock sample) only show a fall in total REE content from AA7 to AA8 (fig. 33-E). The samples AA2 (Vatnahverfi), AA9 (Qagssiarssuk), AA12 (Agpat/Puissagtaq) and AA15 (Nunatak) are not associated with other fluorite samples (fig. 33-F).

Most of the samples have a weak negative Ce anomaly, which may be inherited from the primary fluid or been caused by slightly oxidizing conditions through transportion to the place of precipitation by adsorbtion by oxyhydrates such as FeO(OH) as suggested by Möller & Morteani (1983). On the other hand, this weak Ce anomaly is very much dependant on the chondrite values to which the samples are normalised, and may have no meaning at all.

The general development of the REE pattern goes from a high to a lower REE content accompanied by a differentiation between the LREE and the HREE with Yb/La ratio from about 0.01-0.02 up to about 0.3 and even 0.75. Within the group of heavy RE elements the trend of the curve generally continue to fall towards Lu, but in sample AA9 and AA11 a enrichment is noted. The chondrite normalised REE diagrams indicate the possibility that much of the fluorite has the same source.

3.3.4 Sample/sample normalisation

The RE-elements have possibly been transported as F-complexes in fluids originating from the alkaline intrusions and with a possible mixture of meteoric waters. It was, therefore, felt that a more meaningful or more easily interpretable distribution would be forthcomming if the results were normalised against a fluorite sample from one of the alkaline intrusions. As the chondrite normalised results show a closer resemblage to the Motzfeldt than to the Ilímaussaq results, fluorite sample AA1 was used in the sample/sample normalisation. This sample also has a REE pattern very similar to whole rock REE patterns from the youngest units of the centre (fig. 33). The sample/sample plots are illustrated in fig. 34.

In the sample/sample normalisation to AA1 a group of 7 samples (AA2, AA4, AA7, AA8, AA10 & AA12 - fig. 34-A) show very similar trends. The REE contents are all lower than AA1 except for AA2, which has a higher Lu content. The samples in this group have a positive Eu anomaly compared to AA1, and show a general enrichment towards the HREE.

Sample AA9 and AA11 (fig. 34-B) are partly different from the previous group of samples. They have a positive Eu anomaly but are not so strongly depleted in LREE as the first group of samples or enriched in HREE.

The two samples AA13 and AA14 differ from the previous samples by being depleted in the LREE towards Tb and then with a small increase in the LREE (fig. 34-C).

The samples A5 and A6 have the same LREE pattern as the first group (fig. 34-D), but are depleted in HREE compared to AA1, with a relative maximum at Eu (AA5) or Tb (AA6).

From the grouping of the sample/sample normalisation curves (fig. 34) it seems possible that most of the samples could originate from a fluid coming from the Motzfeld Centre. AA13, AA14 and AA15 also show a different pattern. Sample AA15 is thought to be pre-Gardar and AA14 & AA13 are possibly more associated with the Ilímaussaq intrusion. Whole rock REE patterns from the youngest units from Ilímaussaq are very similar to those from Motzfeldt (fig. 34) (Bailey et al., 1978; Armour-Brown et al. 1984). As fluorite in the Ilímaussaq intrusion is very rare, no REE data from this mineral exists, and the association of the fluorite with fluids coming from the Motzfeldt Centre may be strongly biased because of lack of data from fluorite in the Ilímaussaq intrusion.

3.3.5 Tb/La - Tb/Ca diagram

By plotting the Tb/La ratio against the Tb/Ca ratio (fig. 35) it is possible to determine if the fluorite has a pegmatitic, a hydrothermal or a sedimentary origin (Möller et al.,1976; Möller & Morteani, 1983). The Tb/Ca ratio defines the chemical environment from which the fluorite is generated while the Tb/La ratio represents the degree of fractionation. Three possible evolution trends in the development of the F-rich fluids is shown on fig. 35. These trends are fractionations of REE, remobilisation of fluorite and interaction with calcite Two samples fall clearly in the pegmatitic field - AA1 and AA11, which also have the highest Th contents. Also AA9 and AA10 (and AA3) fall in the pegmatitic field but very close to the provisional boundary to the hydrothermal field. The rest of the samples fall in the hydrothermal field. As the Ca analytical results are only semi-quantitative and the boundary provisional AA10 and AA3 may actually belong to the hydrothermal field.

From the Tb/La - Tb/Ca diagram fluorite samples AA7 and AA8 from the same rock sample (Mellemlandet) show an apparent fractionation in the REE from AA8 to AA7. Otherwise the two samples have parallel REE curves. The samples AA13 and AA14 (Agpat), AA3 and AA4 (Puissagtaq) and AA10 and AA11 (Qagssiarssuk) show a remobilisation of the fluorite. Sample AA1, AA5 and AA6 show also show a remobilisation of fluorite, but the trends of the curves in the sample/chondrite normalised diagram indicated a combination of a fractionation of the REE and an interaction with calcite.

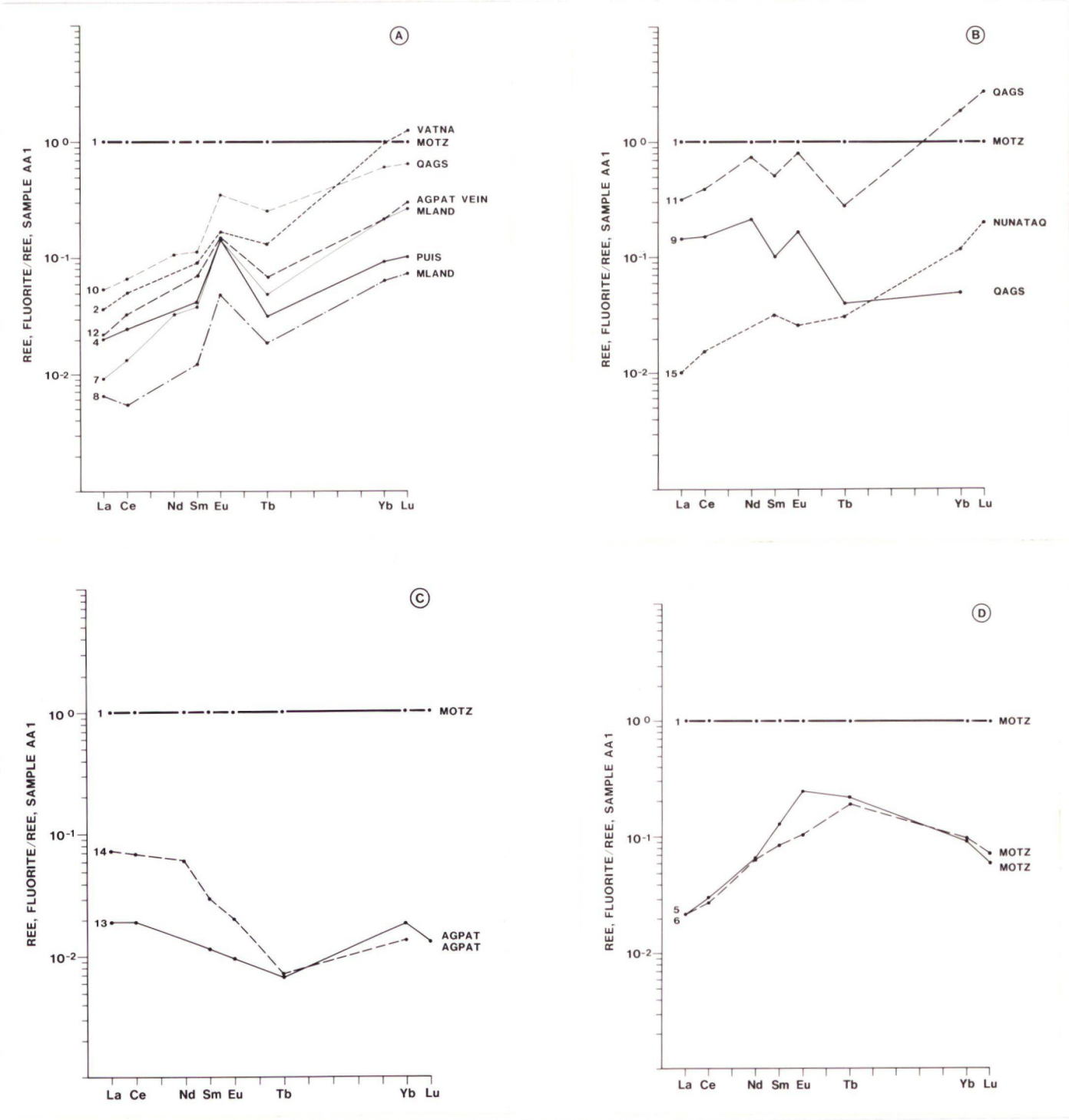

Fig. 34. Sample/sample normalised REE distribution in fluorite samples. The samples have been grouped into 4 classes according to their trend - see text for reference.

Sample AA15 is relatively enriched towards the HREE with a weak negative Eu anomaly compared with AA1, and is separated by its REE pattern from the other fluorite samples. It is of Ketilidian age have a metamorphic origin.

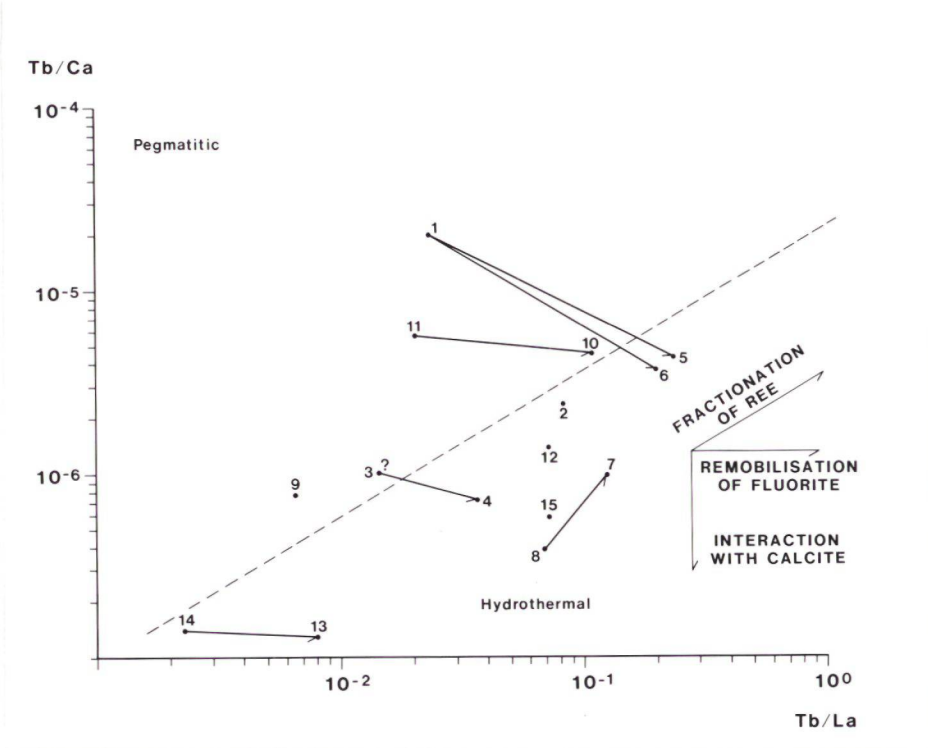

Fig. 35. Scatter diagram Tb/La - Tb/Ca in fluorite samples, with pegmatitic and hydrothermal fields indicated and the possible evolution trends for the fluorite shown as arrows.

3.3.6 Th - Tb/La diagram

As Th is expected to occur in the high temperature area, the pegmatitic field, a Th-Tb/La scatter diagram was constructed (fig. 36). This diagram show a distinct fall in Th content in the fluorite samples with increasing fractionation, and the highest Th contents are found in the samples plotting in the pegmatitic field of the Tb/La-Tb/Ca diagram.

3.3.7 Sr/Ca - Tb/La diagram

The Sr content in the Motzfeldt fluorite samples is high and very low in the Agpat sample. A Sr/Ca - Tb/La scatter diagram was therefore constructed (fig. 37) to see if any grouping of the samples occurred. Most samples plot in one reasonably well defined area with AA14 clearly off and AA9 and AA15 in between. There is a general reduction of the Sr/Ca ratio with increasing fractionation. From this diagram it seem like the samples group in a field aound the Motzfeldt samples.

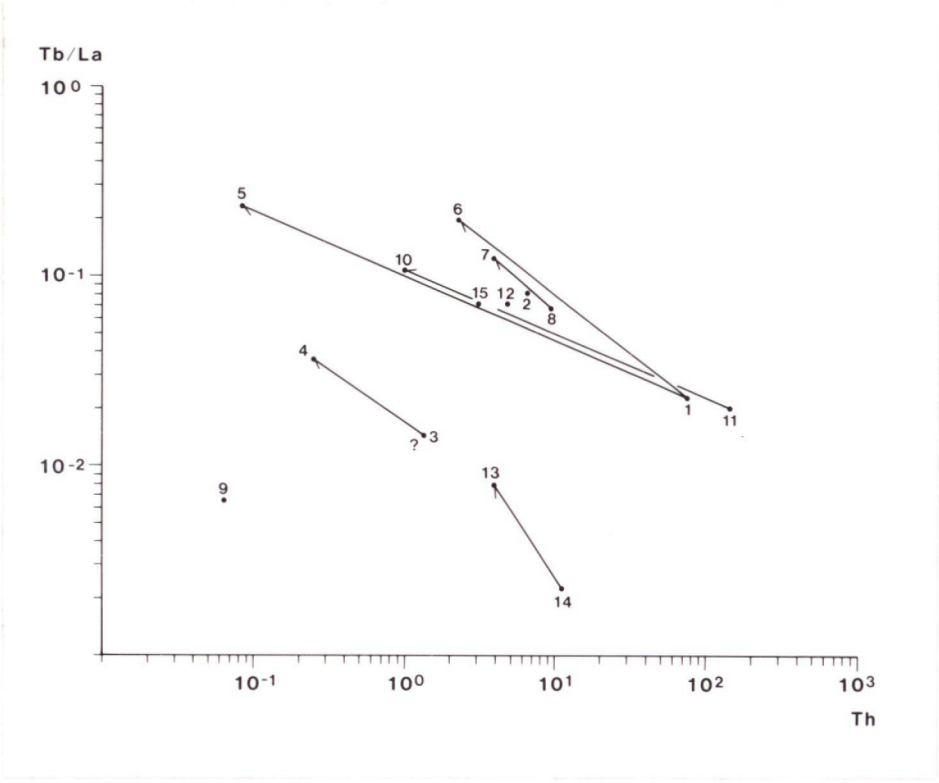

Fig. 36. Scatter diagram Th - Tb/La for fluorite samples with possible evolution trends.

3.3.8 Discussion and conclusions

REE analyses of fluorite gave a variation in total REE content from 10 up to 1600 ppm. The sample/chondrite diagrams illustrate a great variation between the different degrees of fractionation between LREE and HREE with Tb/La ratios from 0.005 up to 0.754, most samples show negative Eu anomaly.

The source of the fluorite associated with fractures in the Granite Zone may have been the different alkaline magmas which were rich in fluorine. The chondrite and sample/sample REE normalisation diagrams have been used to classify the fluorite samples. Three of the samples are from the Motzfeldt Centre and there is no doubt about their origin. Eight other samples have a very similar REE pattern in the sample/sample normalisation to a Motzfeldt fluorite sample, which indicates that the Motzfeldt Centre or cogenetic magmatic body is their source. The Agpat samples are best associated with the Ilímaussaq intrusion, and the nunatak sample of Ketilidian metamorphic origin stands alone. The Mellemland samples may have had another source other than Motzfeldt because of the absence of an Eu anomaly, although their sample/sample normalisation pattern points to this intrusion. The Mellemland samples are not associated with any uranium occurrences, which indicate oxidizing conditions in the fluids (Möller & Morteani, 1983).

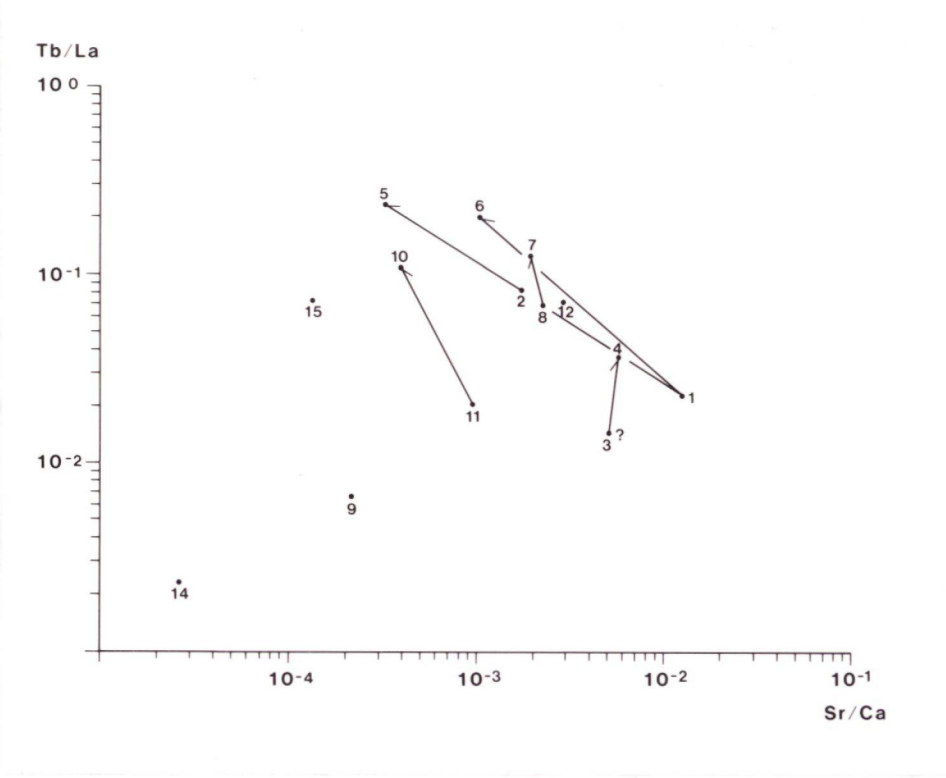

Fig. 37. Scatter diagram Tb/La - Sr/Ca for fluorite samples with possible evolution trends.

The temperature conditions under which the fluorite was precipitated is indicated by the Tb/Ca-Tb/La diagram (Möller et al., 1976). Few of the fluorite samples fall in the pegmatitic field of the diagram and most in the hydrothermal field, which is in agreement with geological observations. This is also supported by the Th-Tb/La diagram, where a distinct fall in the Th content is associated with increasing fractionation. The change from the pegmatitic to the hydrothermal field therefore shows a decrease in the participation of Th in the mineralising fluids. The Tb/La-Sr/Ca diagram shows a very low Sr/Ca ratio for the Agpat samples pointing to Ilímaussaq as source, where the other samples group around the Motzfeldt samples indicating Motzfeldt Centre as source.

The hydrothermal fluids were possibly a mixture of hydrothermal and meteoric waters (Nyegaard et al., 1986) and this mixing may account for the differences in the REE pattern for the Motzfeldt fluorite and the fluorite in fractures in the granite. The position in space and time of the uranium occurrences and the associated fluorite may, therefore, strongly influence the REE patterns of the

fluorite, and a distinction between fluorite associated with U/Th occurrences and barren veins cannot be made from the REE pattern at this stage of investigation.

Interaction between hydrothermal fluids and wall rock has not been taken into consideration in the previous discussion, but chloritisation is normally associated with the uranium occurrences. This process has been shown to introduce heavy REE into the system (Alderton et al., 1980) and may explain the increase of HREE in some of the fluorite samples

This preliminary investigation of the REE contents in fluorite associated with Gardar Th and U mineralisation has given useful results and better understanding of the mineralisation processes. It is recommended that work of this kind continues and more samples and minerals considered. An investigation of the REE pattern for calcite, which is also associated with the uranium occurrences, and their oxygen and carbon isotope ratios will greatly facilitate the classification of the occurrences and the origin of the hydrothermal fluids as Möller et al. (1979, 1984) have shown for Pb-Zn vein deposits. Also the REE partition coefficients between minerals associated with the occurrences and in the wall rock can greatly help the evaluation of the uranium occurrences (Chatterjee, 1985; Guichard et al., 1979 and Möller et al., 1976). These investigations should be combined with fluid inclusion studies to determine the temperature, pressure and composition of the hydrothermal regimes.

4 APPRAISAL OF EXPLORATION METHODS

4.1 Statement of problem and background

The exploration problem can be simply stated: having defined the Granite Zone as a uraniferous district which methods are most efficient in locating uraniferous mineral occurrences?

Since 1980 a number of different exploration methods have been employed during the Syduran and Sydex projects including analysis of lineaments and faults, helicopter-borne gamma-spectrometry and total gamma measurements, ground measurements of electromagnetism and total gamma radiation, radon emmanometry, heavy mineral panning and sieving of stream sediment in the field, stream water and spring and seep water sampling, soil sampling and ion absorbers in the soil. The following is a discussion of where and when particular methods should or should not be used.

The best exploration method is of course one which is related to the primary nature of the mineral occurrences and to the secondary environment. In the Granite Zone these are pitchblende ore-shoots located in the faults and fractures of Gardar age. They could also include unconformity type deposits which could be hidden by the overlying Eriksfjord Formation. The wall rock of the faults and fractures, is altered and less resistant to weathering and they have, therefore, been followed by erosive features and buried under surficial deposits. The problem is, therefore, to use methods, which can locate hidden uranium mineral occurrences.

4.2 Geochemical methods

Geochemical methods which have been used successfully at the reconnaissance phase, suffer, at the follow-up phase, by the high mobility of uranium in the secondary environment. As has been well documented elsewhere, uranium is mobile in neutral water and extremely mobile if there are carbonate ions present. Organic matter, on the other hand, absorbs uranium and has an extremely high concentration factor. Peat with 4920 ppm U (sample no. 297757) has been measured below a small stream which contains 1-6 ppb U (sample no. 296252) A concentration factor of 10^6 times. It is interesting to note that the eU analyses (gamma-spectrometric assay) for the same sample was only

93 ppm U. As it takes about 10 000 years for uranium to reach equilibrium with its daughter elements ^{214}Bi, this difference shows how quickly (in the order of 1000-2000 years) the organic material accumulates uranium. There is no evident source for this uranium and there are no well developed lineaments in the area where uranium minerals are likely to occur. It must therefore be interpreted as a false anomaly. It illustrates the problem of interpretating drainage geochemical data and its limitations in exploration at the follow-up stage.

4.2.1 Heavy mineral concentrates, and wet sieving and decanting of stream sediment.

Two methods have been tried in order to eliminate anomalies in the stream sediment caused by the absorption of uranium by organic material. The first approach was to wet sieve the sample in the field and decant the water and the organic material, and fine clay fraction which were still in suspension after some 20 minutes of settling time. This procedure was originally developed to reduce sample variability of stream sediment when organic material is present (Plant, 1971). The second method was to concentrate the heavy mineral by panning . For various reasons outlined below neither method seems to be a satisfactory solution for systematic use in the Granite Zone.

The wet sieving and decanting after 20 minutes was only capable of removing part of the organic material. The loss of weight on ignition (LOI), which is a reasonably accurate measure of the organic content in the sediment sample, all show a consistent loss of between one half and one quarter of the dry sieved sediment after decanting (Table 8). The relationship of uranium to the organic material can be seen from the proportional decrease in the uranium content. The three sites in which there was no significant reduction in uranium content (296801, 297122 & 297128) were all well washed sediment containing very little organic material. The problem of organic material in the sediment is, therefore only partially solved by wet sieving and decanting.

Panning of stream sediment eliminated all organic material and the uranium content of the heavy mineral concentrates was correspondingly reduced (Table 8) with the exception of one sample (296801) which has increased in value by an insignificant amount. This sample was taken at a site where the stream was immediately below Vein II at Puissagtaq uranium showing (Armour-Brown et al., 1984) and it was thought that this relatively high level of uranium may constitute an anomaly derived from this mineral occurrence. To test this hypothesis it was necessary to identify the uranium bearing mineral phase in the heavy mineral concentrate. In order to do this the non-magnetic, heavy mineral (>3.3 SG) fraction was separated from the panned heavy mineral

Table 8. Uranium ppm (U) and loss of ignition (LOI) in % in stream sediment from dry sieved, wet sieved and decanted after 20 minutes, and panned heavy mineral concentrate from the same sample sites

sample site no.	dry sieved sample U	dry sieved sample LOI	wet sieved and decanted U	wet sieved and decanted LOI	panned heavy-mineral concentrate U	panned heavy-mineral concentrate LOI
296090	170.00	13.46	141.00	10.17	25.00	0.00
296499	115.00	19.05	104.00	10.05	11.00	0.00
296500	125.00	21.33				
296095			141.00	0.13	2.00	0.00
296801	58.50	4.86	55.10	3.02	62.00	0.00
296802	540.00	27.90	386.00	12.63	43.00	0.00
296803	347.00	17.92	320.00	8.00	97.00	0.00
297105	292.00		120.00		53.00	
297108	716.00		136.00		95.00	
297122	19.00		20.10		17.80	
297128	3.96		4.70		3.00	

concentrate along with another 3 samples for which there was no known reason for the high uranium value in the panned, heavy mineral fraction. Uranium analysis of the various fractions of two of these showed that uranium was higher in the non-magnetic, heavier mineral fraction (Table 9). Autoradiographs of thin sections made from this fraction revealed that between 0.4-0.7 % of the grains were the source of alpha radiation.

The minerals causing the radiation depended to some extent on the area from which the samples were collected. Samples taken from the stream immediately below the vein II (sample site 295358) at Puissagtaq contained mostly zoned zircon grains with fine inclusions (1-5 microns in diameter) of uranothorianite or uranothorite (fig. 38) (Table 10).

The zoned zircon is presumably derived from the granite whilst the uraniferous niobium minerals are probably derived from the radioactive Gardar microsyenite dykes. There are a number of them known to occur upstream from sample 296356.

Table 9. Uranium content of different fractions of the panned heavy mineral concentrate

Sample no.	U ppm in acid (10M HNO3) extractable acid				
		magnetic		non-magnetic	
	total	mag	weak mag.	light	heavy
296356	97	38	96	136	153
296358	8	5	7	2	59
297103	34		5	26	45
297115	50		83		106
	weight in grams				
296356	11.3	3.4	2.8	4.8	0.3
286358	14.3	4.0	2.6	7.4	0.3

Table 10. Microprobe analyses of radioactive minerals in the heavy, non-magnetic fraction of panned mineral samples from stream sediment

A. no.	S. no.	G. no.	UO_2	PbO	ThO_2	TiO_2	FeO	CaO	Ce_2O_3	Y_2O_3	Zr_2O	SiO_2
6	2963581	1	3.158	0.011	38.809	0.823	23.188	1.182	0.275	3.113	0.000	9.37
7	2963581	2	6.705	0.379	58.340	0.027	2.973	1.025	0.632	0.238	0.000	15.01
8	2963581	2	6.443	0.000	61.589	0.014	3.837	0.789	0.512	0.293	0.000	14.41
9	2963581	3	0.000	0.451	0.160	0.000	0.219	0.000	0.014	0.330	64.268	37.59
10	2963581	3	4.746	0.922	56.006	0.042	0.527	1.208	0.255	1.250	10.308	22.69
11	2963581	4	11.510	1.930	6.416	0.419	1.338	0.156	0.437	0.450	48.195	29.19
12	2963581	4	0.000	0.360	0.284	0.059	0.492	0.055	0.055	2.033	66.840	35.84
61	2963561	2	6.090	0.463	52.923	0.343	4.083	0.329	1.760	3.336	0.000	15.03
62	2963561	2	7.106	0.199	53.463	0.472	3.274	0.384	1.860	3.212	0.000	14.92
63	2963561	3	2.768	1.969	0.229	2.281	2.741	6.058	0.823	0.000	1.016	2.84
64	2963561	3	2.744	0.704	0.295	3.350	1.469	15.964	0.753	0.000	1.849	0.00
65	2963561	4	6.379	0.503	0.004	3.807	2.532	1.772	2.004	0.000	0.000	7.66
66	2963561	5	0.000	0.000	0.682	0.606	20.250	0.318	0.046	0.268	0.000	28.64
67	2963561	5	4.150	0.647	41.003	0.517	13.120	0.857	0.481	0.812	0.000	15.13

A. no.: Analytical no., S. no.: Sample no., G. no.: Grain no.

A. no.	Mineral
6	Inclusion in zircon
7	Uranothorianite inclusion in zircon
8	Uranothorianite inclusion in zircon
9	Zircon with inclusions
10	Uranothorite inclusion in zircon grain above (analytical no. 9)
11	Uraniferous zircon inclusion in zircon (anal. no. 12)
12	Zircon
61	Uranothorianite inclusion in zircon
62	Uranothorianite inclusion in zircon
63	Unknown uraniferous mineral probably pyrochlore
64	Unknown uraniferous mineral probably pyrochlore
65	Unknown uraniferous mineral
66	Unknown iron silicate with inclusions
67	Uranothorianite inclusion in iron silicate (anal. no. 66)

In the Qagsiarssuk area they could be derived from radioactive Gardar dykes or else from glacial transported material from the Motzfeldt Centre. In either case the source of the uraniferous grains is not the pitchblende veins as these minerals have never been found in association with them.

Considering the time it takes to make a panned heavy mineral concentrate (about 15-30 min) and the uncertainty of the interpretation of the results it can be concluded that heavy mineral panning is not an efficient way of locating pitchblende in this environment.

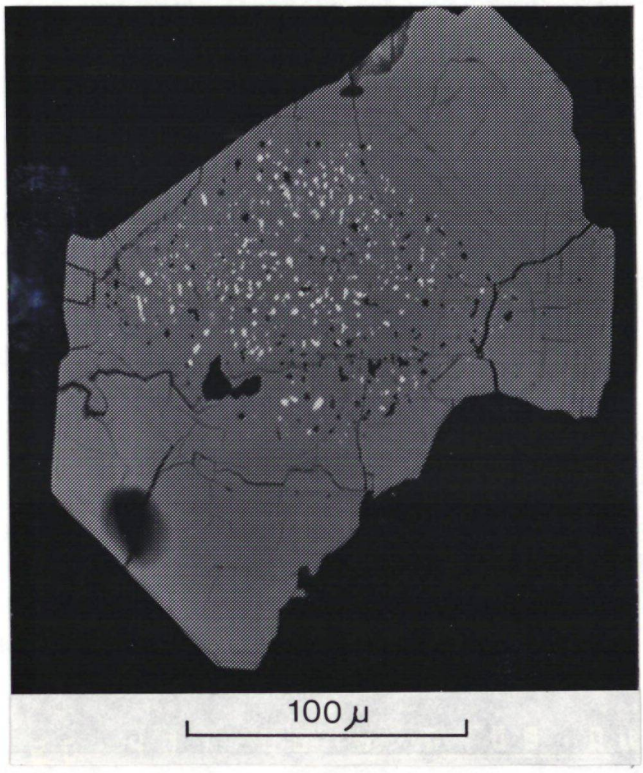

Fig. 38. BEI of zoned zircon (grey) with inclusions of uranothorite (white) in heavy mineral concentrate in sample no. 296356.

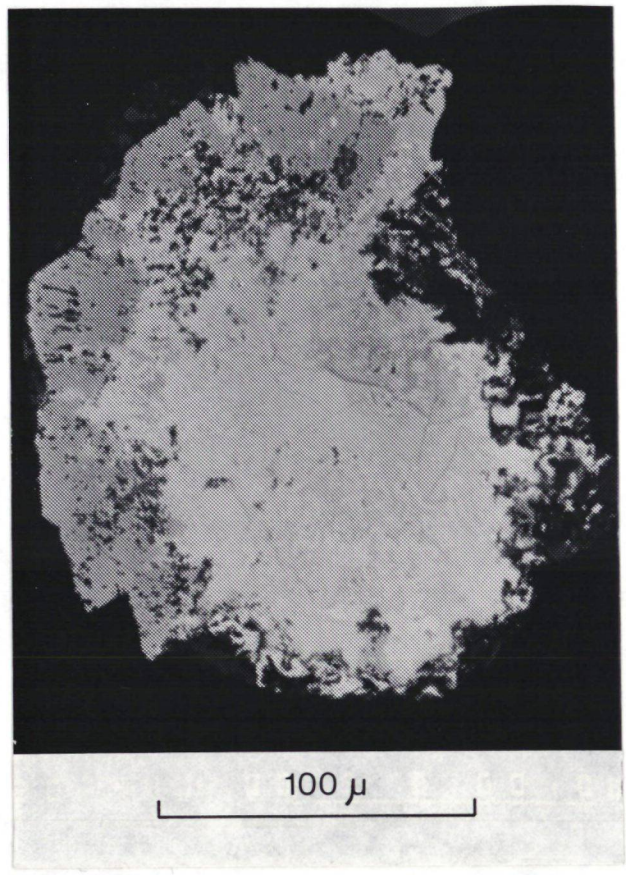

Fig. 39. BEI of uraniferous pyrochlore. Grey phase is zircon and white is uraniferous pyrochlore in heavy mineral concentrate in sample no. 296358.

4.2.2 Water sampling in the Qagssiarssuk area

Geochemical prospecting using water samples from streams and lakes was carried out in the Qagssiarssuk area. The water sampling was carried out because previous reconnaissance sampling in South Greenland (Armour-Brown et al., 1982) and more detailed water sampling in the granite area of Vatnahverfi (Armour-Brown et al., 1984) has proved successful. The purpose was to test the method in this area which is underlain by granite, carbonatitic rocks, sandstone, lava and a dyke swarm. The purpose was also to test the usefulness of lake water samples as this sample media has not been used in uranium prospecting in South Greenland. The terrain is rather flat, lying below 400 m.a.s.l., and to a great extent covered by vegetation. Many small streams and lakes are found and the area is covered by 88 lake water and 111 stream water samples. The samples are analysed for uranium, fluorine, pH and conductivity.

4.2.2.1 Lake water samples

The maximum and minimum values for the lake water samples are 9.82 and 0.39 ppb U respectively. The arithmetic mean is 0.94 and the geometric mean 0.76 ppb U. The histogram for uranium (fig. /40) shows a lognormal distribution but the plot of the cumulative percentages on probability paper show that the population plots on a line with a kink around the 70% percentile (fig. /41). Therefore, two populations seem to exist. The high values are associated with water having a pH higher than 7, which is probably caused by a carbonate content (fig. 42).

To illustrate the areal distribution of the uranium in lake water, the samples have been grouped into 4 classes and plotted (fig. 43). The class limits used are the 50,80 and 90 percentiles with the following number of samples and ppb U:

below 50	percentile	49	samples	below 0.70	ppb U
50-80	-.-	19	-.-	0.70 - 0.95	ppb U
80-90	-.-	13	-.-	0.96 - 1.30	ppb U
above 90	-.-	7	-.-	above 1.30	ppb U

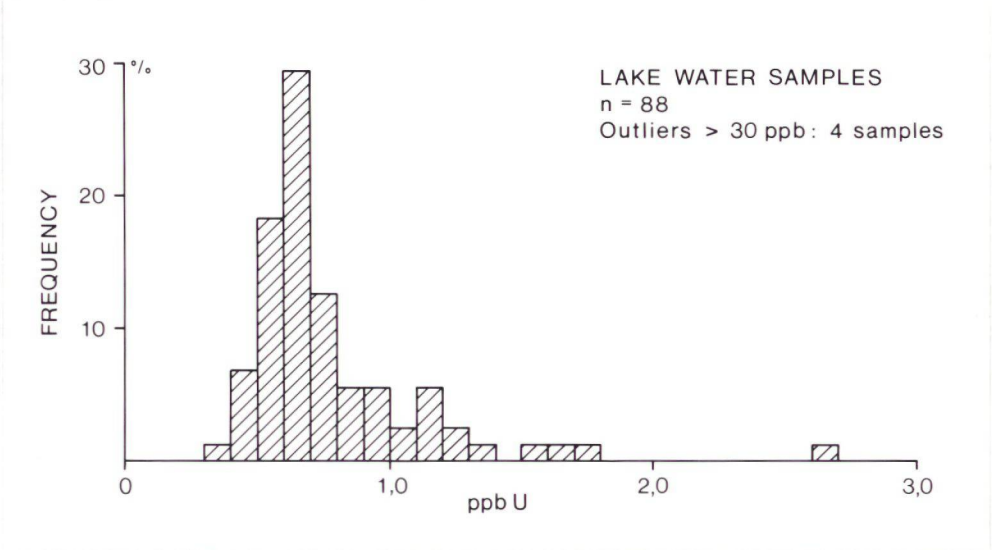

Fig. 40. Histogram of U in lake water samples - the Qagssiarssuk area.

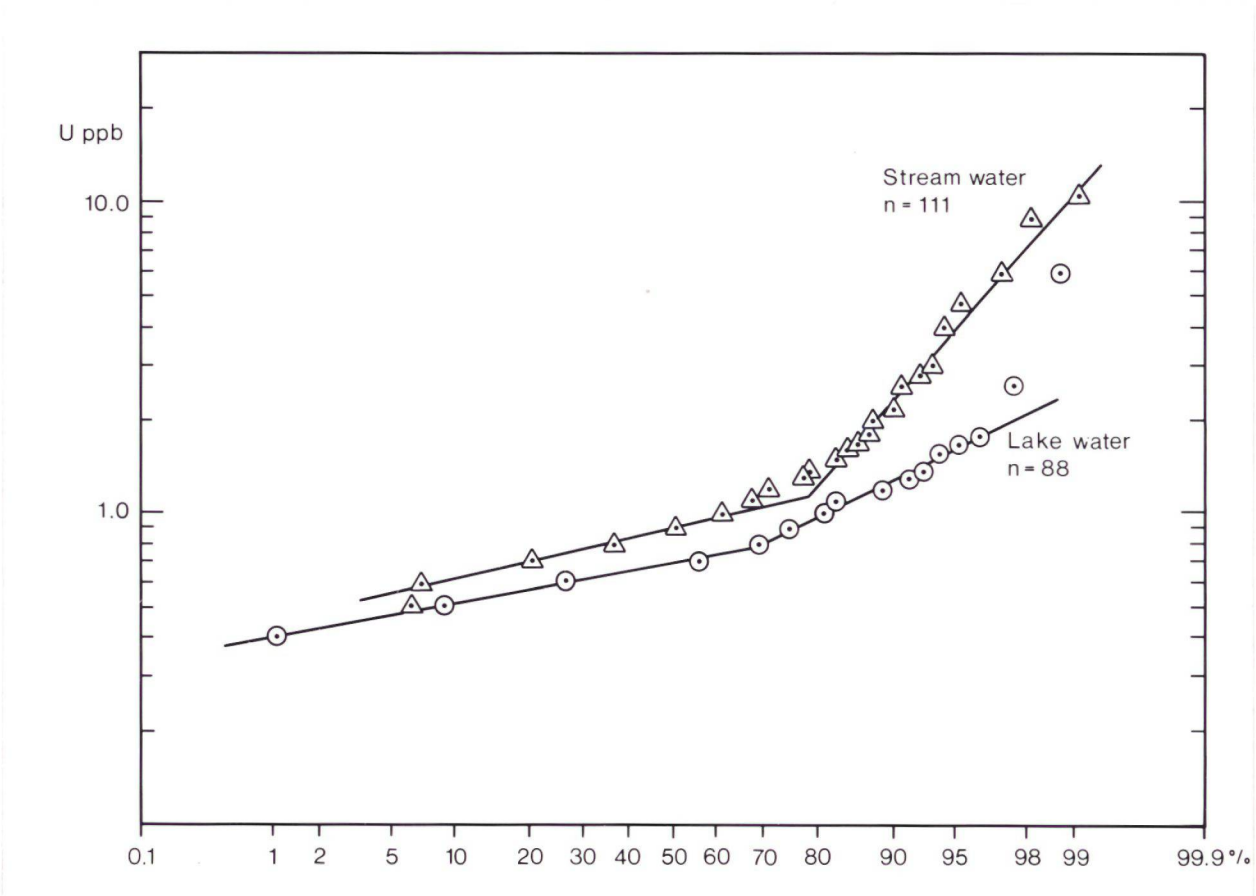

Fig. 41. Cumulative frequency curves of uranium in stream water and lake water from the Qagssiarssuk area.

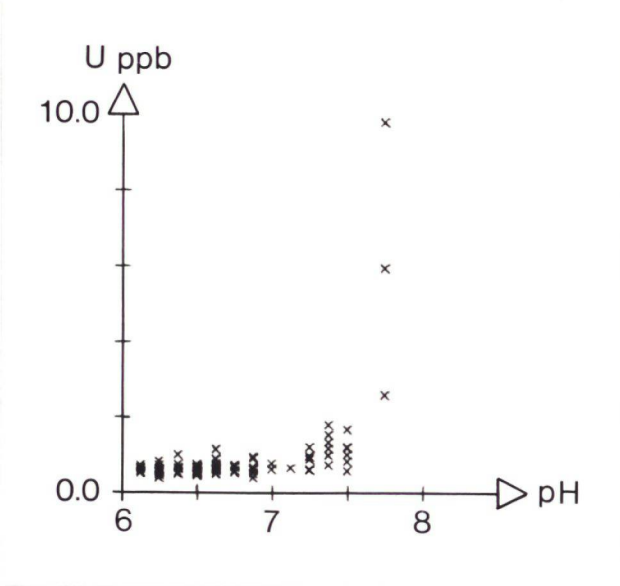

Fig. 42. U-pH scatter diagram for lake water samples, the Qagssiarssuk area.

The highest values are found in the northern part of the area (fig. 43) underlain by granite with carbonatite diatremes, and the carbonatitic rocks are causing the higher pH and carbonate complexing. The samples between the 80 and 90 percentile are more scattered over the area, but many lie in the sandstone, which are interbedded with carbonatitic volcanic flows and tuffs. SW of Qagssiarssuk. The single sample in the sandstone/lava area to the south is anomalous.

The fluorine content in the lake water samples vary between 0.02 and 1.70 ppm with a arithmetic mean at 0.15 ppm and a geometric mean at 0.10 ppm. The highest values (> 80 percentile) are sometime found associated with high U contents or with the carbonatitic rock in the Qagssiarssuk area.

4.2.2.2 Stream water samples

The maximum and minimum uranium values in the stream water samples are 13.90 and 0.06 ppb respectively, and the histogram (fig. /44 /& /41) has the same features as seen for the lake water samples. The arithmetic mean is 1.45 ppb U and the geometric mean 1.04 ppb. Several of the high U values are associated with pH higher than 7, and also in this case carbonate complexing occur (fig. 45). The water samples are also grouped into 4 classes with the following values:

below 50	percentile	57	samples	below 1.40	ppb U
50-80	-.-	31	-.-	0.90 - 1.40	ppb U
80-90	-.-	12	-.-	1.41 - 2.30	ppb U
above 90	-.-	11	-.-	above 2.30	ppb U

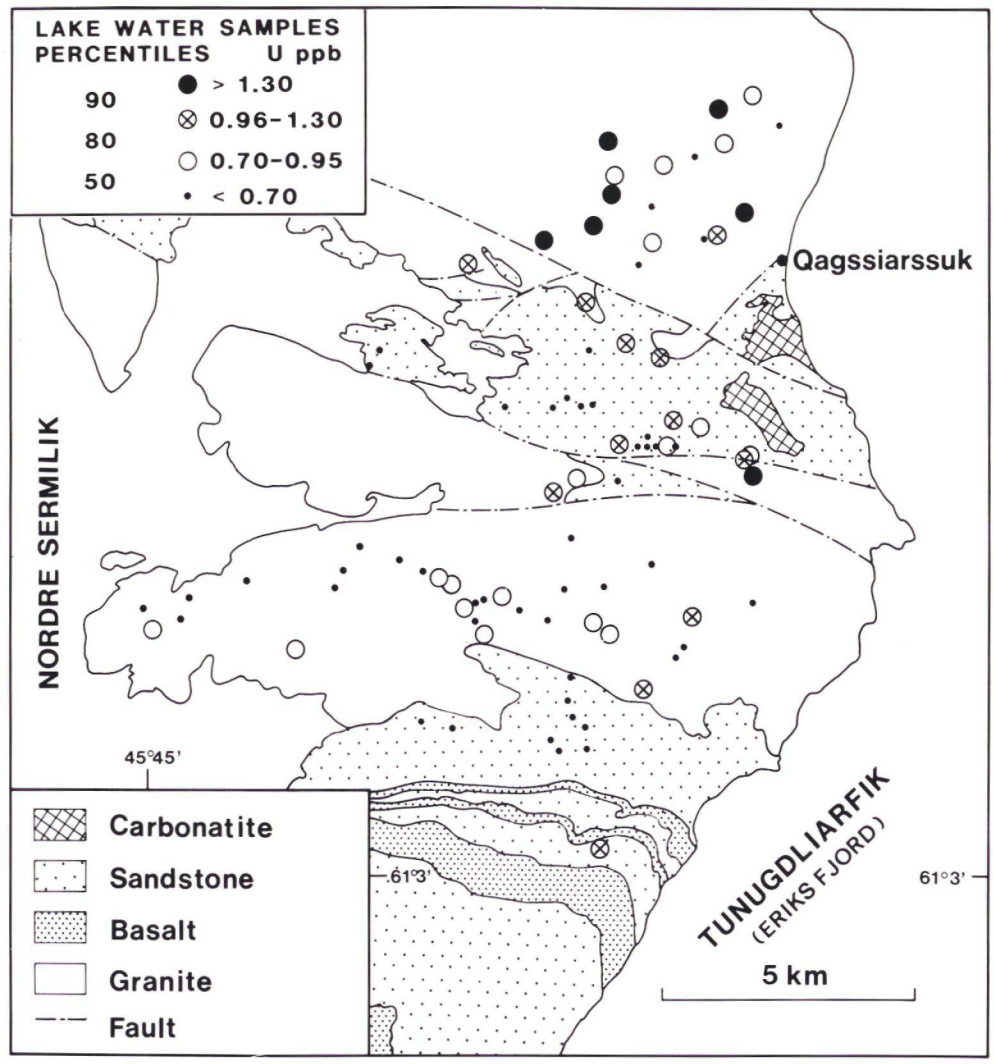

Fig. 43. Distribution of lake water samples in the Qagssiarssuk area divided into 4 classes.

The highest values (fig. 46 - above the 90 percentile) are found in the northern part of the area as the lake water samples, but also in the western part. The samples in the 80-90 percentile class are mainly found in the granite area to the south.

The fluorine content in stream water samples vary between 0.06 and 1.50 ppm with an arithmetic mean at 0.21 ppm and a geometric mean at 0.21 ppm. Also for this sample type the correlation between U and F is very low.

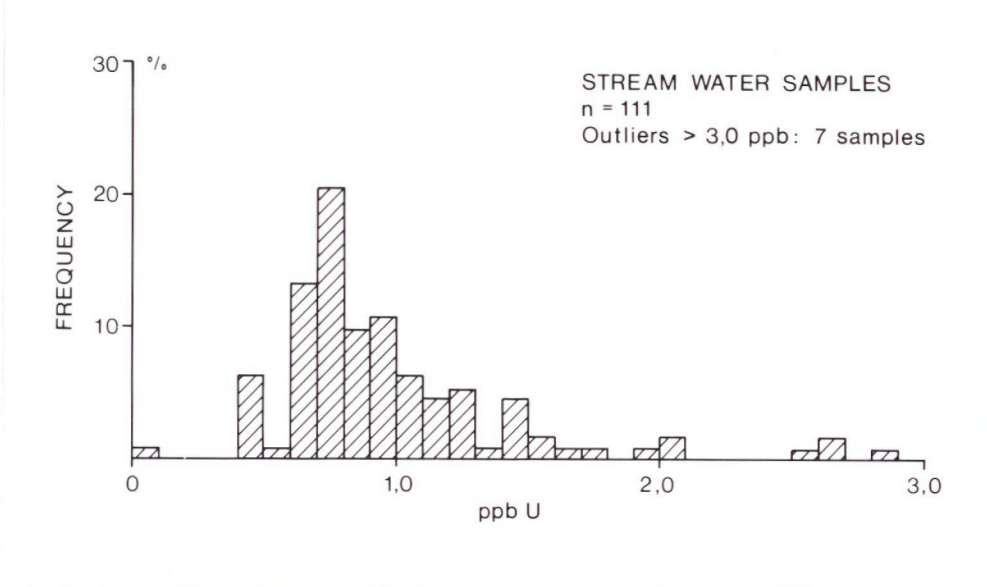

Fig. 44. Histogram of U in stream water samples - the Qagssiarssuk area.

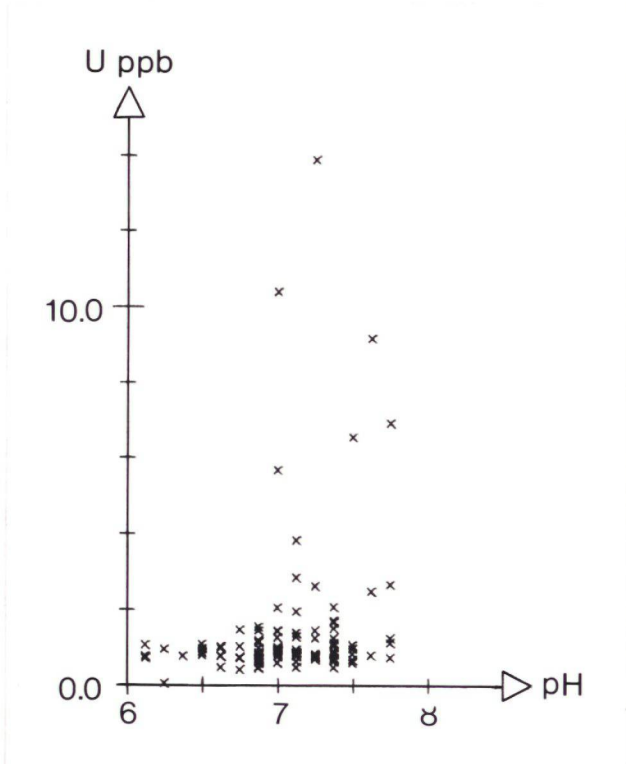

Fig. 45. U-pH scatter diagram for stream water samples, the Qagssiarssuk area.

4.2.2.3 Discussion and conclusions

The two sample media (streams and lakes) give more or less the same distribution of anomalous samples over the area with a lower U content in the lake water samples than in the stream water samples. The results do not lead to specific uranium mineral occurrences, but outline areas where other forms of uranium prospecting should be carried out. The northern part of the sampled

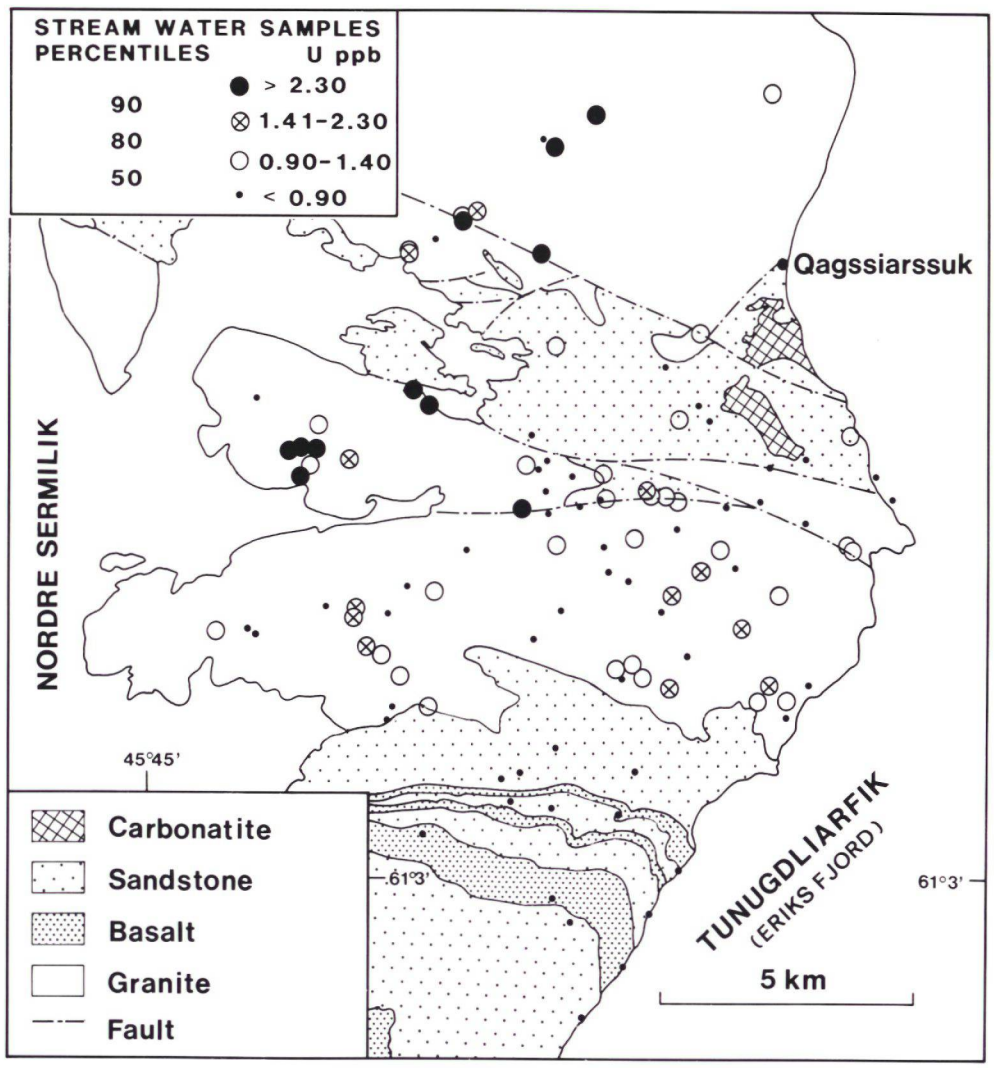

Fig. 46. Distribution of stream water samples in the Qagssiarssuk area divided into 4 classes.

area is clearly high in uranium although some of the uranium rich water samples can be explained by carbonate complexing. Only two localities with uranium mineral occurrences are found in this area, but it has not been prospected in detail. The western part is also anomalous and here pitchblende and brannerite occurrences are found. U and F are not well correlated, although samples with high uranium (> 80 percentile) sometimes will be high also in F (> 80 percentile) both for lake and stream water samples. This is probably because fluorite in this area is found both associated with the carbonatitic rocks with no uranium mineral occurrences and with pitchblende vein occurrences. In this area fluorite analyses cannot be used in combination with U as an indicator for uranium mineral occurrences.

One anomalous lake water sample was found in the sandstone/lava area to the southwest where also pitchblende and brannerite occurrences were found. The stream water samples from this area vary from 0.42 to 0.93 ppb U with an average of 0.71 ppb U, and compared with samples from a previous geochemical sampling (Armour-Brown et al., 1982) in other parts of the sandstone area where the uranium content often gave 0.00-0.05 ppb U, these samples are rather high, also taking the rainy field season 1984 into consideration field season 1984. Therefore the sandstone area between Qagssiarssuk and Narssaq merits more prospecting based on the water sampling results. As the background values for uranium are lower than in the granite area (Armour-Brown et al., 1982) it is necessary to treat samples from the Eriksfjord Formation separately to establish background and threshold values.

An important advantage of water over stream sediment as sampling medium is that the uranium contained in water is derived from a single cycle of erosion. Lake and stream water supplement each other and both media should be considered in future uranium exploration. The sample coverage of the prospected area will be much better, and as the method is quick it will not add much to the field costs. The lake water will probably be less influenced by rainfall than the stream water and therefore be more suitable for comparison of samples taken during different years. Stream water samples taken during previous field seasons from the same stream localities in the Qagssiarssuk area have much higher uranium values, and can not be compared with 1984 samples.

4.2.3 Soil sampling and ion absorbers placed in the soil

Soil sampling and ion absorbers placed in the soil were tried along three short profiles in the Puissagtaq area in order to evaluate these techniques as a method of localising pitchblende when it is buried beneath overburden. When the overburden is residual, soil sampling should be an adequate method for localising buried mineral occurrences. When the overburden is transported, however, for example glacial tills and slope sheetwash or covered by peat, it was felt that ion absorbers may be more useful.

Ion absorbers have been used mostly for surface water sampling (Asmund, 1974). Recent development in Russia of cloth impregnated with ion-absorbent resin has made the use of ion absorbers in the soil a more practical proposition (Lukashev, 1983). It works on the principle that metal ions tend

to move from the weathering rocks below in response to electrochemical forces through the overburden in the interstitial water along the grain boundaries. If ion absorbers are buried in the ground for a period then they will accumulate metal ions in proportion to the metal flux through the soil, which in turn will depend on the metal source and the nature of the secondary environment. A number of successful cases using this technique over known ore bodies in different terrains have been documented by Lukashev (1983). As metal ions will tend to migrate through different overburden at different rates and will be particularly susceptible to the water content, it is important that only sorbents buried in a similar type of overburden are compared. According to Lukashev's experience the sorbents should be left in the soil for a minimum of about 3 months depending on the nature of the overburden.

Four lines of soil samples, radiometric measurements and ion absorbers have been made in the Puissagtaq area over the three known veins described in the 1984 report (Armour-Brown et al., 1984). Attempts to buy the absorbers used by Lukashev from the USSR were delayed by bureaucracy. After the 1984 field season the Russian licensing authorities eventually came up with a price of $5000 for 200 absorbers, including ashing and analysis. Three types of absorber were used: MnO as a fine black powder made by Henrik Stendal at the Central Geological Institute of the University of Copenhagen, a fine resin called Chelex100 with a 100-200 mesh size and a coarse resin called Pyragolone. The first two absorber materials were packed into filter paper and the third was packed into nylon cloth. None of these methods were particularly satisfactory because the filter-paper covered absorbers were extremely difficult to retrieve without damaging them, and if the soil was dry the coarse resin in the nylon cloth was not so well in contact with the soil so that uptake of the pore water could not be so efficient. The superiority of the cloth impregnated with resin, such as those described by Lukashev, was evident. Firstly the cloth will maintain better contact with the surrounding soil and, therefore, take up the pore water better and secondly retrieval is quick and easy and sure, especially if a piece of string has been attached to it before burial.

The four lines were selected to intersect the known pitchblende occurrences and their projections, the continuation of geophysical anomalies and to be in different kinds of soil. The results of all the sampling media at each site are listed in the Appendix V.

The lines over vein I are in the relatively flat terrain just to the east of the Puissagtaq lake. They both ran from north to south and were measured in reference to the (0,0) point (note that this point corresponds to line 100E, 0

surveyed for the geophysical measurements made in 1982 (Armour-Brown et al., 1984). Line 12.5 W ran north-south through a waterlogged marshy area underlain by a peat horizon (Ao), which has formed over a poorly sorted glacial till of greater depth than 1.7 m. The absorbers were placed at the interface between the peat and the till, which was usually at about 30 cm depth. A second line was placed 15 m east of the 0,0 point where there was poorly developed soil over glacial sediments and till. Both lines were positioned so that they crossed the possible projection of the E-W striking vein I and the geophysical anomaly defined by the very low frequency (VLF-EM) measurements made in 1982.

The results of the three different kinds of absorber were comparable. They each seem to be able to absorb U ions within the 65 days that they lay in the soil. The coarser resin in the small bags tended to give lower values when the soil was drier otherwise differences are no more than would be expected by sample precision. The results from the fine resin in the filter paper are compared with the soil sample and scintillometer result along line 12.5 W (fig. 47). In this water saturated soil the ion absorbers give a well defined and narrower anomaly than the soil samples. The highest value is directly over the extension of the vein. The highest soil sample value is slightly displaced to the south while the scintillometer anomaly is slightly displaced to the north of the vein. The contrast between anomalous and background data is 100 fold for both types of sample media whereas the scintillometric value is only 3-5 times. The results confirm Lukashev´s findings which show that the ion absorbers in the soil give strong contrasts and correspond closely with underlying minerals. The results from line 15 E has not been reproduced in a figure, because they showed no significant variation above background levels in any of the sample media. It must be concluded that the pitchblende vein does not continue eastwards below the line despite the VLF-EM anomaly.

The results from ion absorbers and soil samples from a line crossing over vein II gave similar background results even over the vein. Clearly the soil at this locality is transported, possibly a combination of glacial and slope sheetwash. Either the ion sorbents were not left in the soil for long enough or else those laid over the vein disturbed the upward movement of the pore water when burying them. A large pit was dug at this point so that five of each sample type could be placed in the ground at roughly the same position so that sample variance could be measured. Only the MnO sorbent contained a consistent but insignificant 1 ppm U at this location.

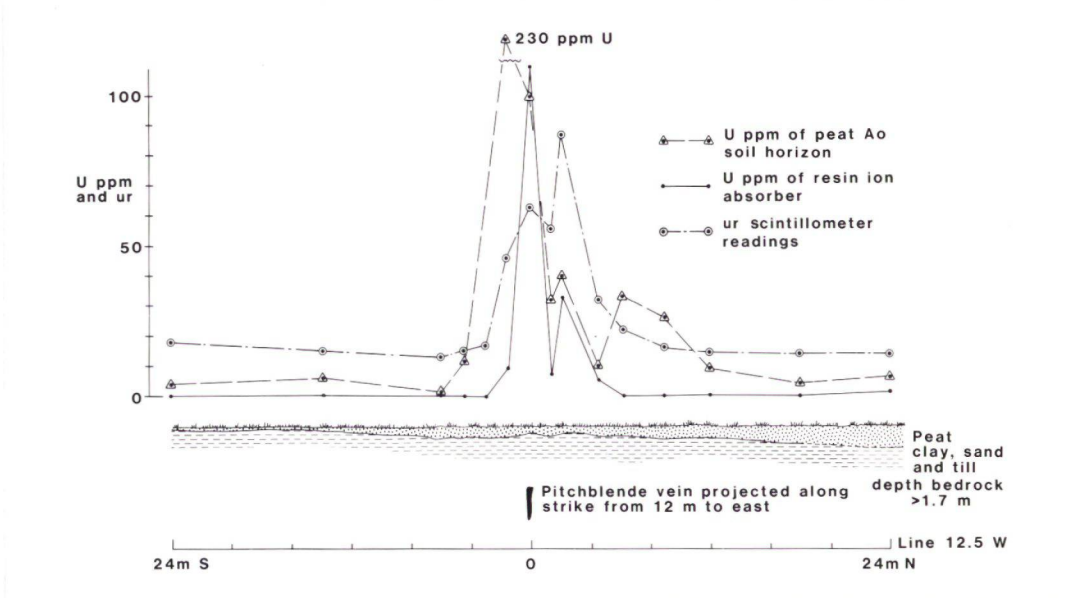

Fig. 47. Uranium values and radioactivity in soil and ion absorbers along line 12.5 W, Vein I, Puissagtaq.

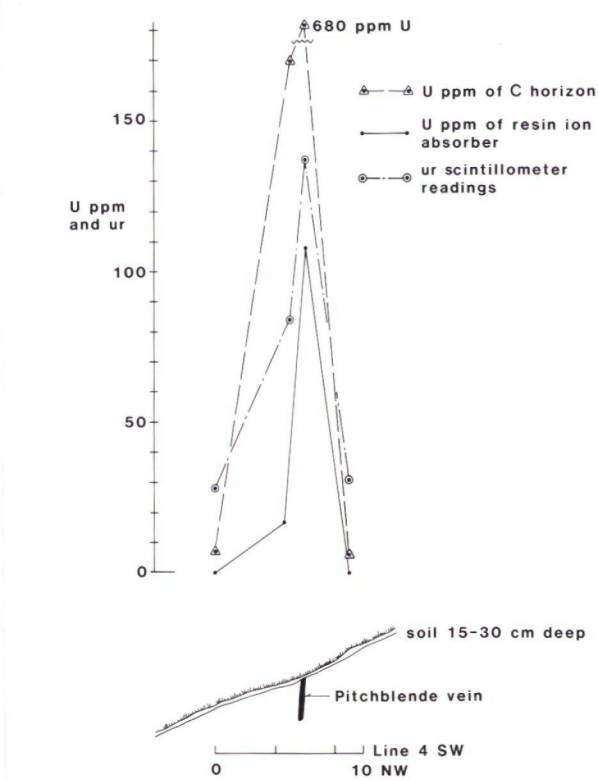

Fig. 48. Uranium values and radioactivity in soil and ion absorbers along line 4 SW, Vein III, Puissagtaq.

The line crossing vein III was on a steep slope where the soil was very shallow and probably residual with some local sheetwash transport. Some of the results are illustrated in (fig. 48). The resin ion absorber in filter paper shows the same strong contrast but the soil samples has an equally strong contrast. The soil samples, however, show a slight displacement downhill whereas the ion absorber anomaly lies directly over the pitchblende vein. Considering the thin nature of the soil it is hardly surprising that the scintillometer data also showed good correspondence with the pitchblende vein.

The general conclusion from these studies are that ion sorbents may be useful where the overburden is so thick that it masks the radioactivity, and where it is suspected that it is transported so that soil sampling is probably not effective. Although 2 months is ample time to allow U-ion absorption if the soils are saturated, it may be too short for dry well drained soils. Longer periods should be tried for these soil types in an orientation study. Before proceeding further with the method the correct sorbent cloth should be acquired and an orientation survey made over a known uranium occurrence which has preferably been tested by drilling so that its full extension under the overburden is known.

They may be particularly useful to check whether electromagnetic geophysical anomalies are uraniferous. Judging from the results of line 12.5W on Vein I and on Vein III it may also be useful for narrowing possible drilling targets as the anomalies appear to be located more exactly over actual mineral occurrences than soil sample data. On the other hand the broader expression of the soil sample anomalies will be more useful initially as they form a larger target and therefore fewer soil samples to define them.

4.3 Geophysical methods

4.3.1 Helicopter-borne and ground radiometric methods

Helicopter-borne radiometric methods which worked well at the reconnaissance stage of exploration have proved less efficient at the follow-up stage. None of the pitchblende veins have been located by helicopter surveys. Even where mineralisation was known to occur the helicopter-borne instrumentation did not give a response high enough to be recognised as an anomaly. This is due firstly to the fact that the radiation from the pitchblende is often masked by overburden and secondly that the measurement is diluted by the country rock which is barren of radiation.

Airborne radiometric results in particular give a very good estimate of the background radioelement content of the rocks. The likelihood, however, of detecting veins from the air is small even if they are exposed, because of the narrowness of the pitchblende occurrences. It must be concluded that helicopter-borne gamma-ray methods are not an effective method of follow-up exploration for pitchblende veins in the Granite Zone.

Ground radiometric prospecting, on the other hand, has proven effective providing the overburden is not deeper than 1 m. It is also useful for tracing radioactive boulders back to their source. Their instant response makes them extremely useful instruments both for locating and quickly evaluating uranium mineral occurrences. In the Granite Zone, however, there are many thorium dominated radioactive mineral occurrences, which are also detected and cannot be differentiated with total count scintillometers. Light single-channel gamma-spectrometers should be used in the field to overcome this problem.

It is, however, not often possible to eliminate areas from having any U-potential with ground scintillometry because knowledge of the depth of overburden is usually lacking.

It can be concluded that airborne radiometric methods are of limited use in searching for pitchblende occurrences in the Granite Zone. Ground radiometric instruments are, on the other hand, essential for good prospecting are easy to use and give immediate results. Their use should be extended to light single-channel gamma-spectrometers so that radioactivity from uranium and thorium could be differentiated in the field.

4.3.2 EM-VLF and magnetics in the Qagssiarssuk area

During the first half of the field season 1984 a very low frequency electromagnetic (VLF-EM) and magnetic survey was carried out in the Qagssiarssuk area by the Geophysical Section at GGU. (Thorning & Boserup, 1985). The main aim of the work was to make a traverse over the major fault zones in the area, over the granite and sandstone and their contact and the many dykes in this part of the Granite Zone to test the usefulness of these methods in an area with complex geology. Because of the terrain the profiles are broken but cover some of the geological features of the area. The preliminary results of this work show that these geophysical methods work as well in this area as they did at the Puissagtaq uranium prospect (Armour-Brown et al., 1984, and Nyegaard & Thorning, 1983). Unfortunately the results are not available at time of writing, but the conclusions from the Puissagtaq area

also cover the work in the Qagssiarssuk area, and are as follows (Armour-Brown et al., 1984):

1: It is possible to map the extent of fault zones by a combination of magnetics and VLF-EM.
2: The position of the individual conductors probably corresponds to faults and fractures.
3: Magnetic susceptibilities are generally lower in the fault zone than outside. The fault zone is therefore defined as a broad magnetic low.

In future prospecting geophysical methods - VLF-EM and magnetics - can be very useful in delineating the faults in the Granite Zone especially if it is carried out as an airborne survey over a wide area. They will also be useful in combination with other prospecting methods to outline possible drilling targets.

1.1 SUMMARY OF RESULTS AND CONCLUSIONS

The prospecting in the Qagssiarssuk area and on the nunatak north of Nordre Sermilik has contributed new interesting information about the uranium geology in the Granite Zone of South Greenland. The study of the Gardar structural setting of the Ivigtut-Julianehåb region gave new results, which will be valuable in future geological work or exploration in this area.

The following summarises the main results and conclusions:

1. The prospecting for uranium in the Qagssiarssuk area resulted in many new findings of uranium mineral occurrences in both the Julianehåb granite and in the sandstone of the Eriksfjord Formation.

2. The uranium mineral occurrences found close to the granite and sandstone contact indicate possibilities for uranium occurrences of the unconformity type known from the Athabasca Basin in Canada and the Pine Creek Geosyncline in Australia. This is particularly true of the two anomalous zones found in the sandstone where uranium and chlorite are associated together. The development of clay minerals are characteristic of the haloes found in association with unconformity type deposits.

3. The mineral assemblage of the uranium bearing veins in the Granite Zone is simple with mainly pitchblende and hematite with associated pyrite and chalcopyrite. Brannerite is found widespread in the altered and fractured granite as pseudomorphs after sphene and other Ti-bearing minerals in the wall rock or as veinlets both in granite and sandstone associated with chlorite.

4. The gangue minerals associated with the pitchblende veins are mainly quartz with some calcite, chlorite, fluorite and hematite. In the brannerite veinlets they are mainly calcite, chlorite and fluorite.

5. A REE study of fluorite suggests that the Motzfeldt complex was the source of the hydrothermal fluids.

6. A possible source for the uranium in this hydrothermal system was found on the nunatak north of Nordre Sermilik. Here, uraninite was found in rafts of gneiss in the Julianehåb granite. Isotopic age determinations on the uraninite gave 1780 +/-8 Ma, which corresponds to the age of the late Julianehåb granite. This finding demonstrates that uranium in non-resistate minerals was available in the granitic basement prior to the Gardar Period and may have been leached out by weathering, meteoric or hydrothermal waters.

7. It is proposed that the hydrothermal system was derived from the Gardar alkaline intrusions and driven by the heat that they produced. Uranium may have been derived from the late volatile phases of these intrusions. Its source could also have been oxygenating, meteoric waters hydrothermal fluids, which carried uranium in solution from the uraniferous basement rocks. The mixing of these two fluid systems in the still active Gardar faults could well have created the geochemical conditions for the precipitation of uranium.

8. The analysis of lineaments and faults in the Ivigtut-Julianehåb region showed that the lineament development was particularly intense between Neria in the north and the 10 km wide NE-SW trending lineament that runs through the Vatnahverfi area in the south.

9. The region could be divided into large blocks bounded by faults which have reacted differently to the regional stress field partly because of the original inherent structures of the blocks and partly because of local stress features. For example within the Gardar graben structure NW-SE trending faults are particularly well developed.

10. The regional stress field responsible was a E-W sinistral simple shear throughout the Gardar Period, which rotated anti-clock wise by about 20^{o}. The tension direction of this regional stress system was NW-SE and has given rise to the NE-SW striking tension features such as the graben and dyke swarms. It could also account for the crustal thinning which allowed the upwelling of the mantle and the development of the alkaline intrusions.

11. It is suggested that a major NE-SW sinistral transcurrent fault of Mesozoic age cross cuts the region south of Nunarssuit with a 40 km offset. Such an offset accounts better for the present distribution of the alkaline complexes in relation to the Gardar structural development.

12. Water sampling in the Qagssiarssuk area showed relatively high values in the sandstone areas prospected and a detailed geochemical water sampling programme in these areas is strongly recommended as a possible method to locate areas with unconformity type uranium occurrences.

13. Sampling of heavy mineral concentrates by panning will probably not be an efficient or effective way of locating pitchblende veins in the Granite Zone.

14. The studies with resin ion sorbents placed in the soil in the Puissagtaq uranium prospect showed that this method of prospecting may be useful as areas with thick overburden, but more orientation studies are necessary where the soil is relatively dry to prove that the method can be generally applied.

16. The magnetic and EM-VLF survey in the Qagssiarssuk area gave good results and the methods are useful in mapping fault zones. A survey over the whole Granite Zone could be used for locating fault zones especially in the basement below the Eriksfjord Formation where uranium deposits of the unconformity type may occur associated with faults.

17. The finding of many uranium mineral occurrences in the Qagssiarssuk and on the nunatak area by ground scintillometry shows that this is an efficient method of locating and evaluating them.

2 RECOMMENDATIONS

Uranium mineral occurrences continue to be found wherever exploration work is carried out in the Granite Zone, demonstrating beyond doubt that this is a uranium mineral district. The chances of finding an economic uranium mineral showing in this district must be rated very high if prospecting were to be continued. Recommendations for future work can be put under three headings: 1) detailed studies af mineral occurrences found during follow-up work, 2) continued exploration in the rest of the Granite Zone for uranium mineral occurrences, and 3) academic geological and geophysical studies which will help elucidate the geology of the area to give a more detailed framework of the geological history and the genesis of the uranium occurrences.

Detailed studies

Following the 1984 field seasons the two zones which were found in the Eriksfjord sandstone must be particularly recommmended for further detailed work. Both these anomalies strongly resemble haloes of the unconformity type of uranium deposits found under the Athabasca sandstone in Canada with minor uranium mineralisation associated with clay minerals. Following the work by Hoeve Quirt (1985) and Mellinger et al (1985) the clay minerals associated with the uranium occurrences in the Eriksfjord sandstones should be analysed. If these give interesting results clay analysis should be done on a systematic regional basis in order to detect variations in the illite chlorite content. If the results of this work are used in conjunction with EM-VLF and magnetic results then drilling targets could be outlined.

A third area which deserves more detailed investigation is the wide and well defined fault that runs E-W at Puissagtaq across the Igaliko peninsula. This should be surveyed by VLF-EM and magnetometer along its whole length, in order to define drilling targets under overburden or bedrock.

Follow-up exploration

Only about a quarter of the Granite Zone has been prospected so far. Further work should proceed first by detailed (1:5000-10,000) photogrammetric studies of the structural blocks outlined in this report so that the lineaments can be defined. Detailed scintillometric prospecting with water sampling should then

be made along these features. Light single channel gamma-ray spectrometers should be used in the field so that radioactivity from U can be differentiated from Th in the field.

Thermoluminesence of the quartz veins can be used to determine if uranium containing fluids have passed through the fracture system (Hochman Ypma, 1984), and a halo around ore bodies can be detected. Therefore quartz veins located in the fault zones with and without uranium mineral occurrences should be collected and thermoluminesence studies carried out to determine if uranium was present in the fluid phase and thereby help in narrowing down interesting areas.

Geological and geophysical studies

It can not be recommended, however, that any of the above work be carried out under the present oversupply of Uranium on the world market and if there is not the political wish to drill and exploit any resources that are found. Until such a time there are numerous purely geological studies which could be made to give not only a better understanding of the geology but also to set constraints for the various models that have been proposed for the structural development and intrusion of the Gardar alkaline rocks, and the related hydrothermal activity. Such work might also show that there are other elements of economic interest associated with this very widespread hydrothermal activity.

Studies of mineralogy, fluid inclusions, rare earth elements and carbon, oxygen and sulphur isotopic studies on vein material are of great interest. These studies would aid in the establishment of the relationships of the veins to the Gardar central complexes and the genesis of fluorite, carbonate, quartz and sulphide minerals associated with the pitchblende and thereby characterise the Gardar hydrothermal activity.

There still remain important regional geological and geophysical information which would greatly aid in the interpretation of the genesis and development of the Gardar province in general. These include a regional aeromagnetic survey, a gravimetric survey and lower age limit for the development of the Gardar.

The regional aeromagnetic survey made by the Kryolitselskabet Øresund A/S and processed at the Institute of Mathematical Statistics and Operations Research, the Technical University of Denmark (Conradsen et al., 1984) display some of the details that can be extracted from such a survey. The continuation of the magnetic survey over the Inland Ice (Thorning et al., 1985) will reveal the full extent of the Gardar province and elucidate some of the major fault displacements.

Combined ground EM-VLF and magnetic surveys over fault zones have been

carried out with success, and an airborne EM-VLF over the Granite Zone, would greatly support the structural interpretation of the Gardar structures and hence support the prospecting for uranium vein type occurrences associated with these structures.

The gravimetric survey carried out by Blundell (1978) has already established the presence of a 30 km wide, NE-SW elongated gravity "high" centered on the Ilímaussaq intrusion. This work should be extented to include as much of the Granite Zone as is economically feasible to test whether there is a similar anomaly under the Motzfeldt Centre, and whether it can support Upton & Emeleus´ (1986) hypothesis based on petrochemical data, that the Gardar igneous rocks in the central lying area between Tugtutôq - Ilímaussaq zone was tapping a more deeply seated zone of the mantel than the Nunarssuit zone to the north.

The initiation of the Gardar period has never been adequately dated. It is bracketed by late Ketilidian granite and early dolerite dykes of Gardar age and occurred between 1600 and 1310 Ma (Allaart, 1983). It presumably started about 1400 Ma as indicated by palaeomagnetic data (Piper, 1977) with rifting and the penecontemporaneous sedimentation of the Eriksfjord Formation. It would be useful to confirm the exact date by isotopic methods so that time constraints could be placed on the Gardar structural and igneous development.

REFERENCES

Alderton, D.H.M., Pearce, J.A. & Potts, P.J. 1980: Rare earth element mobility during alteration: Evidence from Southwest England. Earth Planet. Sci. Lett., 49, 149-165.

Allaart, J.H. 1969: The chronology and petrography of the Gardar dykes between Igaliko Fjord and Redekammen, South Greenland. Rapp. Grønlands geol. Unders., 25, 26pp.

Allaart, J.H. 1973: Descriptive text to Geological map of Greenland 1:100 000, Julianehåb 60 V 2 Nord. Copenhagen: Grønlands geol. Unders. (also Meddr Grønland 192,4) 41pp.

Allaart, J.H. 1983: Descriptive text to Geological map of Greenland 1:100 000, Narssarssuaq 61 V.3 Syd. Copenhagen: Grønlands geol. Unders., 20 pp.

Armour-Brown, A. & Wallin, B. 1985: Ketilidian uranium mineral occurrences in South Greenland. Report of activities, 1984. Rapp. Grønlands Geol. Unders. 125, 66-74.

Armour-Brown, A. 1986: Geology and evaluation of the uranium occurrence at Igdlorssuit, South Greenland. The South Greenland Exploration Programme 1984-1986, Report No. 2. Unpubl. internal GGU rep.

Armour-Brown, A., Tukiainen, T. & Wallin, B. 1982: Pitchblende vein discoveries in the Proterozoic Ketilidian granite of South Greenland. Geol. Rundschau 71, 73-80.

Armour-Brown, A., Tukiainen, T. & Wallin, B. 1982: The South Greenland uranium exploration programme, Final Report of reconnaissance results. Unpubl. internal GGU rep., 107 pp.

Armour-Brown, A., Tukiainen, T., Wallin, B., Bradshaw, C., Emeleus, C.H. 1983: Uranium exploration in South Greenland. Rapp. Grønlands geol. Unders. 115, 68-75.

Armour-Brown, A. Steenfelt, A. & Kunzendorf, H. 1983: Uranium districts defined by reconnaissance geochemistry in South Greenland. J. Geochem. Explor., 19, 127-145.

Armour-Brown, A., Tukiainen, T., Nyegaard, P. & Wallin, B. 1984: The South Greenland Exploration Programme. Final report of progress 1980-1983. Unpubl. internal G.G.U. rep., 107 pp.

Asmund, G. 1974: Hydrogeochemical investigations on river water in West, South and East Greenland. Rapp. Grønlands geol. Unders. 65, 71-73.

Baer, A.J. 1981: A Greenvillian model of Proterozoic plate tectonics. In Kröner, A. (ed.): Precambrian plate tectonics. Elsevier. 353-385.

Bailey, J., Gwozdz, R., Rose-Hansen, J. & Sørensen, H. 1978: Preliminary geochemical work on the Ilímaussaq alkaline intrusion, South Greenland. Rapp. Grønlands geol Under. 90, 75-79.

Bak, J., Sørensen, K., Grocott, J., Korsgård, J.A., Nash, D. & Waterson, J. 1975: Tectonic implications of Precambrian shear belts in western Greenland. Nature 254, 566-569.

Berthelsen, A. 1962: On the geology of the country around Ivigtut, SW-Greenland. Geol. Rdsch. 52, 269-280.

Berthelsen, A. & Henriksen, N. 1975: Descriptive text to Geological map of Greenland 1: 100 000, Ivigtut, 61 V 1 Syd. Grønlands geol. Unders., Copenhagen (also Meddr Grønland 185, 1) 210 pp.

Berthelsen, A. & Noe-Nygaard, A. 1965: The Precambrian of Greenland. In: Rankama, K. (ed.) Precambrian, Vol 2., Interscience Publishers. 113-262.

Blundell, D.J. 1978: A gravity survey across the Gardar Igneous Province, SW Greenland. Jl. Geol. Soc. Lond. 135, 545-554.

Chatterjee, A.K. 1985: Rare earth elements and oxygen isotopic signatures for the distribution, mobilization and concentration of uranium in the South Mountain Batholith, Nova Scotia. In: Concentration mechanisms of uranium in geological environments. Program and extended abstracts, Nancy, France, 155-162.

Guichard, F., Church, T.M., Treuil, M. & Jaffrezic, H. 1979: Rare earth in barites: distribution and effects on aqueous partitioning. Geochim. Cosmochim. Acta 43, 983-997.

Conradsen, K., Nilsson, G., Thyrsted, T. & Nielsen, B.K. 1985: Application of remote sensing in uranium exploration in South Greenland. Unpubl. internal DTH rep., IMSOR, The Tecnical University of Denmark, 157 pp.

Delaloyle, M. 1979: The total lead method. In: Jäger, E. & Hunzinker, J.C. (edit.) Lectures in Isotope Geology, 132-133. Springer-Verlag, Berlin.

Emeleus, C.H. 1964: The Grønnedal-Ika alkaline complex, South Greenland. The structure and geological history of the complex. Bull. Grønlands geol. Unders. 45 (also Meddr Grønland 172,3) 75 pp..

Emeleus, C.H. & Upton B.G.J 1976: The Gardar period in southern Greenland. In: Escher, A. & Watt, W.S. Geology of Greenland, 152-181. Copenhagen: Geol. Surv. Greenland.

Emeleus, C.H. & Stephenson, D. 1970: Field work between Tunugdliarfik and Tasiussaq. Rapp. Grønlands geol. Unders. 28, 30-32.

Ferguson, J. & Goleby, A.B. (edit.) 1980: Uranium in the Pine Creek Geosyncline. IAEA, Vienna. 760 pp.

Ghisler, M. 1968: The geological setting and mineralizations west of Lilianmine, South Greenland. Rapp. Grønlands geol. Unders. 16, 53 pp.

Hansen, J. 1968: A study of radioactive veins containing rare-earth minerals in the area surrounding the Ilímaussaq alkaline intrusion in South Greenland. Bull. Grønlands geol. Unders. 76 (also Meddr Grønland 181, 8) 47 pp.

Harry, W.T. & Oen Ing Soen 1964: The pre-Cambrian basement of Alangorssuarq, South Greenland, and its copper mineralization at Josvaminen. Bull. Grønlands geol. Unders. 47 (also Meddr Grønland 179), 72 pp.

Henriksen, N. 1960: Structural analysis of a fault in South-West Greenland. Bull. Grønlands geol. Unders. 26 (also Meddr Grønland 162,9) 15 - 41.

Hochman, M.B.M. & Ypma, P.J.M 1984: Thermoluminescence as a tool in uranium exploration. J. Geochem. Explor. 22, 313-331.

Hoeve, J. & Sibbald, T.I.I. 1978: Mineralogy and geological setting of unconformaty-type uranium deposist in Northern Saskatchewan. In: Kimberley, M.M. (ed.) Short course in uranium deposits: Their mineralogy and origin. Short cource handbook Vol 3. Min. Assoc. Can., 457-474.

Hoeve, J., Sibbald, T.I.I., Ramaekers, P. & Lewry, J.F. 1980: Athabasca Basin unconformaty-type uranium deposits: A special class of sandstone-type deposits? In: Ferguson, J. & Goleby, A.B. (edit.) Uranium in Pine Creek Geosyncline. IAEA, Vienna, 575-594.

Hoeve,J. & Quirt, D. 1985: A stationary redox front as a critical factor in the formation of high-grade, unconformity-type uranium ores in the Athabasca Basin, Saskatchewan. In: Concentration mechanisms of uranium in geological environments, Program and extended abstracts, Nancy, France, 219-224.

Hood, P. & Bower, M.E. 1973: Low-level aeromanetic surveys of the continental shelves bordering Baffin Bay and the Labrador Sea. In: Hood, P. (ed.) Earth Science Symposium on Offshore Eastern Canada. Geol. Surv. Can., Paper 71-23, 573-598.

Irving, E. & McMglynn, J.C. 1981: On the coherence, rotation and palaeolatitude of Laurentia in the Proterozoic. In: Kröner, A. (ed.) Precambrian plate tectonics. Elsevier. 563-598.

Kalsbeek, F.& Taylor, P.N. 1985: Isotopic and chemical variation in granites across a Proterozoic continental margin - the Ketilidian mobile belt of South Greenland. Earth Planet. Sci. Lett., 73, 65-80.

Knudsen, C. 1986: Apatite mineralisation in carbonatite and ultramafic intrusions in Greenland. Unpubl. internal GGU rep., 176 pp.

Koeppel, V. 1968: Age and history of uranium mineralization of the Beaverlodge area, Saskatchewan. Geol. Surv. Can. Paper 67-31, 11 pp.

Le Pichon, X, Sibuet, J.-C. & Franchetenau, J. 1977: The fit of the continents around the North Atlantic Ocean. Tectonophysics 38, 47-51.

Lukashev, V.K. 1983: Mode of occurrence of elements in the secondary environment. In Björklund, A. (ed.) Proceedings of the 10th International Geochemical Exploration Symposium. Vol. 21, no. 1-3, 73-88.

Mellinger, M., Quirt, D. & Hoeve, J. 1985: Geochemical signatures of uranium deposition in the Athabasca Basin of Saskatchewan (Canada). In: Concentration mechanisms of uranium in geological environments, Program and extended abstracts, Nancy, France, 205-209.

Möller, P. & Morteani, G. 1983: On the geochemical fractionation of rare earth elements during the formation of Ca-minerals and its application to problems of the genesis of ore deposits. In: Augustithis, S.S (ed.) The significance of trace elements in solving petrogenetic problems & controversies, pp 747-791. Theophrastus, Athens.

Möller, P.,Parekh, P.P. & Schneider, H.-J. 1976: The application of Tb/La-Tb/Ca abundance ratios to problems of fluorspar genesis. Mineral. Deposita, 11, 111-116.

Möller, P.,Parekh, P.P. & Simon, P. 1976: Seltene Erden als geochemische Indikatoren für die Genese von Fluorit und Calcit auf Gang und Kluft-lagerstatten im Weserbergland (Nordwest-Deutschland) und benachbarten Gebieten. Geol. Jb. D 20, 77-112.

Möller, P., Morteani, G., Hoefs, J. & Parekh, P.P. 1979: The origin of ore-bearing solution in the Pb-Zn veins of the western Harz, Germany, as deduced from rare-earth elements and isotope distributions in calcites. Chem. Geol., 26, 197-215.

Möller, P., Morteani, G. & Dulski, P. 1984: The origin of calcites from Ob-Zn veins in the Harz Mountains, Federal Republic of Germany. Chem. Geol., 45, 91-112.

Nyegaard, P. 1985: Uranium exploration in the Qagssiarssuk area, South Greenland. Report of Activities 1984. Rapp. Grønlands geol. Unders. 125, 74-78.

Nyegaard, P. & Thorning, L. 1983: Geophysical and geological fieldwork on fault structures at the Igaliko peninsula, South Greenland. Rapp. Grønlands geol. Unders. 115, 75-79.

Nyegaard, P., Armour-Brown, A. & Steenfelt, A. 1986: Vein type uranium mineral occurrences in South Greenland. In: Fuchs, H.D. (ed.) Vein type uranium deposits. IAEA-TECDOC 361, I.A.E.A., Vienna, 43-55.

Piper, J.D.A. 1976a: Palaeomagnetism of marginal syenites and fractionated rocks of the Ilímaussaq intrusion, South Greenland. Bull. geol. Soc. Denmark 25, 89-97.

Piper, J.D.A. 1977: Magnetic stratigraphy and magnetic-petrologic properties of Precambrian Gardar lavas, South Greenland. Earth Planet. Sci. Lett. 34, 247-263.

Piper, J.D.A. 1977: Palaeomagnetism of the Giant Dykes of Tugtutôq and Narssaq Gabbro, Gardar igneous province, South Greenland. Bull. geol. Soc. Denmark 26, 85-94.

Piper, J.D.A 1982: The Precambrian palaeomagnetic record: the case for the Proterozoic supercontinent. Earth Planet. Sci. Lett. 59, 61-89.

Piper, J.D.A. & Stearn, J.E.F. 1977: Palaeomagnetism of the dyke swarms of the Gardar igneous province, South Greenland. Phys. Earth Planet. Inter. 14, 345-358.

Plant, J. 1971: Orientation studies on stream sediment sampling for a regional geochemical survey in Northern Scotland. Trans. Inst. Min. Metall. 80, 324-344.

Poulsen, V. 1964: The sandstones of the Precambrian Eriksfjord Formation in South Greenland. Rapp. Grønlands geol. Unders. 2, 16 pp.

Pulvertaft, C.T.R. 1967: Geological map of Greenland 1:100 000, 60 V.1 Nord Nunarssuit. Copenhagen. Grønlands geol. Unders.

Roberts, D.E. & Hudson, G.R.T. 1983: The Olympic Dam copper-uranium-gold deposit, Roxby Downs, South Australia. Econ. geol. 78, 799-822.

Robinson, S.C. 1955: Mineralogy of uranium deposits, Goldfields, Saskatchewan. Geol. Surv. Can. Bull. 31, 128 pp.

Ruhlmann, F. 1985: Mineralogy and metallogeny of uraniferous occurrences in the Carswel structure. In Laine, R., Alonso, D. & Svab, M. (edit.) The Carswell structure uranium deposits, Saskatchewan. Geol. Ass. Can., Special paper 29, 105-120

Ruzicka, V. & Littlejohn, A.L. 1982: Notes on mineralogy of various types of uranium deposits and genetic implications. In: Current research, Part A, Geol. Surv. Can. Paper 82-1A, 341-349.

Schönwandt, H.K. 1983: Interpretation of ore microstructures from a seleneous Cu-mineralization in South Greenland. Neues Jahrbuch Miner. Abh. 146, 302-332.

Steenfelt, A. 1972: Beskrivelse af pulaskite, heterogen foyait, sodalit-foyait, naujait og kakortokit på Kvanefjeldsplateauet, Ilímaussaq. Unpubl. dissertation, Univ. Copenhagen (also Unpubl. internal GGU rep.) 58 pp.

Stephenson, D., 1976: A simple-shear model for the ductile deformation of high-level intrusions in South Greenland. J. geol. Soc. Lond. 132, 307-318.

Stewart, J.W. 1964: The earlier Gardar igneous rocks of the Ilímaussaq area, South Greenland. Unpublished Ph.D. Thesis, Univ. Durham, England, 423 pp.

Stewart, J.W. 1970: Precambrian alkaline-ultramafic/carbonatite volcanism at Qagssiarssuk, South Greenland. Bull. Grønlands geol. Unders. 84 (also Meddr Grønland 186,4) 70 pp.

Tanner, W.F. 1962: Surface structural patterns obtained from strike-slip models. Jour. Geol. 70, 101-107.

Thorning, L. & Boserup, M. 1985: Geophysical field work in relation to mineral exploration programmes in South Greenland. Rapp. Grønlands geol. Unders. 125, 78-83.

Thorning, L., Bower, M., Hardwick,. C.D. & Hood, P.J. 1985: Greenland ice cap aeromagnetic survey 1984: reconnaissance lines in southern Greenland. Rapp. Grønlands geol. Unders. 125, 83-84.

Tremblay, L.P. 1958: Geology of uranium deposits of Beaverlodge region, Saskatchewan,. UN 2nd Inter. Conf. Peaceful Uses of Atomic Energy, Geneva 2, 491-497

Tremblay. L.P. 1978: Geological setting of the Beaverlodge-type of vein-uranium deposit and its comparison to that of the unconformaty-type. In: Kimberley, M.M. (ed.) Short course in uranium deposits: Their mineralogy and origin. Mineralogical Association of Canada, 431-456.

Upton, B.G.J. 1974: The alkaline Province of South-West Greenland. In Sørensen, H. (ed): The alkaline rocks. John Wiley & Sons. 221-238.

Upton, B.G.J. & Blundell, D.J. 1978: The Gardar igneous province: evidence for Proterozoic continental rifting. In Neumann, E.R. & Ramberg, I.B. (eds.) Petrology and Geochemistry of Continental Rifts, 163-172.

Upton, B.G.J. & Fitton, T.G. 1985: Gardar dykes north of the Igaliko Syenite Complex, southern Greenland. Rapp. Grønlands geol. Unders. 127, 24 pp.

Upton, B.G.J. & Emeleus, C.H. 1986: Mid-Proterozoic alkaline magmatism in South Greenland: The Gardar Province. Spec. Publ. Geol. Soc. London. (in press).

Van Breemen, O., Aftalion, M. & Allaart, J.H. 1974: Isotopic and geochronologic studies on granites from the Ketilidian mobil belt of South Greenland. Bull. geol. Soc. Amer. 85, 403-412.

Watt, W.S. 1969: The coast-parallel dike swarm of southwest Greenland in relation to the opening of the Labrador Sea. Can. J. Earth Sci. 6, 1320-1321.

Wedepohl, K.H. (ed.) 1978: Handbook of Geochemistry. Vol II/5. Springer Verlag.

Wilde, A.R., Wall, V.J. & Bloom, M.S. 1985: Wall-rock alteration associated with unconformity-related uranium deposits Northern Territory, Australia: Implications for uranium transport and depositional mechanisms. In Concentration mechanisms of uranium in geological environments, Program and extended abstracts, Nancy, France, 231-239.

Williams-Jones, A.E. & Sawiuk, M.J. 1985: The Karpinka lake uranium prospect, Saskatchewan: A possible metamorphosed middle Precambrian sandstone-type uranium deposit. Econ. Geol. 80, 1927-1941

APPENDIX I

ANALYTICAL RESULTS OF ROCK SAMPLES FROM THE GRANITE ZONE

U>100 ppm and U/Th>1.0. All values in ppm.
Sample locations: Map 2.

GGU No	eU	U	eTh	Zr	Nb	Y	Cu	Zn	Pb
244154	-	112	-	312	3609	291	23	1880	12
244169	-	190	-	1264	4579	961	74	1275	67
244176	-	160	-	1229	3062	595	64	2847	88
244191	-	171	-	2137	3977	967	48	393	44
252947	525	353	14	24	19	35	0	25	108
252948	-	1950	-	119	125	141	54	64	731
252952	2590	2370	256	639	348	260	24	118	232
277581	-	125	-	-	-	-	-	-	-
277584	-	165	-	-	-	-	-	-	-
277595	1830	1740	11	270	180	106	57	188	444
277596	-	194	-	53	19	7	14	79	140
287136	12700	13300	2090	143	274	123	44	72	656
287146	2860	3620	7	87	121	72	68	21	464
297601	894	910	15	232	72	49	0	50	183
297684	8844	5770	13	293	139	90	41	126	376
297696	-	7890	-	-	-	-	-	-	-
297697	-	193	-	245	32	26	95	60	338
297698	12674	10300	111	1333	655	709	47	155	344
297699	-	36300	-	1078	1036	554	110	72	2492
297700	2273	568	0	410	40	83	24	45	42
297710	1100	10	0	39	4	0	19	41	389
297711	561	517	12	399	150	51	94	246	42
297713	284	11	6	81	7	0	1	32	109
297718*	-	16900	-	21804	198599	26872	573	172	1184
297721	1020	892	28	191	59	79	45	80	231
297726	277	85	0	29	0	84	17080	160	949
297727	-	118	-	29	12	96	31312	225	1437
297733	4450	3550	38	191	103	119	-	-	-
297734	742	121	27	261	27	12	9	52	111
297736	207	48	2	242	14	103	-	-	-
297746	147	139	4	344	30	55	-	-	-
297748	282	381	120	209	59	76	17	83	103
297749	-	614	-	407	47	82	4	79	313
297802	-	152	-	4470	2057	321	105	483	96
297835	570	664	70	2961	764	367	109	237	116
297836	149	154	72	5927	607	451	68	372	103
297841	-	2230	-	647	578	226	61	252	1052
297872	17000	15700	335	327	480	282	-	-	-
297873	9370	6070	0	-	-	-	-	-	-
297875	1990	2050	3	901	271	105	21	59	112
297877	22000	38800	4880	537	975	533	-	-	-
297883	229	176	21	262	30	28	4	93	54
297889	201	298	17	229	54	40	0	50	18

* This sample is pure allanite, and the analytical results are dubious

ANALYTICAL RESULTS cont.

GGU No	eU	U	eTh	Zr	Nb	Y	Cu	Zn	Pb
297901	16500	13700	450	2458	1005	707	-	-	-
297902	1888	2670	531	748	326	301	0	65	63
297903	759	1040	256	666	178	209	21	33	71
297909	-	267	-	329	96	37	11	570	34
297918	958	948	133	7634	27018	494	101	276	61
297920	-	824	-	26378	33047	877	34	2908	301
297929	633	584	107	68	42	43	0	34	58
297932	283	258	158	4437	169	687	26	50	69
298002	-	134	-	644	139	85	24	151	38
298004	190	229	104	298	13	87	9	46	41
298005	551	530	199	378	51	113	15	50	28
298010	157	488	26	167	30	32	0	60	131
298015	284	488	49	240	39	27	528	60	70
298018	1020	114	0	76	25	16	38	53	208
298019	-	732	-	284	91	60	39	150	151
298030	837	124	7	208	21	40	215	126	145
298031	1210	93	4	240	13	41	124	81	381
298032	-	2970	-	247	29	32	134	79	148
298034	483	528	14	249	26	27	135	74	157
298040	106	92	95	255	148	182	45	168	84
298046	101	106	5	1472	182	71	76	104	188
298048	-	159	-	382	112	43	55	65	68
304201	171	-	0	206	26	23	0	40	18
304202	414	-	21	95	33	132	18	62	1
304204	612	-	0	10	29	24	88	0	49
304205	5323	-	16	369	186	109	37	37	183
304206	114	-	38	-	-	-	-	-	-
304208	293	-	3	256	40	58	13	24	23
304211	610	-	0	259	57	43	0	100	0
304212	8401	-	245	445	275	297	0	10	674
304213	130	-	124	1980	249	3198	41	49	0
304214	688	-	277	161	134	379	28	80	183
304215	1133	-	60	9701	181	523	25	81	49
304216	953	-	390	48717	1523	3241	73	86	23
304217	259	-	31	321	188	144	0	25	6
304218	422	-	0	136	40	45	441	9	38
304220	432	-	94	811	90	248	7	40	0
304221	703	-	202	613	71	716	35	104	0
304222	385	-	131	263	40	266	57	43	0
304223	274	-	211	4035	179	775	15	38	0
304224	3880	-	219	450	237	217	598	56	1312
304225	2794	-	0	374	84	73	31	108	4
304226	1138	-	26	186	54	31	49	60	99
304227	331	-	0	168	31	84	42	44	14
304228	374	-	16	243	48	88	0	35	0
304230	187	-	29	4296	207	164	32	46	0
304231	727	-	326	62538	1683	2108	96	77	22
304232	5620	-	16	521	181	157	420	49	104
304233	591	-	153	172	42	195	42	39	5
304234	11500	-	3	245	281	142	469	12	436
304235	440	-	22	225	34	44	0	55	17
304238	863	-	49	466	43	245	53	40	6
304239	832	-	87	393	84	345	159	131	0

ANALYTICAL RESULTS cont.

GGU No	eU	U	eTh	Zr	Nb	Y	Cu	Zn	Pb
304240	750	-	100	3126	85	527	67	71	0
304241	536	-	138	7084	116	658	43	91	0
304242	502	-	41	12643	158	449	94	74	0
304244	2080	-	2	625	154	99	866	62	65
304245	652	-	45	4912	144	371	55	77	0
304246	1220	-	25	480	71	310	46	107	0
304249	290	-	0	-	-	-	-	-	-
304250	17400	-	72	-	-	-	-	-	-
304251	8020	-	97	-	-	-	-	-	-
304252	7630	-	0	-	-	-	-	-	-
304253	26900	-	0	-	-	-	-	-	-
304254	9610	-	0	-	-	-	-	-	-
304256	90800	-	3580	-	-	-	-	-	-
304257	13700	-	89	-	-	-	-	-	-
304258	44200	-	431	-	-	-	-	-	-
304259	62200	-	1760	-	-	-	-	-	-
304260	39400	-	781	-	-	-	-	-	-
304261	63100	-	1550	-	-	-	-	-	-
304271	2827	-	0	324	75	45	33	17	109
304272	3938	-	3	93	51	92	195	87	1006
304273	739	-	0	236	38	63	6	164	47
304274	147	-	8	44	3	113	9656	292	1711
304276	13994	-	434	867	492	208	18	75	536
304277	7021	-	0	163	74	77	30	140	120
304282	9528	-	2402	-	-	-	-	-	-
304307	2286	3100	130	-	-	-	-	-	-
304317	28700	-	782	-	-	-	-	-	-
304344	1650	-	0	-	-	-	-	-	-
304401	290	-	43	-	-	-	-	-	-
304410	276	440	153	204	146	128	60	391	3239
304414	391	492	70	71	109	56	0	0	11
304417	619	643	82	372	49	32	0	13	16
304423	146	-	22	-	-	-	-	-	-
304424	793	470	0	168	59	14	0	17	26
304428	298	795	51	578	87	55	0	51	0
304430	458	617	54	139	48	75	13	211	0
304431	845	1120	321	343	63	149	0	32	4
304432	250	-	21	-	-	-	-	-	-
304433	383	447	67	1508	45	231	58	103	20
304436	468	460	3	163	52	119	238	552	1594
304437	1030	1120	158	518	46	269	11	52	57
304439	1070	1430	28	413	132	239	27	149	87
304442	1020	1530	36	269	52	52	484	34	321
304445	5300	1270	207	1017	495	355	47	32	249
304447	525	-	26	-	-	-	-	-	-
304505	220000	-	23000	-	-	-	-	-	-
304506	172	-	19	-	-	-	-	-	-
304508	110	-	23	-	-	-	-	-	-
304510	327000	-	59000	-	-	-	-	-	-
304516	612	-	15	1265	645	107	58	135	78
304517	39400	-	1100	-	-	-	-	-	-
304526	1369	-	60	-	-	-	-	-	-
304527	2850	-	1900	-	-	-	-	-	-

ANALYTICAL RESULTS cont.

GGU No	eU	U	eTh	Zr	Nb	Y	Cu	Zn	Pb
304528	383	-	33	-	-	-	-	-	-
304535	1690	-	0	-	-	-	-	-	-
304543	628	-	6	-	-	-	-	-	-
304544	2620	-	44	-	-	-	-	-	-
304545	124	-	25	-	-	-	-	-	-
304556	162	-	28	352	29	36	74	51	5
304579	768	-	18	1068	289	80	45	83	38
304580	158	-	26	376	32	90	10	123	16
304581	1730	-	0	145	46	100	0	39	13
304582	1110	-	45	-	-	-	-	-	-
304594	430	-	0	-	-	-	-	-	-
304604	1362	-	28	238	59	57	24	1	42
304815	570	-	0	-	-	-	-	-	-
304828	148	-	42	-	-	-	-	-	-
304831	558	-	1	-	-	-	-	-	-
304834	127	-	5	-	-	-	-	-	-
304844	253	-	24	-	-	-	-	-	-
304858	6410	-	0	-	-	-	-	-	-
304860	238	-	0	-	-	-	-	-	-
304863	286	-	138	-	-	-	-	-	-
325011	374	37	3	656	48	20	4	9	129
325013	345	99	92	34	12	9	16	159	0
325019	152	22	18	69	9	21	2	6	342
325020	811	19	12	207	18	13	2	25	155
325021	6038	126	47	47	7	13	72	4	329
325040	141	133	11	35	8	8	0	0	0
325041	1766	1160	5	125	28	28	220	48	269
325051	104	110	28	295	26	118	102	17	0
325064	267	236	6	106	16	66	34	172	21
325065	254	395	61	256	40	157	43	46	131
325066	5551	43500	1160	653	391	543	27	234	2886
325067	20038	26800	0	549	267	326	69	176	3569
325068	310	194	2	279	20	10	0	46	20
325070	1212	815	0	263	20	109	158	202	125
325071	1200	1450	18	143	15	151	3075	309	1144
325073	12232	13000	0	465	165	476	23	55	914
325074	636	664	40	826	139	179	56	369	144
325075	394	381	25	440	73	52	37	328	62
325096	4706	2040	0	1160	120	57	41	150	263
325097	822	1680	1	1861	52	78	33	47	137
325104	469	539	149	1119	1305	1164	286	182	336
325112	891	535	0	76	24	10	2	14	37
325121	12136	3700	0	114	56	75	47	64	613
325122	647	638	0	133	25	27	25	68	58
325125	422	313	11	318	24	44	64	101	32
325126	1510	1280	53	349	46	58	20	187	194
325127	731	235	38	375	23	63	19	283	243
325128	1034	772	23	449	27	59	271	44	142
325129	708	864	5	389	28	25	0	120	250
325130	499	431	29	351	21	46	10	62	84
325131	207	123	15	356	26	44	13	102	62
325133	3728	3290	60	320	44	137	19	71	338
325134	679	500	23	313	21	109	3	21	103
325135	929	173	12	267	30	41	80	148	243

ANALYTICAL RESULTS cont.

GGU No	eU	U	eTh	Zr	Nb	Y	Cu	Zn	Pb
325137	1064	1620	14	372	39	79	19	52	0
325217	203	261	124	2827	730	196	38	201	90
325219	2248	1740	35	312	36	40	0	53	28
325223	7245	-	201	-	-	-	-	-	-
325306	13355	-	600	-	-	-	-	-	-
325307	9911	-	90	-	-	-	-	-	-
325312	11590	-	0	-	-	-	-	-	-
325318	16386	-	19	-	-	-	-	-	-

eU eTh : Gamma-spectrometry, Risø and fieldlab.
U : Delayed neutron counting, Risø
Zr, Nb, Y, Cu, Zn, Pb : EDX, Risø

APPENDIX II

MAJOR ELEMENT ANALYSES FROM SOUTH GREENLAND

All units in %, n.d.: not detected

GGU No	(1) 325011	(2) 325021	(3) 325041	(4) 325070	(5) 325086	(6) 325103	(7) 325104	(8) 325112
SiO_2	87.21	91.64	90.46	43.74	75.41	46.29	20.14	91.07
Al_2O_5	2.63	1.96	4.33	16.61	6.79	10.46	3.24	2.56
Fe_2O_5	3.97	0.58	2.32	7.06	1.75	11.95	5.18	0.98
FeO	1.60	0.87	0.97	10.05	1.99	1.07	0.85	1.20
MgO	0.60	0.51	0.37	3.69	1.12	1.02	1.11	0.28
CaO	0.11	0.88	0.20	5.61	1.01	2.25	37.64	0.30
Na_2O	0.34	1.02	0.87	3.91	1.61	0.29	4.25	1.59
K_2O	0.80	0.66	1.59	1.34	3.01	8.97	1.46	0.74
TiO_2	1.59	0.10	0.21	3.19	0.30	2.66	0.83	0.19
MnO	0.01	0.01	0.09	0.13	0.34	0.04	0.06	0.11
P_2O_5	0.05	0.04	0.04	0.45	0.20	2.13	29.84	0.04
SUM	98.91	98.27	101.45	95.78	93.53	87.13	104.60	99.06

GGU No	(9) 325122	(10) 325125	(11) 325126	(12) 325128	(13) 325133	(14) 325134	(15) 325135	(16) 325137
SiO_2	72.31	50.72	62.05	67.48	54.42	68.57	54.30	61.19
Al_2O_5	5.54	14.98	13.49	16.35	16.77	13.63	14.97	14.23
Fe_2O_5	3.50	4.74	1.83	2.69	6.10	2.25	10.37	10.96
FeO	4.47	1.97	2.69	0.35	4.20	1.09	1.88	1.56
MgO	1.36	2.93	1.82	0.40	2.97	0.79	1.99	1.20
CaO	1.13	4.77	2.93	0.92	1.50	0.79	2.96	0.55
Na_2O	0.70	5.43	2.08	3.51	5.07	3.56	1.87	3.06
K_2O	0.82	2.63	3.88	4.94	4.48	4.80	3.74	2.49
TiO_2	0.96	1.14	0.65	0.80	0.53	0.57	2.51	0.63
MnO	0.28	0.11	0.10	0.03	0.14	0.03	0.15	0.02
P_2O_5	0.78	0.68	0.32	0.38	0.31	0.23	1.69	0.29
SUM	91.85	90.10	91.84	97.85	96.49	96.31	96.43	96.18

GGU No	(17) 325308	(18) 325309	(19) 325310	(20) 325313	(21) 325316	(22) 325322
SiO_2	76.80	89.01	61.36	70.30	59.66	61.84
Al_2O_5	11.89	5.06	17.26	11.67	17.07	10.33
Fe_2O_5	1.01	0.02	2.70	0.70	2.88	11.40
FeO	0.59	1.31	2.66	1.57	n.d.	5.60
MgO	0.34	0.10	1.91	0.28	0.81	0.40
CaO	0.21	1.61	3.67	0.23	0.46	1.71
Na_2O	3.00	2.12	4.66	1.44	6.22	4.09
K_2O	7.13	0.23	4.59	7.19	6.67	2.59
TiO_2	0.05	0.06	0.68	0.16	0.39	1.72
MnO	0.01	0.01	0.09	0.01	0.06	0.17
P_2O_5	0.02	0.00	0.30	0.02	0.11	0.10
SUM	101.05	99.53	99.88	93.57	94.33	99.95

ANALYTICAL METHOD: XRF, Durham, England. Fe+2/+3, GGU

1. Sandstone, brecciated and with brannerite, Ingnerulalik
2. Sandstone, brecciated and with pitchblende, Ingnerulalik
3. Sandstone, brecciated and with pitchblende, Ingnerulalik
4. Dolerite, altered and with branerite and sec. U minerals, Nunakutdlak
5. Granite, red, altered, associated with Th-rich joints, Ingnerulalik
6. Granite, altered and with dyke fracments, Th dominated, Qagssiarssuk
7. F-apatite rich rock, altered and brecciated, Qagssiarssuk
8. Sandstone, brecciated and with brannerite, Nunakutdlak
9. Sandstone, brecciated and with brannerite and sec. U minerals, Sitdlisit
10. Diorite, altered and with brannerite, Kangerdlua
11. Granite, altered, brecciated with coffinite and sec. U minerals, Kangerdlua
12. Granite, altered, red and with brannerite, Kangderlua
13. Diorite, altered and with pitchblende, Kangerdlua
14. Aplite with brannerite, Kangerdlua
15. Diorite, altered and with brannerite, Kangerdlua
16. Granite, altered and with brannerite, Kangerdlua
17. Gneiss, feldspatic, red, Nunatak
18. Gneiss, feldspatic, white, Nunatak
19. Granite, Nunatak
20. Gneiss, white and with sulphides, Nunatak
21. Microsyenitic dyke, grey, Nunatak
22. Magnetite bands marginal to red aplite, Th-dominated, Nunatak

TRACE ELEMENT ANALYSES

All units in ppm

GGU No	(1) 325011	(2) 325021	(3) 325041	(4) 325070	(5) 325086	(6) 325103	(7) 325104	(8) 325112	(9) 325122	(10) 325125
V	715	158	114	213	24	219	121	110	933	128
Cr	105	66	63	88	14	274	2	218	3561	16
Ni	1	2	9	89	5	18	31	17	27	0
Cu	5	135	358	163	149	0	228	22	4	82
Zn	10	6	61	220	200	69	177	25	68	112
Ga	7	4	5	30	11	17	0	4	12	23
Rb	31	24	83	87	92	140	23	29	34	81
Sr	13	7	22	284	154	1256	5470	5	194	244
Y	10	4	7	29	70	83	280	3	8	18
Zr	607	53	124	250	240	1012	1237	81	128	329
Nb	73	6	16	15	0	610	2049	41	17	19
Ba	178	205	3090	609	3357	30733	17821	77	752	791
La	39	12	15	48	331	6555	1359	13	39	84
Ce	35	12	15	79	535	5014	1310	15	28	93
Nd	8	0	0	0	334	3840	1334	0	0	73
Pb	284	664	687	303	374	194	712	176	151	85
Th	8	7	6	0	1659	1244	169	5	2	9
U	43	151	1532	899	0	34	587	601	643	341

GGU No	(11) 325126	(12) 325128	(13) 325133	(14) 325134	(16) 325137	(17) 325308	(18) 325309	(19) 325310	(20) 325313	(22) 325322
V	107	72	436	97	54	5	6	71	4	126
Cr	22	29	41	23	6	24	59	54	20	0
Ni	0	0	1	3	0	0	0	7	0	3
Cu	12	445	5	23	0	0	9	9	0	0
Zn	228	56	101	34	67	14	11	79	22	241
Ga	19	23	31	19	20	18	8	23	19	27
Rb	176	174	210	164	151	158	8	133	201	125
Sr	242	245	90	78	110	86	90	673	149	178
Y	20	22	34	37	24	12	3	28	14	70
Zr	298	426	287	276	383	620	445	382	321	1330
Nb	26	30	26	21	28	11	5	24	24	16
Ba	554	991	859	680	353	86	31	2181	126	261
La	57	53	81	38	84	8	20	46	27	1835
Ce	71	88	175	46	114	10	21	60	25	1658
Nd	45	24	92	11	37	0	0	44	1	913
Pb	496	317	889	246	124	75	15	23	61	174
Th	17	18	30	27	20	29	18	7	22	898
U	1527	732	3338	505	1694	48	23	17	12	233

Analytical method: XRF, Durham, England

APPENDIX III

ANALYTICAL RESULTS OF FLUORITE

Ca is in % and semi-quantitative, SNo is GGU sample number and ID is Risø ID number.

Area	Motz	Vatna	Puis	Puis	Motz	Motz	Mland	
SNo	297940	304240	304282	304506	304606	304609	304812	304812
ID	AA1	AA2	AA3	AA4	AA5	AA6	AA7	AA8
Na	411.0	397.0	308.0	168.0	403.0	82.7	53.4	59.9
Ca%	55.0	60.0	57.0	48.6	55.8	56.7	54.6	54.4
K	n.d.	n.d.	n.d.	n.d.	n.d.	n.d.	201.0	346.0
Sc	0.220	7.76	0.696	1.811	0.122	0.052	1.589	0.538
Cr	11.5	6.7	10.7	11.5	0.54	4.58	0.7	1.39
Fe	2313.0	1558.0	6780.0	6700.0	30.0	467.0	103.0	500.0
Co	5.08	0.82	1.32	3.03	0.351	1.183	0.195	0.301
Zn	134.5	4.9	19.2	24.7	7.56	13.0	n.d.	7.4
As	21.5	6.64	n.d.	n.d.	n.d.	n.d.	n.d.	n.d.
Rb	n.d.	n.d.	23.0	n.d.	n.d.	n.d.	n.d.	n.d.
Sr	6980.0	1044.0	2911.0	2799.0	181.0	584.0	1064.0	1223.0
Ag	81.9	n.d.	n.d.	n.d.	n.d.	n.d.	n.d.	n.d.
Sb	6.67	n.d.	n.d.	n.d.	n.d.	n.d.	n.d.	n.d.
Cs	n.d.	n.d.	0.39	n.d.	n.d.	n.d.	n.d.	n.d.
Ba	n.d.	1340.0	21000.0	n.d.	n.d.	n.d.	n.d.	n.d.
La	473.00	17.30	40.00	9.69	10.21	10.42	4.34	3.03
Ce	781.00	39.40	271.20	19.6	24.24	21.88	10.40	4.14
Nd	253.00	n.d.	178.00	n.d.	17.1	16.5	8.4	n.d.
Sm	69.00	6.27	38.40	2.927	8.86	5.89	2.660	0.855
Eu	5.99	1.006	1.19	0.875	1.478	0.624	0.843	0.293
Tb	11.08	1.44	0.58	0.356	2.416	2.093	0.546	0.210
Yb	13.50	13.05	3.14	1.26	1.24	1.32	2.92	0.864
Lu	1.65	2.055	0.32	0.170	0.100	0.120	0.445	0.120
Hf	1.30	0.54	0.23	0.23	n.d.	0.123	n.d.	n.d.
Ta	6.86	n.d.	n.d.	n.d.	n.d.	0.078	n.d.	0.094
Th	76.1	6.52	1.36	0.25	0.084	2.26	3.86	9.61

n.d. : not detected. Results are in ppm (except for Ca).

Area	Qags	Qags	Qags	Agpat vein		Agpat	Nunatak
SNo	325069	325085	325086	325224	325230	325230	325302
ID	AA9	A10	A11	A12	A13	A14	A15
Na	400.0	68.4	83.0	220.5	276.0	465.0	84.0
Ca%	57.9	61.3	54.5	54.6	57.5	56.5	59.6
K	n.d.	n.d.	n.d.	n.d.	n.d.	n.d.	n.d.
Sc	0.373	0.879	1.037	1.204	0.047	0.041	0.174
Cr	24.4	11.9	5.6	5.3	1.28	0.53	3.07
Fe	1560.0	2392.0	1332.0	1658.0	434.0	760.0	754.0
Co	2.40	1.87	0.47	0.374	0.235	0.214	0.263
Zn	42.9	26.5	43.6	15.6	7.8	20.7	9.6
As	n.d.	2.08	n.d.	n.d.	0.24	0.43	0.99
Rb	n.d.	n.d.	n.d.	5.3	n.d.	n.d.	n.d.
Sr	125.0	240.0	516.0	1590.0	n.d.	15.0	80.0
Ag	n.d.	n.d.	4.8	n.d.	n.d.	n.d.	n.d.
Sb	n.d.	n.d.	n.d.	n.d.	0.09	0.27	0.67
Cs	0.21	n.d.	n.d.	n.d.	n.d.	n.d.	n.d.
Ba	n.d.	102.0	n.d.	n.d.	n.d.	n.d.	n.d.
La	67.8	25.48	149.8	10.52	9.15	34.4	4.75
Ce	117.0	51.5	303.6	26.0	15.20	53.0	12.13
Nd	54.	27.	189.	n.d.	n.d.	15.3	n.d.
Sm	6.96	7.74	35.3	4.81	0.786	2.108	2.239
Eu	0.991	2.11	4.82	0.901	0.057	0.123	0.157
Tb	0.447	2.78	3.07	0.761	0.074	0.079	0.346
Yb	0.68	8.24	24.70	2.90	0.249	0.180	1.580
Lu	n.d.	1.075	4.47	0.500	0.021	n.d.	0.330
Hf	0.148	n.d.	n.d.	n.d.	0.225	0.140	0.302
Ta	0.452	n.d.	n.d.	n.d.	n.d.	0.160	n.d.
Th	0.065	1.008	148.3	4.78	3.96	11.37	3.09

n.d. : not detected. Results are in ppm (except for Ca).
Analytical metod: INAA, Risø National Labratory

Motz : Motzfeldt centre
Vatna : Vatnahverfi area
Puis : Puissagtak uranium prospect
Mland : Mellemlandet
Qags : Qagssiarssuk area
Agpat vein : Agpat area, in granite
Agpat : Agpat
Nunatak : Nunatak area

APPENDIX IV

MICROPROBE DATA ON DIFFERET URANIFEROUS MINERALS

Units in %, n.d.: not detected, MA: Chemical age in Ma.
(Pitchblende, brannerite, coffinite, kasolite, curite? a.o.)

PITCHBLENDE: (*: altered)

SNO	325041	325041	325041	325041	325041	325041	325041
UO_2	76.96	77.18	79.27	79.11	76.20	78.13	78.01
PbO	13.71	14.10	11.72	11.79	13.80	13.33	14.41
ThO_2	n.d.	0.15	n.d.	n.d.	n.d.	n.d.	n.d.
FeO	0.02	0.04	n.d.	0.08	0.07	0.05	0.10
CaO	3.91	4.09	4.36	4.41	2.91	3.29	3.26
Ce_2O_3	0.09	0.05	0.13	0.17	0.01	n.d.	0.10
Y_2O_3	n.d.	n.d.	0.42	0.07	0.18	0.13	0.29
SiO_2	0.58	0.60	0.55	0.67	0.93	0.84	0.80
MA	1184	1209	1003	1010	1201	1193	1222

SNO	325041	325041	325041	325041	325041	325041	325041
UO_2	77.98	77.99	75.60	79.12	78.57	78.56	77.18
PbO	14.44	13.08	15.72	12.68	11.44	11.40	13.64
ThO_2	0.14	n.d.	n.d.	n.d.	n.d.	n.d.	0.13
FeO	0.05	0.05	0.03	0.05	0.10	0.17	0.04
CaO	2.86	3.33	4.21	3.41	4.34	4.65	3.09
Ce_2O_3	0.06	0.08	n.d.	0.11	0.14	0.04	n.d.
Y_2O_3	n.d.	0.18	n.d.	n.d.	n.d.	n.d.	n.d.
SiO_2	0.87	0.76	0.10	0.62	0.64	0.60	0.78
MA	1224	1122	1354	1078	989	986	1175

SNO	325041	325041	325041	325066*	325066	325066	325066
UO_2	76.62	82.10	77.38	59.91	70.96	68.23	69.95
PbO	11.77	7.14	12.31	19.52	15.38	18.34	15.44
ThO_2	n.d.	0.20	0.14	n.d.	n.d.	n.d.	n.d.
FeO	0.08	0.18	0.06	0.69	0.58	0.31	0.37
CaO	3.10	4.31	3.19	0.77	2.46	1.69	2.38
Ce_2O_3	0.08	n.d.	0.14	0.48	0.40	0.47	0.49
Y_2O_3	0.14	n.d.	0.32	0.15	0.28	0.35	0.18
SiO_2	0.78	0.47	0.82	1.72	0.57	0.59	0.59
MA	1038	615	1070	1957	1403	1679	1424

PITCHBLENDE cont.

SNO	325066*	325073	325073	325073	325073	325073	325073
UO_2	62.55	74.86	73.61	74.60	73.63	73.93	75.28
PbO	20.45	10.32	11.21	12.15	12.32	11.96	10.03
ThO_2	0.07	n.d.	n.d.	0.05	n.d.	0.06	0.24
FeO	0.69	1.13	1.64	0.41	1.30	0.29	0.65
CaO	0.85	3.61	3.19	2.16	2.74	2.59	3.69
Ce_2O_3	0.44	0.99	0.52	0.83	0.96	0.85	0.74
Y_2O_3	0.42	1.01	1.48	1.38	1.38	0.65	1.31
SiO_2	1.94	0.75	0.80	0.48	0.81	0.79	0.69
MA	1963	942	1030	1093	1120	1087	912

SNO	325073	325073	325073	325073	325073	325073	325073
UO_2	71.51	65.91	73.28	72.31	75.79	70.74	76.74
PbO	10.10	11.24	9.21	10.84	8.63	12.87	8.47
ThO_2	0.08	n.d.	n.d.	n.d.	0.01	0.03	n.d.
FeO	3.18	0.25	0.20	0.24	0.23	0.37	0.27
CaO	3.52	2.48	3.57	3.52	3.85	0.03	3.52
Ce_2O_3	0.86	3.27	1.56	1.53	1.47	1.33	1.15
Y_2O_3	1.19	0.90	1.09	0.84	1.27	1.26	1.50
SiO_2	2.04	0.37	0.33	0.33	0.28	0.26	0.45
MA	962	1139	866	1016	791	1205	768

SNO	325073	325121	325121	325121	325121	325121	325133
UO_2	68.47	61.63	79.27	77.45	78.77	78.27	61.03
PbO	10.87	9.31	13.30	12.89	13.82	13.87	17.54
ThO_2	n.d.	n.d.	n.d.	n.d.	n.d.	n.d.	n.d.
FeO	0.42	4.67	0.19	0.56	0.12	0.11	0.55
CaO	1.03	0.80	1.92	1.19	1.97	1.69	2.41
Ce_2O_3	0.94	n.d.	0.01	0.07	0.10	0.02	1.02
Y_2O_3	0.18	0.18	0.36	0.28	0.21	n.d.	0.51
SiO_2	0.31	8.56	0.07	0.47	0.15	0.14	4.32
MA	1069	1023	1123	1115	1168	1178	1773

PITCHBLENDE cont.

SNO	325133*	325133	325133	325133	325133	325133	325133
UO_2	59.62	65.72	53.63	71.94	69.66	61.05	74.54
PbO	14.81	8.76	14.80	7.98	9.63	10.42	10.38
ThO_2	n.d.	0.02	n.d.	n.d.	0.01	n.d.	n.d.
FeO	0.47	0.82	0.34	0.43	0.31	0.62	0.55
CaO	2.19	3.40	1.89	3.99	3.24	2.64	4.61
Ce_2O_3	0.93	1.51	0.72	1.24	1.00	0.77	1.19
Y_2O_3	0.19	0.46	0.31	0.56	0.69	0.12	0.57
SiO_2	4.07	1.15	6.95	0.66	0.37	9.27	0.35
MA	1573	913	1715	772	944	1140	950

SNO	325133	325133
UO_2	74.97	73.18
PbO	11.91	10.03
ThO_2	n.d.	n.d.
FeO	0.32	0.76
CaO	4.05	4.42
Ce_2O_3	0.99	1.29
Y_2O_3	1.95	0.70
SiO_2	0.32	0.70
MA	1070	937

BRANNERITE: (*: Absite - Th-rich variety)

SNO	325066	325112*	325112	325112	325121	325121	325122
UO_2	43.67	21.30	18.53	47.43	48.77	44.69	49.42
PbO	0.45	0.40	0.50	1.61	1.99	1.57	0.97
ThO_2	n.d.	10.51	n.d.	n.d.	n.d.	n.d.	n.d.
TiO_2	37.21	37.46	55.13	34.97	32.91	31.15	36.47
FeO	1.93	2.62	3.93	3.81	4.13	4.81	3.82
CaO	3.46	4.14	1.48	4.49	1.81	1.83	2.91
Ce_2O_3	0.36	5.27	n.d.	0.02	n.d.	n.d.	n.d.
Y_2O_3	1.12	1.83	n.d.	0.24	0.33	n.d.	0.24
SiO_2	2.83	3.16	7.78	0.13	1.75	3.36	1.80

BRANNERITE cont.

SNO	325122	325122	325122	325125	325125	325126	325126
UO_2	47.13	25.58	46.21	31.68	21.70	47.27	49.97
PbO	1.05	1.24	1.05	2.35	2.42	0.57	1.97
ThO_2	n.d.	0.08	0.11	n.d.	0.09	n.d.	0.23
TiO_2	35.17	22.05	33.82	48.88	60.33	35.46	36.72
FeO	4.61	13.01	4.12	3.73	4.85	2.78	3.55
CaO	3.41	1.12	2.88	1.93	1.31	4.44	4.96
Ce_2O_3	n.d.	0.36	n.d.	0.61	0.48	0.20	0.77
Y_2O_3	n.d.	0.31	n.d.	1.26	3.37	0.69	0.92
SiO_2	1.80	12.93	1.93	2.72	4.14	1.76	n.d.

SNO	325126	325133	325133	325133	325133	325133	325133
UO_2	46.60	40.32	42.46	41.77	39.00	39.52	41.39
PbO	0.80	3.20	2.01	1.54	2.06	2.54	2.25
ThO_2	0.09	n.d.	0.07	n.d.	n.d.	n.d.	n.d.
TiO_2	37.61	34.67	33.46	33.30	34.03	32.37	35.21
FeO	3.77	3.25	3.16	3.53	3.07	3.00	2.53
CaO	5.55	2.79	3.18	3.23	3.22	2.94	3.34
Ce_2O_3	0.04	1.15	0.56	0.58	1.12	1.11	1.07
Y_2O_3	0.79	0.74	0.75	0.54	0.81	0.74	1.11
SiO_2	n.d.	3.87	3.37	2.96	3.84	3.38	3.32

SNO	325133	325133	325137	325137	325137	325137	325137
UO_2	43.52	39.10	31.85	28.01	37.92	30.29	26.41
PbO	1.50	3.25	0.41	0.57	0.33	0.53	0.81
ThO_2	0.14	0.15	n.d.	0.01	0.01	0.16	0.42
TiO_2	35.02	33.86	35.83	50.28	34.07	39.89	47.95
FeO	3.01	3.32	4.75	4.39	4.08	4.76	3.71
CaO	3.01	2.44	1.67	1.19	2.47	1.11	0.94
Ce_2O_3	0.23	1.33	0.52	0.41	0.88	0.71	0.35
Y_2O_3	0.53	0.91	1.41	n.d.	1.44	1.07	0.76
SiO_2	2.37	3.99	7.21	4.24	4.12	6.10	1.84

BRANNERITE cont.

SNO	325137	325137	325137	325137	325137	325137	325137
UO_2	29.01	30.49	29.71	44.52	42.22	43.77	28.57
PbO	0.68	0.65	0.38	0.73	0.97	1.60	0.94
ThO_2	0.40	0.12	0.05	n.d.	0.04	0.02	0.09
TiO_2	41.10	40.86	27.64	35.54	34.62	33.32	45.17
FeO	11.05	4.55	19.51	3.94	4.03	3.98	4.68
CaO	1.43	1.41	1.47	3.54	2.69	3.05	1.63
Ce_2O_3	0.78	0.59	0.83	0.71	0.58	0.64	0.58
Y_2O_3	4.84	1.06	1.39	1.09	0.90	1.02	1.03
SiO_2	2.62	5.61	3.35	1.36	1.46	1.74	2.88

SNO	325137	325137	325137	325137	325137
UO_2	33.23	26.19	44.44	30.81	48.03
PbO	0.52	0.04	0.66	0.69	0.87
ThO_2	0.12	n.d.	n.d.	n.d.	0.27
TiO_2	40.88	32.18	34.08	20.80	34.47
FeO	3.68	7.35	5.19	4.91	3.95
CaO	1.74	1.11	3.00	1.95	3.15
Ce_2O_3	0.70	0.91	0.70	0.51	0.61
Y_2O_3	1.81	0.15	0.98	0.43	0.90
SiO_2	3.71	2.28	1.77	36.45	1.50

COFFINITE:

SNO	325126	325126	325126	325126	325126	325126	325126
UO_2	61.04	59.27	61.75	60.49	66.61	65.95	66.67
PbO	5.39	1.09	2.39	0.26	1.02	0.33	0.87
ThO_2	n.d.	n.d.	n.d.	0.06	n.d.	n.d.	n.d.
FeO	0.12	2.30	0.24	1.47	0.27	0.20	0.82
CaO	5.05	6.31	4.17	7.01	6.22	7.92	8.02
Ce_2O_3	0.20	n.d.	0.14	0.11	n.d.	n.d.	0.02
Y_2O_3	0.43	n.d.	0.45	0.24	0.50	n.d.	n.d.
SiO_2	14.41	12.38	13.67	13.45	14.45	14.31	14.63

COFFINITE cont.

SNO	325126	325126	325126	325126	325126	325126	325126
UO_2	65.67	63.72	59.65	55.00	66.31	67.46	67.61
PbO	0.92	0.85	0.07	0.20	0.49	1.22	n.d.
ThO_2	n.d.	0.17	n.d.	0.09	n.d.	n.d.	n.d.
FeO	0.32	3.93	1.77	3.31	1.23	0.73	1.40
CaO	6.11	6.11	6.69	5.61	6.15	6.56	7.10
Ce_2O_3	0.04	0.05	0.07	0.14	0.21	0.15	0.02
Y_2O_3	0.15	n.d.	0.42	0.09	0.25	n.d.	n.d.
SiO_2	14.13	14.33	11.07	13.80	11.57	14.42	15.31

SNO	325126	325126	325126	325126
UO_2	61.55	55.93	57.91	57.97
PbO	0.64	0.28	0.70	2.37
ThO_2	0.07	n.d.	n.d.	n.d.
FeO	0.83	0.25	0.26	0.63
CaO	6.98	5.40	6.01	4.58
Ce_2O_3	0.15	n.d.	0.05	0.21
Y_2O_3	n.d.	0.12	0.33	0.25
SiO_2	14.79	19.81	13.71	20.56

KASOLITE:

SNO	325041	325041	325041	325041	325041	325041	325041
UO_2	44.20	44.30	43.48	43.61	43.13	44.49	46.04
PbO	34.93	35.35	32.81	34.93	34.48	34.40	33.91
ThO_2	n.d.	0.03	n.d.	n.d.	n.d.	n.d.	n.d.
TiO_2	0.02	n.d.	n.d.	0.08	n.d.	n.d.	0.03
FeO	0.11	0.10	0.14	0.09	0.14	0.49	0.27
CaO	n.d.	n.d.	n.d.	n.d.	n.d.	0.01	0.01
Ce_2O_3	n.d.	0.06	0.01	0.13	0.06	n.d.	0.11
Y_2O_3	0.60	n.d.	0.44	0.02	n.d.	0.38	1.47
SiO_2	9.89	9.90	9.80	9.66	9.72	9.99	8.58

KASOLITE cont.

SNO	325071	325071	325071	325071	325071	325073	325073
UO_2	44.14	44.41	44.71	44.32	47.92	44.28	46.67
PbO	35.70	34.27	33.92	34.80	34.15	34.39	27.90
ThO_2	n.d.	n.d.	n.d.	n.d.	n.d.	n.d.	n.d.
TiO_2	n.d.	0.01	0.05	n.d.	n.d.	n.d.	0.09
FeO	0.14	0.34	0.50	0.67	0.05	0.22	0.52
CaO	n.d.	n.d.	n.d.	0.04	n.d.	n.d.	0.18
Ce_2O_3	0.12	n.d.	0.05	0.05	n.d.	0.02	0.35
Y_2O_3	n.d.	0.07	n.d.	n.d.	n.d.	0.14	n.d.
SiO_2	9.33	9.51	10.18	9.40	7.65	9.01	1n.d.

SNO	325122	325126	325126	325126	325126	325126	325126
UO_2	46.80	39.97	44.38	41.99	43.81	45.40	43.00
PbO	31.46	25.01	30.85	25.14	26.46	30.02	24.35
ThO_2	n.d.	0.07	n.d.	n.d.	n.d.	n.d.	1.17
TiO_2	0.27	n.d.	0.01	n.d.	0.08	0.01	0.05
FeO	1.00	0.82	0.32	4.88	3.83	0.87	2.80
CaO	0.58	0.62	0.29	0.97	1.47	0.32	0.98
Ce_2O_3	0.17	n.d.	0.18	0.22	0.01	0.39	0.05
Y_2O_3	0.02	0.30	0.08	n.d.	0.14	n.d.	n.d.
SiO_2	11.49	9.74	9.71	9.95	9.33	10.97	9.51

SNO	325126	325126	325126	325126	325126	325126	325126
UO_2	39.38	45.41	53.82	37.35	43.87	46.56	42.28
ThO_2	n.d.	n.d.	n.d.	n.d.	n.d.	n.d.	n.d.
FeO_2	0.52	0.60	0.50	5.07	1.59	2.53	1.00
CaO	0.69	0.32	0.96	1.24	0.50	0.58	0.66
Ce_2O_3	0.24	0.22	0.24	0.19	0.36	0.35	0.42
Y_2O_3	0.07	0.08	0.08	n.d.	n.d.	0.26	0.25
SiO_2	7.43	9.86	11.77	13.10	16.82	10.65	9.84

CURITE ?

SNO	325071	325071	325071	325071	325071	325071	325071
UO_2	66.09	64.59	67.15	65.36	64.69	61.88	62.88
PbO	22.08	22.26	22.16	21.18	21.53	20.35	20.57
ThO_2	n.d.	n.d.	n.d.	0.05	n.d.	n.d.	n.d.
TiO_2	n.d.	0.01	0.02	0.03	0.01	n.d.	0.04
FeO	0.05	0.06	n.d.	0.01	0.05	0.08	0.48
CaO	n.d.	n.d.	n.d.	n.d.	n.d.	0.01	n.d.
Ce_2O_3	0.05	0.10	0.10	0.01	0.03	0.05	0.09
Y_2O_3	n.d.	0.14	n.d.	n.d.	0.21	n.d.	0.31
SiO_2	n.d.	n.d.	n.d.	n.d.	n.d.	0.06	n.d.

Fe-RICH SECONDARY U MINERAL:

SNO	325041	325041	325041	325073	325073	325126	325126
UO_2	28.65	29.78	29.25	11.18	25.07	39.53	48.42
PbO	5.96	6.09	5.79	11.88	18.26	2.03	2.73
ThO_2	n.d.	n.d.	n.d.	n.d.	12.14	n.d.	0.22
TiO_2	0.04	0.02	0.01	n.d.	n.d.	0.04	n.d.
FeO	37.78	37.18	38.11	42.88	15.52	18.77	23.19
CaO	0.61	0.57	0.61	0.18	0.58	3.86	1.44
Ce_2O_3	0.10	n.d.	0.02	0.35	0.13	n.d.	0.09
Y_2O_3	n.d.	0.30	n.d.	0.43	0.26	n.d.	n.d.
SiO_2	4.36	4.60	4.44	13.08	10.27	15.76	11.08

Pb-Ca-U MINERAL:

SNO	325131	325131	325131	325131	325131	325131	325131
UO_2	36.08	42.02	18.74	45.36	48.85	53.72	27.63
PbO	28.52	10.96	56.53	25.09	18.87	15.66	40.98
ThO_2	n.d.	n.d.	n.d.	n.d.	n.d.	n.d.	n.d.
FeO	0.94	3.53	0.37	2.44	3.18	3.05	0.46
CaO	2.79	5.13	0.03	1.73	5.29	4.56	9.76
Ce_2O_3	0.90	1.34	0.05	0.43	1.21	1.69	0.42
Y_2O_3	1.05	1.46	0.40	0.64	1.95	n.d.	0.72
SiO_2	3.53	3.32	0.50	8.14	4.32	3.10	2.49

REE MINERALS (carbonates or phosphates): (*: bastnasite ?)

SNO	325103	325103	325103	325103	325103	325103	325103
UO_2	n.d.	n.d.	0.31	n.d.	n.d.	0.12	0.34
PbO	0.24	0.27	n.d.	0.38	n.d.	0.03	n.d.
ThO_2	0.04	n.d.	0.10	2.56	0.11	0.04	3.98
TiO_2	1.58	1.74	1.61	n.d.	1.33	1.46	n.d.
FeO	0.01	0.03	0.02	0.49	0.08	0.02	2.31
CaO	0.09	0.06	0.01	0.72	0.04	0.04	0.59
Ce_2O_3	17.02	16.89	16.95	27.41	15.81	15.54	20.74
Y_2O_3	0.34	0.23	n.d.	0.76	n.d.	0.17	0.72
SiO_2	n.d.	n.d.	n.d.	0.01	n.d.	0.03	20.58

SNO	325103	325103	325103	325103	325103	325103	325103
UO_2	0.20	n.d.	0.20	n.d.	n.d.	0.01	0.23
PbO	0.02	n.d.	0.06	1.19	0.27	0.08	0.25
ThO_2	n.d.	0.16	0.10	3.76	n.d.	n.d.	n.d.
TiO_2	1.62	1.50	1.60	n.d.	1.83	1.85	n.d.
FeO	n.d.	0.10	0.07	0.37	n.d.	0.02	0.01
CaO	n.d.	n.d.	n.d.	0.53	0.02	0.01	0.72
Ce_2O_3	16.42	16.02	16.28	27.21	18.74	19.44	34.77
Y_2O_3	0.17	0.23	n.d.	0.74	n.d.	0.29	0.04
SiO_2	n.d.	n.d.	n.d.	0.20	n.d.	n.d.	0.32

SNO	325112	325112	325112	325122	325122*	325131*	325131*
UO_2	0.04	n.d.	0.10	3.62	n.d.	0.26	0.12
PbO	0.06	0.01	0.14	0.18	0.11	0.31	0.10
ThO_2	0.06	0.15	1.32	n.d.	0.13	0.19	n.d.
TiO_2	n.d.	n.d.	1.86	n.d.	0.22	n.d.	n.d.
FeO	2.82	0.59	0.28	7.76	1.12	1.94	2.02
CaO	0.50	0.50	0.06	0.24	11.47	13.74	13.39
Ce_2O_3	29.95	34.97	18.13	22.27	23.41	21.30	18.82
Y_2O_3	0.20	0.20	n.d.	6.26	1.42	1.71	0.34
SiO_2	6.26	0.49	3.45	7.70	n.d.	n.d.	6.99

APPENDIX V

URANIUM CONTENT OF SOIL HORIZONS AND SORBENTS AND RADIOACTIVITY OVER PITCHBLENDE VEINS, PUISSAGTAQ

Vein I, line 12.5 W

Soil sample no.	Hor.	Sample loc.	U ppm in soil and sorbents: Soil	Sorbents: MnO	Sorbents: Resin fine	Sorbents: Resin coarse	Rad. ur
282301	Ao	0.0	269.00	21.20	110.00	56.60	63
282302	A1	0.0	1250.00				
282303	Ao	1.5S	266.00	8.98	8.86	11.30	46
282304	A1	1.5S	37.50				
282305	Ao	3.0S	7.60	0.00	0.00	0.37	17
282306	A1	3.0S	5.98				
282307	Ao	4.5S	3.91	0.00	0.00	0.00	15
282308	Ao	6.0S	3.76	0.00	0.00	0.00	13
282309	Ao	14.0S	5.09	0.00	0.00	1.68	15
282310	A1	14.0S	6.50				
282311	C	14.0S	5.74				
282312	Ao	24.0S	4.13	1.71	0.00	0.40	18
282313	A1	24.0S	4.02				
282314	C	24.0S	6.45				
282315	Ao	1.5N	202.00	1.45	7.23	11.00	56
282316	A1	1.5N	46.00				
282317	Ao	2.2N	351.00	9.33	33.50	35.10	87
282318	A1	2.2N	30.60				
282319	Ao	4.5N	156.00	1.47	4.71	3.96	32
282320	A1	4.5N	11.80				
282321	Ao	6.0N	7.20	0.00	0.00	0.37	22
282322	Ao	9.0N	6.70	0.00	0.00	0.60	16
282323	Ao	12.0N	8.09	0.00	0.00	0.00	14
282324	A1	12.0N	6.59				
282325	Ao	18.0N	7.94	0.00		0.43	14
282326	Ao	24.0N	7.50	0.00	1.18	1.64	14
282327	A1	24.0N	9.72				
282328	C	24.0N	9.34				

Vein I, line 15 E

Soil sample no.	Hor.	Sample loc.	U ppm in soil and sorbents: Soil	Sorbents: MnO	Resin: fine	Resin: coarse	Rad. ur
282329	Ao	0.0N	4.49	0.96	0.00	0.67	18
282330	A1	0.0N	5.58				
282331	Ao	1.5N	6.19	0.00	1.17	0.97	17
282332	A1	1.5N	4.89				
282333	Ao	3.0N	5.90	0.00	0.00	0.61	16
282334	A1	3.0N	5.50				
282335	Ao	4.5N	5.72	0.00	1.36	2.78	18
282336	A1	4.5N	7.03				
282337	Ao	6.0N	5.20	0.00	0.00	0.00	18
282338	Ao	9.0N	4.32	0.00	0.00	2.33	17
282339	A1	9.0N	5.11				
282340	C	9.0N	6.71				
282341	Ao	12.0N	5.95	0.62	0.00	0.52	16
282342	A1	12.0N	6.59				
282343	C	12.0N	7.23				
282344	Ao	15.0N	6.72	0.00	1.48	0.75	19
282345	Ao	21.0N	8.03	0.00	0.00	0.52	16
282346	Ao	26.0N	7.47	0.00	0.00	0.43	15
282347	Ao	1.5S	5.45	0.00	0.00	1.15	18
282348	A1	1.5S	5.07				
282349	C	1.5S	5.67				

Vein I, line 15 E

Soil sample no.	Hor.	Sample loc.	U ppm in soil and sorbents: Soil	Sorbents: MnO	Resin: fine	Resin: coarse	Rad. ur
282350	Ao	3.5S	5.05	0.67	0.00	1.86	15
282351	A1	3.5S	5.40				
282352	C	3.5S	5.36				
282353	C	3.5S	4.97				
282354	Ao	9.0S	5.09	0.00	0.00	0.00	21
282355	A1	9.0S	4.59				
282356	Ao	15.0S	4.27	0.62	1.46	2.56	20
282357	A1	15.0S	6.25				

Vein II, line 18 E

Soil sample no.	Hor.	Sample loc.	U ppm in soil and sorbents: Soil	Sorbents: MnO	Sorbents: Resin fine	Sorbents: Resin coarse	Rad. ur
282358	A1	0.0	6.53	0.00	0.00	0.00	46
282359	A1	0.0	6.65	0.57	1.08	0.00	
282360	A1	0.0	6.98	1.40	0.00	0.00	
282361	A1	0.0	6.72	1.62	0.00	0.00	
282362	A1	0.0	6.88	0.99	0.00	0.00	
282363	Ao	1.5N	5.05	0.00	0.00		42
282364	A1	1.5N	7.07				
282365	Ao	3.0N	4.87	0.00	0.00		41
282366	A1	3.0N	5.80				
282367	Ao	9.0N	4.47	0.73	0.00		26
282368	A1	9.0N	5.71				
282369	Ao	4.0S	5.61	0.72	0.00		44
282370	A1	4.0S	12.00				
282371	Ao	7.5S	6.26	0.96	0.00		49
282372	A1	7.5S	7.30				

Vein II, line 10 E

Soil sample no.	Hor.	Sample loc.	U ppm in soil and sorbents: Soil	Sorbents: MnO	Sorbents: Resin fine	Sorbents: Resin coarse	Rad. ur
282373	Ao	25.0N	5.03		0.00		25
282374	A1	25.0N	5.96				
282375	Ao	51.0N	20.10		0.00		27
282376	Ao	58.0N	21.60		6.86		27
282377	A1	58.0N	28.50				

Vein II, line 12.5 W

Soil sample no.	Hor.	Sample loc.	U ppm in soil and sorbents: Soil	Sorbents: MnO	Sorbents: Resin fine	Sorbents: Resin coarse	Rad. ur
282378	C	6.0NW	1100.00	17.60	108.00	44.50	137
282379	Ao	9.0NW	5.37	0.00	0.00	0.58	31
282380	A1	9.0NW	7.76				
282381	Ao	4.5NW	97.00	9.13	17.20	2.64	84
282382	A1	4.5NW	215.00				
282383	Ao	0.0	7.20		0.00	0.00	28
282384	A1	0.0	7.28				

GRØNLANDS GEOLOGISKE UNDERSØGELSE
THE GEOLOGICAL SURVEY OF GREENLAND

MAP 1.

LINEAMENT MAP OF THE IVIGTUT-JULIANEHÅB REGION

Compiled from geological maps and aerial photos

LINEAMENTS

Mapped faults or lineaments from aerial photos

Interpreted faults

- Major
- Minor

Gardar intrusive complexes

- Late Gardar
- Mid Gardar
- Early Gardar

- Gardar dolerite/gabbro dykes
- Eriksfjord Formation
- Ketilidian and Archaean basement

GARDAR COMPLEXES

A. Grønnedal-Íka
B. Küngnât
C. Ivigtut
D. Nunarssuit
E. Puklen
F. Tugtutôq
G. Narssaq
H. Ilímaussaq
I. Motzfeldt
J. North Qôroq
K. South Qôroq
L. Igdlerfigssalik
M. Klokken

1:250000

0 10 20 30 40

SYDEX Rep. no. 1 1986

GRØNLANDS GEOLOGISKE UNDERSØGELSE
THE GEOLOGICAL SURVEY OF GREENLAND

MAP 2

MAP A

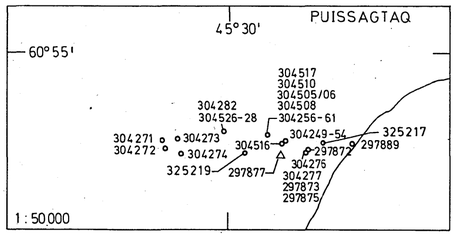

ROCK SAMPLES FROM THE "GRANITE ZONE"

○ 304831 Rock sample U ≥ 100ppm with GGU No. U/Th ≥ 1.0

△ 304535 Boulder U ≥ 100ppm with GGU No. U/Th ≥ 1.0

Parts of 60 V1, 60 V2, 61 V2 and 61 V3.

1:250 000

0 10 20 km

PROJECTION: LAMBERT'S CONICAL ORTHOMORPHIC.
ELLIPSOID: INTERNATIONAL. A = 6378388M - = 1/297.
STANDARD PARALLEL: 61° 30' 00" N

SYDEX Rap. no. 1 1986